Preface

To conclude my study Civil Engineering & Management at the department of Water Engineering & Management I performed a Master project on the evolution of river dunes, especially on the implementation of dune splitting in the two-dimensional vertical (2DV) dune development model (DuDe). My research project started with a trip to New Zealand, where I performed flume experiments together with my daily supervisor, Andries Paarlberg. It has been interesting to see dune development happen only inches before my eyes. The fact that we were so close to the matter and still did not understand why dunes occur and how they progress the way they do is intriguing. My experience in performing flume experiments, obtained during my Bachelor research project was useful but my knowledge about river dunes and sediment transport was limited to one or two courses during my Master. I am pleased to say that I developed much more insight in this matter now and in modelling in general.

To get away from the sand dunes, we took the weekends off to explore the amazing countryside of the Northern Island. During this trip I took the cover photo. The alert observant discovers that leaving the sand dunes behind during the weekends was easier said than done…

New Zealand has been a great experience. I would like to thank Andries for inviting me to join him on the journey to the other side of the world. And for his support during my research, especially for his patience to learn me the details of the DuDe model.

I would like to thank my graduation teacher, Marjolein Dohmen-Janssen for her positive feedback. Subsequently I would like to thank professor Suzanne Hulscher for remembering me to focus on the new aspects of this research and Paul Termes for his enthusiastic responses and ideas.

Besides my committee members I have been talking to one of the developers of the numerical code of the DuDe model, Ruud van Damme. He provided me with ideas to test the applicability of the changes I proposed and improved my understanding of the model by posing the right questions, I would like to thank him for the time and effort he took to help me.

Last but not least, I would like to thank my Dad for providing me with the possibility to study and for his support during my study, especially during the last phase.

Summary

River dunes are submerged bed forms on the bottom of alluvial channels. They form as a result of the complex interaction of water flow and sediment. River dunes influence the water level, by creating additional bed roughness as a result of form drag and can form a threat to shipping activities. Therefore they deserve the attention of river basin managers.

The relevance of physical modelling in contrast to the use of equilibrium predictors or empirical models lies in the applicability in extreme events. Equilibrium predictors do not consider the time component of dune development. Hysteresis for dune height is observed to be strong during a flood wave, which makes the use of equilibrium predictors inaccurate. Empirical modelling depends on calibration with data. The availability of data for extreme events is limited or absent, so the need for physical modelling is strong.

The Dune Development (DuDe) model is developed to describe river dune evolution by combining two-dimensional vertical (2DV) flow equations with a sediment transport formula using a parameterization of flow separation to avoid complex turbulence modeling inside the flow separation zone. Dune growth, migration and merging of river dunes is described well by the DuDe model. Model simulations have shown that the model did not predict equilibrium dimensions. Dunes did not reach a finite length and height.

Therefore, flume experiments have been conducted in Auckland (New Zealand) to observe the process of dune development, especially regarding dune splitting. Dune splitting in the form of initiation of superposed sand wavelets is seen as the mechanism to obtain equilibrium dune dimensions. Superposed sand wavelets develop a flow separation zone and can decrease the migration rate of underlying dunes and even cease migration when they scour the crest of the underlying dune. Therefore the implementation of superposed sand wavelets is seen as the solution to improve the prediction of equilibrium dune dimensions.

There are several ways to implement these superposed wavelets.
The implementation of a random disturbance of the river bed to mimic turbulent structures does not lead to splitting, as the model only supports growth of dunes with a wavelength larger than 0.5 m. Slope effects in the sediment transport formula change the fastest growing mode, but do not enable the random initiation of superposed bed features. Therefore, splitting, based on the superposed wavelets, is implemented in the DuDe model, by superposing a triangular disturbance on the stoss side of dunes, when they exceed a critical length (L_{crit}). This critical length is based on stability analysis, which shows that dunes are able to grow when the wavelength is larger than 0.5 m. These newly formed disturbances are created with an initial wavelet height (H_{wave}) of 6 mm.

Model simulations with this improved model lead to equilibrium dune dimensions. The dunes grow and migrate and eventually reach equilibrium dimensions in the expected period of time. The time to equilibrium and migration rates are in accordance with flume experiments. The model is now able to predict dune development from flat bed to equilibrium as observed in both field and flume.

Sensitivity analysis shows that the equilibrium dimensions depend highly on the critical stoss side length (L_{crit}), but this parameter is based on the stability analysis and is in accordance with the critical length expressed by earlier findings on superposed wavelets. The initial behaviour of the model differs from the experimental observations and therefore the nonlinearity parameter β in the sediment transport equation is reviewed. The variation of β does not lead to a change in the initial model behaviour. It only leads to a complete acceleration of dune development.

An important recommendation to improve the model and to make it feasible for practical application is to revise L_{crit}. The critical stoss side length needs to be representative for the flow and sediment conditions of the area of application. Therefore it is recommended that the critical stoss side length will be determined by a stability analysis, during the model simulations instead of using a fixed value.

Samenvatting (Dutch)

Rivierduinen zijn bodemvormen die zich bevinden op de bodem van rivieren. Ze ontstaan als gevolg van de complexe interactie tussen water stroming en sediment. Rivierduinen beïnvloeden de waterspiegel doordat ze zorgen voor extra bodemruwheid als gevolg van vorm ruwheid (form drag). Ze zijn dus van groot belang voor hoogwaterbescherming en kunnen een bedreiging vormen voor de scheepvaart. Vandaar dat rivierduinen de volle aandacht verdienen van waterbeheerders.

De meerwaarde van fysisch modelleren ten opzichte van evenwichtschatters of empirische modellen om duindimensies te voorspellen ligt in het voorspellen van extreme situaties. Evenwichtschatters houden geen rekening met de tijdsdimensie van duinontwikkeling. Hysterese in de duinhoogteontwikkeling blijkt sterk tijdens hoogwatersituaties. Dit effect kan alleen worden meegenomen als het volgt uit de fysica. Empirische modellen zijn afhankelijk van de beschikbaarheid van data. Vooral voor extreme situaties als piekafvoeren van rivieren is deze ontoereikend. Vandaar de voorkeur voor fysisch modelleren.

Het duin ontwikkelingsmodel (DuDe) is ontwikkeld om rivierduinontwikkeling te beschrijven met behulp van tweedimensionaal verticale (2DV) stromingsvergelijkingen gekoppeld aan een sediment transport formule. Stromingsloslating is afzonderlijk geparameteriseerd om complexe turbulentie modellering in de stromingsloslatingszone te vermijden. Duingroei, migratie en het samengaan van duinen werd reeds goed beschreven door het DuDe model in vergelijking met stroomgoot-experimenten. Echter splitsing van duinen en het bereiken van evenwicht in de duinhoogte en duinlengte ontbrak.

Stroomgoot experimenten zijn uitgevoerd aan de Universiteit van Auckland (Nieuw Zeeland) om duinontwikkeling te observeren, in het bijzonder het splitsen van duinen. Tijdens de experimenten is het ontstaan van zandgolfjes (sand wavelets) op de loefzijde van lange duinen waargenomen. Deze kleine gesuperponeerde bodemvormen zorgen voor een afname van de migratiesnelheid van onderliggende duinen. Ze kunnen zelfs veroorzaken dat een onderliggend duin stopt met migreren wanneer ze de top van het onderliggende duin eroderen.

Er zijn verschillende manieren om deze gesuperponeerde duintjes te modelleren. De implementatie van een willekeurige verstoring van het rivierbed om zodoende turbulente structuren na te bootsen leidt niet tot duinsplitsing, omdat duinen alleen groei vertonen in het model wanneer deze een golflengte hebben groter dan 0.5 m. Daarom is duinsplitsing geïmplementeerd, gebaseerd op de zandduintjes, waargenomen tijdens de experimenten. Deze zandduintjes zijn geïmplementeerd als driehoekige verstoringen op de loefzijde van duinen langer dan de kritische lengte van de loefzijde (L_{crit}). Deze kritische lengte is gebaseerd op stabiliteitsanalyse. Deze analyse laat zien dat duinen groei vertonen wanneer de golflengte 0.5 m overschrijdt. Deze nieuw gecreëerde verstoringen worden gevormd met een initiële hoogte (H_{wave}) van 6 mm.

Model simulaties met deze verbeterde versie van het model laten zien dat evenwicht optreedt in de duindimensies. De duinen groeien en migreren en uiteindelijk bereiken ze een evenwicht binnen de verwachte tijd. De tijd tot evenwicht en de migratiesnelheid van de duinen in evenwicht komen overeen met de waarnemingen tijdens experimenten. Het model is nu in staat om duinontwikkeling te voorspellen van een vlakke bodem tot evenwicht, overeenkomstig de experimenten en veldstudies.

Gevoeligheidsanalyse toont aan dat de evenwichtsdimensies die voorspelt worden met het model weliswaar in hoge mate afhankelijk zijn van de kritische lengte van de loefzijde (L_{crit}), maar deze parameter is bepaald aan de hand van de stabiliteitsanalyse en heeft zodoende dus wel een fysische basis. Daarnaast komt deze parameter overeen met eerdere bevindingen, aangaande de lengte van gesuperponeerde zandduintjes. Het initieel gedrag van het model wijkt af van de duininitiatie waargenomen tijdens de experimenten. De variatie van de nonlineariteits-parameter β leidt echter niet tot een verandering van het initieel model gedrag, enkel tot een algehele versnelling van de duinontwikkeling.

Een belangrijke aanbeveling om het model geschikt te maken voor praktische toepassingen is de bepaling van L_{crit} aanpassen. De kritische lengte van de loefzijde is afhankelijk van de heersende stromings- en sedimentcondities. Het is aan te bevelen gedurende de modelsimulaties op basis van een stabiliteitsanalyse de L_{crit} aan te passen aan de heersende stromingscondities.

Table of Contents

1   Introduction

1.1 River dune modelling

River dunes are present in nearly all fluvial channels and are vital in predicting flow resistance, sediment transport, and deposition within many rivers (Best, 2005).
Dunes occur under sub critical flow conditions and migrate in stream wise direction. They influence the water surface in contrast to ripples. Ripples are also current-generated bed forms but do not influence the water surface because they occupy a smaller portion of the water column. The occurrence of ripples or dunes depends on the grain size and flow strength. Dunes develop at higher flow strengths and relative large grain sizes compared to ripples. (Allen, 1968; Chang, 1988). See Appendix 1 for a detailed classification based on flow characteristics and dimensionless grain size.
The branches of the River Rhine in the Netherlands (see figure 1.1), characterized by a sand-gravel bed in the upstream part and a sand bed in the downstream part of the river system, show migrating dunes, especially during floods (Wilbers & TenBrinke, 2003). Figure 1.1b gives a cross-section of the previous picture, with flow from right to left. The asymmetrical form is clear; river dunes migrate downstream with a relative gentle stoss side and a steep lee side (for details on dune jargon, see section 2.2).
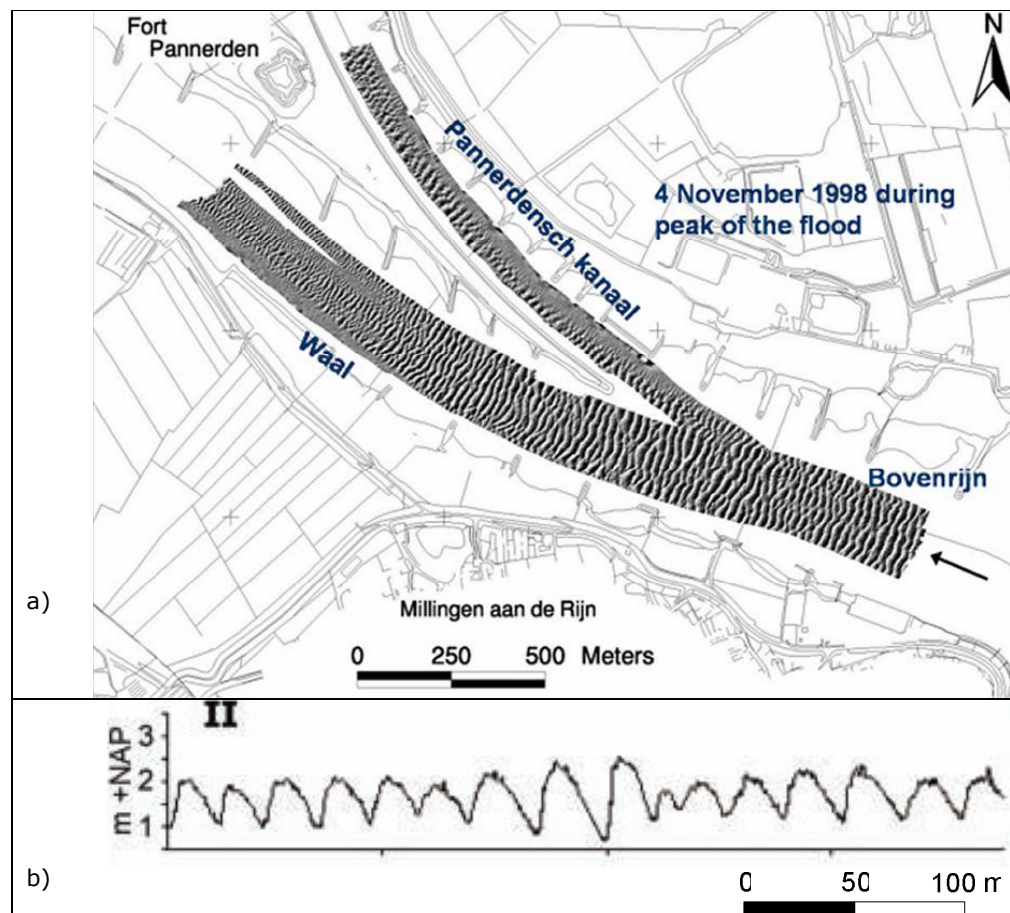
Figure 1.1: a) Dune measurements during high river discharge b) Part of a bed profile showing large dunes with smaller dunes superimposed during flood, on 6 November 1998, flow from right to left. (Wilbers & TenBrinke, 2003).

Dunes grow and migrate as a result of interaction between water flow and bed material as described in section 2.2. Dune growth leads to an increase of the bed roughness as a result of form drag. Bed roughness influences the water depth in a river. The prediction of dunes is therefore important for river managers in the context of flood control. Section 2.1 stresses the need for physical modeling of river dunes based on the dynamic character of bed roughness. Physical modelling has namely value in predicting dune dimensions for extreme events.

Most researchers try to create a physical model based on a coupling of simplified flow equations and a sediment transport formula (Exner, 1920; Kennedy, 1963; Giri & Shimizu, 2006). Other models, however, aim at a more empirical or deterministic approach to describe what is observed during field and flume experiments (Führböter, 1983, Wilbers, 2004; Jerolmack, 2005). A more detailed review on current modelling can be found in section 2.3.

The need for a physical dune development model that is accurate and does not require too much computational effort is strong.

The dune development model (DuDe) is the research object during this Master project. It has been set-up to simulate the development of river dunes in a simplified way with minimum computational effort but based on the underlying physical processes taking place during dune development (section 2.4). It combines a steady two-dimensional vertical (2DV) flow solver to a bed load sediment transport formula. Section 2.5 shows that the DuDe model correctly simulates growth of low angle dunes from an initially disturbed bed. Dunes develop as expected into asymmetrical dunes with a gentle stoss side and a relative steep lee side. However, the existence of a dynamic equilibrium, in which dunes migrate downstream and merge and split as reported by Leclair (2002) and seen during flume experiments (chapter 3), is not observed during model simulations. Dunes keep merging as a result of varying migration rates and grow in height and length until they reach the boundaries of the model domain (section 2.5). Based on empirical methods (Julien & Klaassen, 1995; Van Rijn, 1984) to predict equilibrium dune dimensions, river dune height and length are assumed to reach equilibrium dimensions (Appendix 2). Model simulations with the DuDe model, without implementation of splitting, show that dune dimensions reach excessive proportions and are not in accordance with expected dune dimensions (section 2.5). Flume experiments have lead to the insight that splitting of river dunes occurs on the stoss side of relative long dunes (chapter 3).

Although a generic model or theory that successfully describes all underlying processes of dune evolution -especially the splitting of river dunes- is not available, the goal of this research is to incorporate a splitting mechanism, to obtain realistic dune lengths in the equilibrium stage and to mimic the behaviour observed in flume and field experiments. The lack of a process of splitting or new dune creation in the DuDe model assumed to be the reason for the absence of equilibrium dune dimensions.

Therefore the research objective for this Master project is:

Improving the prediction of equilibrium river dune dimensions, by incorporating dune splitting in the DuDe model for bed form evolution.

The following research questions are formulated to reach this objective:

I   What are the strengths and weaknesses of the DuDe model?
II   What processes are observed during flume experiments that explain the existence of equilibrium dune dimensions?
III   How can splitting of river dunes be implemented in the DuDe model?
IV   Does the implementation of splitting lead to the prediction of equilibrium dune dimensions?

1.2 Methodology & report outline

The lack of a splitting mechanism in the DuDe model is the reason for this research project. The methodology of this research project is visualized in figure 1.2. A comparison of model simulations and flume experiments leads to the derivation of possible splitting mechanisms to implement as model improvements. The model changes are reviewed and implemented and the sensitivity of the chosen parameters is tested. After discussion of the complete process, this leads to interesting conclusions on present improvements and recommendations for future improvements of the DuDe model.

Chapter 2 gives a literature review on dune development and describes the basics (model equations) and possibilities of the DuDe model before splitting has been implemented.

Chapter 3 describes the experimental set up, method and results of the experiments to validate the model and to obtain possible missing processes that explains the inability of the model to predict equilibrium dune dimensions.

Chapter 4 starts with the strengths and weaknesses of the model. Subsequently it presents the implementation of the splitting mechanism and described the model results.

Chapter 5 contains a sensitivity analysis of the model for the non-linearity parameter β in the sediment transport formula and for the two wavelet parameters L_{crit} and H_{wave}.

Chapter 6 discusses the outcomes of this Master research project and the various stages of the project. The main conclusions of this project in the form of answers on the research questions mentioned above and recommendations for future research and application are presented in chapter 7.
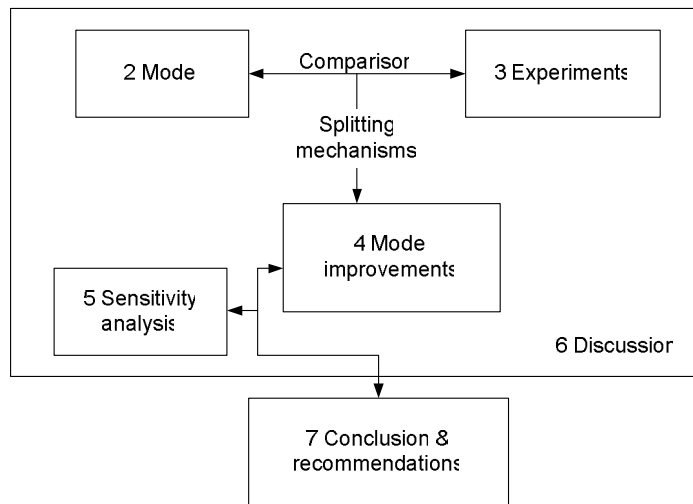
Figure 1.2 Schematic representation of the research methodology.

HIGHLIGHTS Chapter 1: Introduction

- Correct prediction of equilibrium dune dimensions is essential for adequate river management during high river discharge.

- The current DuDe model does not predict equilibrium dune dimensions.

- The goal of this research is to improve the prediction of equilibrium river dune dimensions, by incorporating dune splitting in the DuDe model for bed form evolution.

2   Research background

2.1 Relevance of physical modelling

Field measurements of the Dutch branches of the river Rhine (Wilbers & TenBrinke, 2003) and the Fraser river in British Columbia (Kostachuk & Villard, 1996; Villard, 2003) show a phase lag between the moment of maximum river discharge and the appearance of the highest dunes.
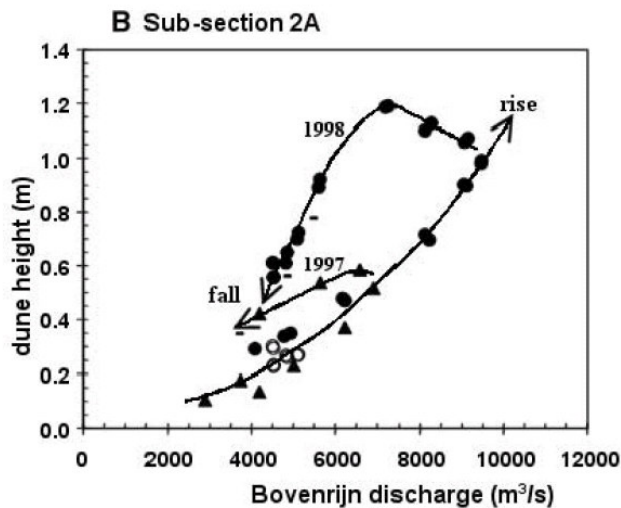

Figure 2.1 Hysteresis in dune height development In the River Rhine [Wilbers & TenBrinke, 2003]

This so called hysteresis effect (figure 2.1) on dune dimensions makes it important to create a physical model to predict equilibrium dimensions. Dune dimensions can not only be described as a function of flow and sediment conditions. It has also a strong time component (figure 2.1). Recent news about climate change and changing weather patterns increases the attention of the public and governments for appropriate water management in general and flood protection in particular. Decision support systems and flood prediction models are used to assist water managers in making the correct decisions.

To improve flood prediction models, dynamic roughness has to be incorporated in these models. The formation of river dunes during high river discharge increases the bed roughness. Water levels depend largely on the bed roughness in the river main channel. The dynamic character of bed roughness as a result of river dunes lies in the phase lag that occurs between the river flood wave and the peak in the bed roughness. Hysteresis, a phase lag between the top river discharge and maximum bed form dimensions, makes it impossible to relate the bed roughness directly to the river discharge. The dune length and height continue to grow, even when the river discharge has started the falling stage. This makes the use of equilibrium predictors unrealistic and underlines the need for a physical based solution for the prediction of river dune evolution during high river discharges. At the moment roughness is used as a calibration parameter for hydraulic modelling.

To incorporate dune evolution in hydraulic model, the need for models with a low complexity and a high accuracy is strong in the field of water managers (Paarlberg, 2007).

2.2 Processes in river dune development

River dunes develop as a result of complex interactions between water flow, sediment transport and bed morphology (figure 2.2). The bed forms are created and altered by the flow and, conversely, the flow is acted upon by the bed forms through the production of form drag and significant changes in local mean flow and turbulence fields (Nelson et al., 1993).
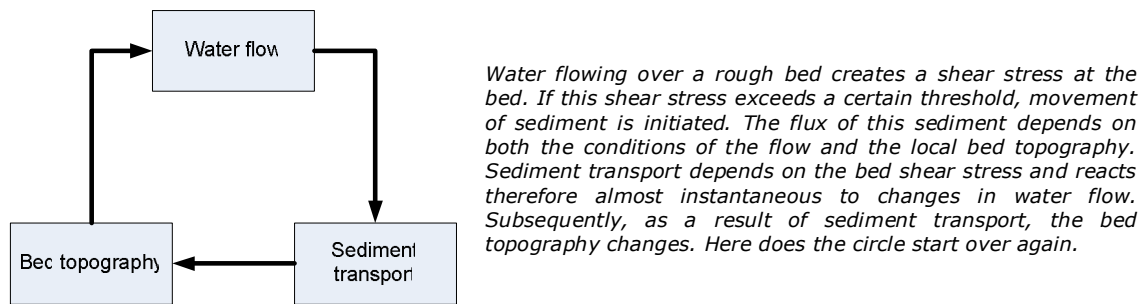

Water flowing over a rough bed creates a shear stress at the bed. If this shear stress exceeds a certain threshold, movement of sediment is initiated. The flux of this sediment depends on both the conditions of the flow and the local bed topography. Sediment transport depends on the bed shear stress and reacts therefore almost instantaneous to changes in water flow. Subsequently, as a result of sediment transport, the bed topography changes. Here does the circle start over again.

Figure 2.2: Morphological cycle

Sediment transport takes place when the bed shear stress exceeds the critical shear stress for grains to move (Appendix 3). If a flat bed is acted upon by turbulent flow capable of producing significant movement of the sediment grain, the bed will be unstable to perturbations and will evolve into a train of bed forms (i.e. ripples and/or dunes) (Nelson et al., 1993). This first stage of river dune development, bed form initiation from flat bed has been subject of research for more than 80 years (e.g. Exner, 1920).
Raudkivi & Witte (1990) claim that since no ripples are formed in laminar flow, the initiation of small disturbances must be a function of turbulence. The first disturbances arise from the turbulent bursting process on the bed surface, but since turbulence is a random or at least very complex process, the apparent order, observed in nature (figure 1.1), must arise from a process of organizing. However, experiments in laminar flow, show that initial bed forms appear in a similar way under sub critical laminar flow. With wavelets forming in the absence of turbulent flow structures, it appears likely that initial bed forms are generated by an instability within the motion of the granular bed material or by a form of shear layer instability. (Coleman & Eling, 2000)
Most research on bed form initiation has focused on two theories. Venditti et al. (2005) examined bed form initiation in unidirectional flow. Linear instabilities (perturbation theory) and bed defects were tested as trigger for dune initiation. The first theory (perturbation theory) is initially proposed by Exner (1920) and later developed by Anderson (1953). Perturbation theory involves the linearization of the equations of motion of both fluid and sediment over a bed perturbation or defect to predict suppression or growth of the perturbation (McLean, 1990). The second theory assumes that all bed forms are a result of propagation of initial bed defects, i.e. accumulations or patches of sediment or holes in the bed that are propagated downstream.
This second theory assumes that these patches grow because flow separation appears behind the crest of these initial dunes. Flow separation occurs at a short distance from the crest of a dune.
River dunes become asymmetric due to unidirectional flow. The top migrates faster than the trough as a result of flow acceleration over the crest, resulting in a gentle stoss side and a steep lee side. If the lee side of a dune becomes too steep for the flow to follow the bed, flow separates. Consequently, a large separation zone develops in the trough. (figure 2.3).
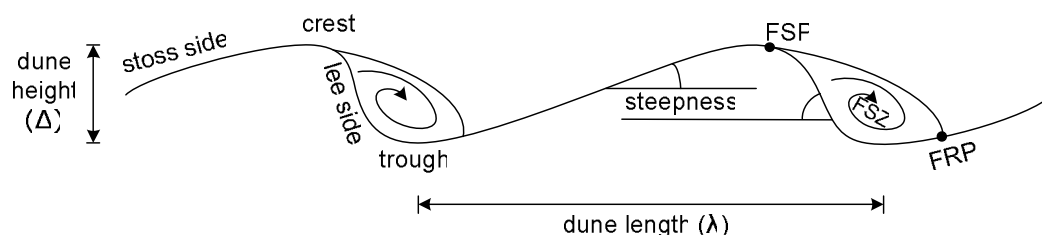

Figure 2.3: Definitions of terms used in river dune research; FSZ = flow separation zone, FSP = flow separation point, FRP = flow reattachment point.

In the flow separation zone, a large eddy is formed where turbulence is generated. This implies energy dissipation and therefore slows down the main flow. It reattaches at a certain distance downstream, at the flow reattachment point (Paarlberg et al., 2005). Flow separation mechanisms are sometimes held responsible for the propagation and growth of these initial bed forms (Raudkivi, 1966).

The migration rate of dunes (c) can roughly be described as the sediment flux over the crest (q_c) of the dune divided by the height of the dune (Δ) (law of Exner-Ertel):

$$c = q_c / \Delta \tag{2.1.1}$$

Assuming a constant sediment flux would imply that dunes migrate with celerities inversely proportional to their heights (Exner, 1920). Initial bed forms travel with velocities reciprocal to their heights with the result that the smaller forms catch up the bigger ones and unite, what in the sense of Haken (1978) corresponds to enslavement (Führböter, 1983). Raudkivi & Witte (1990) agree with this theory and state that bed features created by unidirectional flow of water in alluvial channels are seen to translate downstream at speeds related to their heights. The process of merging as a result of varying celerities is observed also more recently by Nino et al. (2002).

Qualitatively, dune growth is perceived as the outcome of trough scouring, merging of dunes and lee side deposition, in consequence of flow deceleration behind a dune crest. Lee side deposition results also in crest accretion and depends largely on the existence of a flow separation zone, because the size and shape of the flow separation zone influences the local sediment transport (Leclair, 2002).

Bed forms grow as a result of an instability mechanism, induced by the phase lag between sediment transport and the bed topography (Kennedy, 1963; Colombini, 2004). This phase lag is a result of fluid inertia (Dronkers, 2005 ; Charru & Hinch, 2006).

The maximum bed shear stress appears earlier than the dune crest (figure 2.4). Because net sediment transport depends on the gradient in the bed shear stress (positive = erosion, negative = accretion) The crest of a dune grows and a trough scours, when the maximum bed shear stress appears earlier than the dune crest (figure 2.4).
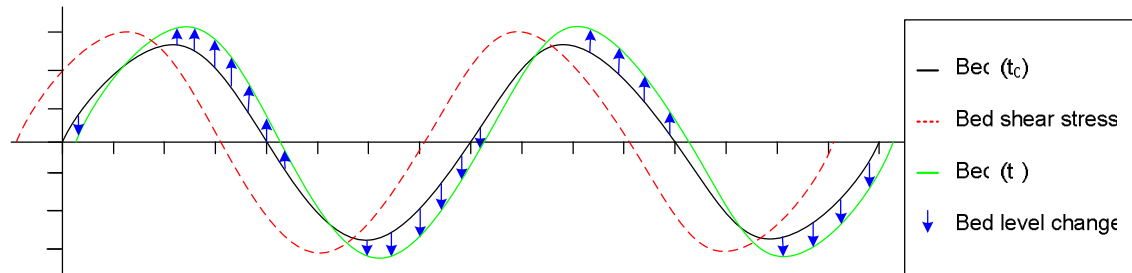

Figure 2.4: Dunes grow when the bed shear stress is out of phase with the bottom configuration.

Colombini (2004) states that: "a simple glance at the linearized form of the Exner's equation for bed evolution (formula 2.1.2; Exner,1920) reveals that if the local sediment transport rate is exactly in phase with the bed elevation, no amplification of bed perturbation is obtained."

$$\frac{\partial h}{\partial t} = -\frac{1}{(1-\varepsilon_0)}\frac{\partial q_b}{\partial x} \tag{2.1.2}$$

(h=bottom elevation [m], t=time [s], ε_0 = void ratio of sediment [-], q_b = sediment flux per unit width [$m^2 s^{-1}$], x = distance in flow direction [m])

The dunes migrate in that case downstream without changing shape (see figure 2.5).
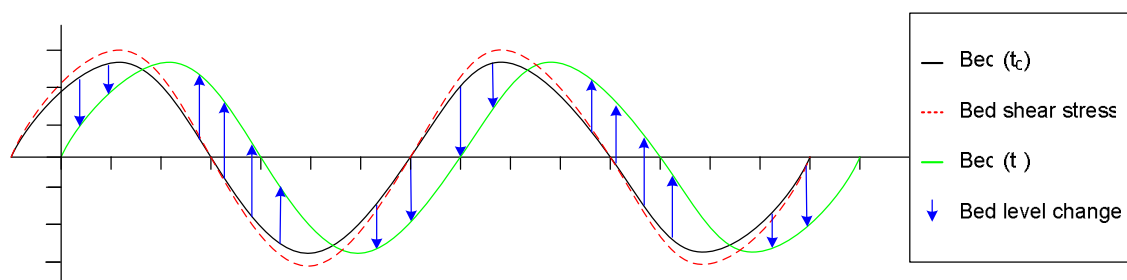
Figure 2.5: Dunes migrate without changing shape, when the bed shear stress is in phase with the bed elevation

However, in the search for an explanation for the finite dune length observed in nature, linear theory is unable to clarify the ability of dunes to reach an equilibrium amplitude. Eventually dune height and length reach equilibrium values in both flume (Coleman, 2005; Van Rijn, 1993) and field experiments (Julien & Klaassen (1995), Wilbers & TenBrinke, 2003). However, reports on flume experiments present mean dune dimensions and lack detailed qualitative descriptions of specific processes (e.g. dune splitting). Equilibrium dune height and length are mainly influenced by flow characteristics, especially the water depth (H). Some equilibrium predictors of river dunes also assume an influence of grain size (Julien & Klaasssen, 1995) and even flow strength (represented by the Froude number (Tsuchiya & Ishizaki, 1967) or Van Rijn's transport parameter T (Van Rijn,1984)).

2.3 Modelling of river dunes

Numerous attempts have been made by researchers to model dune development without modelling all detailed processes. Most models try to create a physical model based on a coupling of simplified flow equations, with some basic assumption regarding turbulence or pressure distribution. Fifteen years ago Nelson et al. (1993) wrote: "Current understanding of the flow-bed coupling is insufficient to produce physically based predictive models for bed form generation and stability under arbitrary flow conditions. This presents a substantial barrier to progress in several areas of geophysics and hydraulics. At present, empirical techniques are used to address these problems and, although these techniques often provide good results over the range of flow and bed form parameters for which they were developed, they typically yield poor results when extrapolated to situations other than those for which they are specifically calibrated. Because one of the primary goals in developing relations for roughness, sediment transport, and bed form geometry is to apply those relations to extreme events or other situations where flow and sediment transport data are difficult or impossible to measure, these empirical methods are inadequate in many cases."
Jerolmack and Mohrig (2005) underlined these findings just recently. However, progress has been made the last 15 years in understanding the fluid dynamics associated with alluvial dunes and has witnessed huge advances in field, laboratory, and numerical investigations (Best, 2005).
Some researchers expect that the most accurate model of bed form evolution will eventually come from detailed numerical solution of the Navier-Stokes equations coupled to some force balance on sand grain and sediment continuity. (e.g. Giri and Shimizu, 2006). However, this model of Giri and Shimizu uses a simplified two-dimensional-vertical numerical implementation of the 3D-flow solver presented by Shimizu et al. (2001), because the application of the 3D flow solver with a sediment transport model for morphodynamic simulation is impractical due to the extremely high computational effort required by such an approach (Giri & Shimizu, 2006). It is clear that numerical modelling of the Navier-Stokes equations in combination with a sediment transport formula requires the use of inventive simplifications in order to make it feasible. In contrast to these physical models, empirical models based on field observations are developed recently (Wilbers, 2004; Jerolmack & Mohrig, 2005). The model of Wilbers (2004) compared dune dimensions obtained by using equilibrium predictors with actual measurements and determines the best fit. Subsequently, Wilbers (2004) developed a model to apply the relaxation and adaptation of dune dimension under unsteady non-uniform conditions. The problem for this model arises when predictions need to be extrapolated to extreme conditions. The model uses calibration data, especially to determine the adaptation constant which determines the time to equilibrium. Therefore this model is not generally applicable, especially for extreme events (Wilbers, 2004).

2.4 DuDe model

The Dune Development model (DuDe) is developed to analyze the morphodynamic evolution of river dunes during river floods (Paarlberg et al, 2006). DuDe consists of a two dimensional vertical (2DV) flow solver and a sediment transport model based on the equations of Meyer-Peter-Müller (1948). The flow solver is a steady version of a model by Hulscher (1996), which is originally developed for simulating offshore sand waves. The currently used numerical implementation is developed by Van den Berg & Van Damme (2005). Hydrostatic shallow water equations are used assuming a constant eddy viscosity.
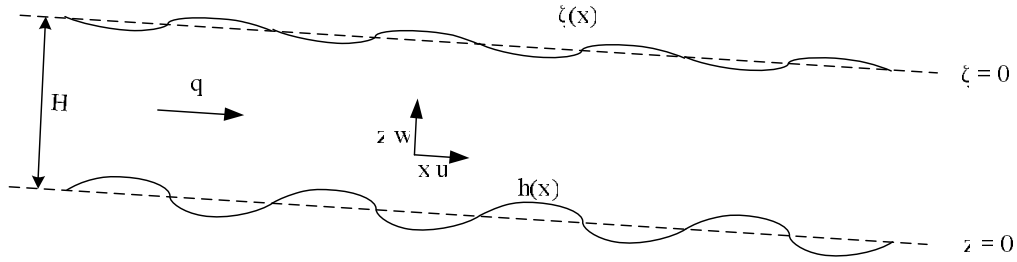

Figure 2.6: Definitions of flow parameters

During a model simulation, the model calculates the flow characteristics based on the bed configuration of the previous time step. Subsequently, the bed shear stress and corresponding sediment transport are derived. The calculation of bed elevation, based on the gradient in sediment transport, is the final step to obtain a new bed profile. This quasi-steadiness of the model is allowed because bed evolution and flow dynamics take place at different time scales. The basic flow and sediment transport equations will be discussed in this chapter. Appendix 4 gives an extended description of the model with the relevant boundary conditions needed to solve these equations. Due to the constant eddy viscosity, flow separation cannot be treated explicitly and is parameterized, which is also described in detail in Appendix 4.

Shallow water equations

Assuming no variations perpendicular to the flow direction and considering incompressible flow, the momentum equation in x-direction reads:

$$u \frac{\partial u}{\partial x} + w \frac{\partial u}{\partial z} = A_v \frac{\partial^2 u}{\partial z^2} - g \frac{\partial \zeta}{\partial x} + g i_b \qquad (2.4.1)$$

The continuity equation reduces, given the assumptions mentioned earlier to:

$$\frac{\partial u}{\partial x} + \frac{\partial w}{\partial z} = 0 \qquad (2.4.2)$$

It turns out that a basic turbulence closure (constant eddy viscosity A_v) in combination with a partial slip condition results in a good representation of the vertical flow structure and therefore in good estimation of the volumetric bed shear stress (τ_b [m²s⁻²]). Boundary conditions, assuming no flow through the boundaries and no wind shear are described in Appendix 4.

Sediment transport equation

The basis for the sediment transport equation used in the DuDe model is first described by Meyer-Peter and Müller (1948). They stated a power law relationship between sediment flux and bed shear stress.
This formula has been modified, as proposed by Komarova & Hulscher (2000), to incorporate two bed slope effects. Firstly (i): as described by Whitehouse (1995), a sloping bed can enhance or reduce the sediment transport rate once sediment is in motion depending on the direction of the slope. For example sediment being transported down a slope will experience a component of its

immersed weight acting down slope. Secondly (ii): a sloping bed will change the value of the threshold shear stress for initiation of motion (Bagnold, 1956).

Intuitively a positive slope (upwards in the direction of flow) increases the threshold shear stress for particle motion. The second bed slope effect is described mathematically by Fredsoe and Deigaard (1992).

The volumetric sediment transport rate q_b [m^2s^{-1}] depends on the local volumetric bed shear stress τ_b [m^2s^{-2}] (see formula 2.2.5). The threshold shear stress increases or decreases depending on the local bed slope (ii) mentioned earlier with a factor λ_1. The volumetric transport rate is also directly influenced by the local bed slope as a result of the other slope effect (i) with a factor λ_2. The parameter α is a proportionality constant = 0.5 s^2m^{-1} and β = 1.5 is a nonlinearity parameter.

The local bed slope h_x is the first derivative of h to x. ϕ_s is the angle of repose of sediment, which depends on the grain diameter and angularity (roundedness) of the sediment (Simons (1957) in: Chang, 1988) and is about 30º for sand in rivers.

$$q_b = \alpha(\tau_b - \lambda_1\tau_{cr,0})^\beta \lambda_2 \qquad\qquad \lambda_1 = \frac{1 + h_x / \tan\phi_s}{\sqrt{1 + (h_x)^2}}$$

$$\tau_{cr,0} = \theta_{cr} g \Delta d_{50} \qquad\qquad\qquad \lambda_2 = \frac{1}{1 + h_x / \tan\phi_s}$$

$$(2.4.3)$$

Bed level changes occur as a result of gradients in the sediment flux distribution, based on the Exner (1920) equation:

$$\frac{\partial h}{\partial t} = -\frac{1}{(1 - \varepsilon_p)}\frac{\partial q_b}{\partial x} \qquad\qquad\qquad\qquad\qquad (2.4.4)$$

This can be explained physically based on continuity of mass, the difference between mass inflow and outflow will be compensated by the change in bed level. A correction is applied for the porosity of the sediment (ε_p = 0.4), because the sediment flux is calculated as volume solid material, and to determine the change in bed elevation including voids, compensation for this 40% void volume is needed.

Parameterization of flow separation

River dunes become asymmetric due to unidirectional flow. The top migrates faster than the trough, resulting in a gentle stoss side and a steep lee side. If the lee side of a dune becomes too steep for the flow to follow the bed, flow separates (figure 2.7). The boundary between the normal flow zone and the flow separation zone is called the separation streamline (SSL). The area underneath the SSL is called the flow separation zone (FSZ). The separation streamline touches the bed again at the flow reattachment point (FRP).
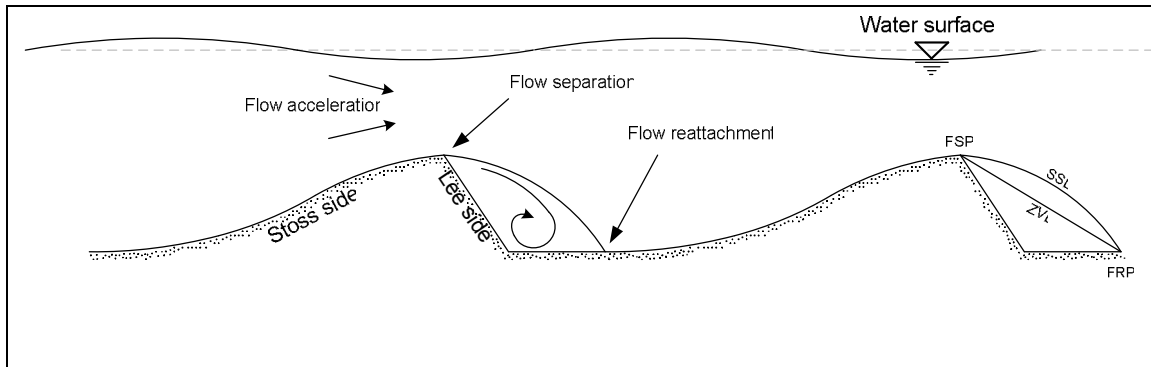

Figure 2.7: Schematisation of river dunes with flow separation characteristics

Due to a constant eddy viscosity in the model, the model does not account for flow separation. Therefore a parameterization based on dune height and the local bed angle at the points of separation is used as described by Paarlberg et al. (2007). The shape of the flow separation zone is found to be independent of flow conditions. (Engel, 1981; Paarlberg et al. 2007). The parameteri-

zation of flow separation is based on a method developed for aeolian dune development by Kroy et al. (2002). For a extensive description of the DuDe model and the parameterization of flow separation, see Appendix 4.

2.5 Model simulations

Default settings

All model results that are presented in this Master thesis have flow and sediment characteristics comparable to the flume environment (chapter 3). These standard settings are:

Flow and sediment characteristics		Dimension
Waterdepth (H)	0.153	[m]
Grain size (d_{50})	$0.8*10^{-3}$	[m]
Bed slope (i_b)	$12*10^{-4}$	[-]
Discharge per unit width (q)	0.076	[m^2s^{-1}]
Numerical properties		
Horizontal grid size (dx)	0.01	[m]
Number of vertical points (Npz)	15	[-]

Table 2.1: Default model settings

Initial model behaviour

The DuDe model needs variability in the initial bed profile to generate dunes, because differences in bed elevation are generated as a result of gradients in the sediment flux (q_x), which are a result of varying local bed gradients (h_x). The simulation starts with a random signal of two grain sizes ($2*d_{50}$) at t_0 to mimic the fact that a flat bed is never perfectly flat. This random signal forms the basis for dune development.

Every mathematical signal can be described as a sum of sinusoidal basis functions (Fourier). As seen in the magnified section of figure 2.8, the enforced random signal diffuses in the first seconds. The smallest wavelengths (largest frequencies) have the largest negative growth rate and therefore disappear fast as seen in earlier performed stability analysis (Paarlberg, 2006). Larger wavelengths (lower frequencies) diffuse slower. This process continues until a wavelength protrudes that grows, as seen after approximately 20 minutes.
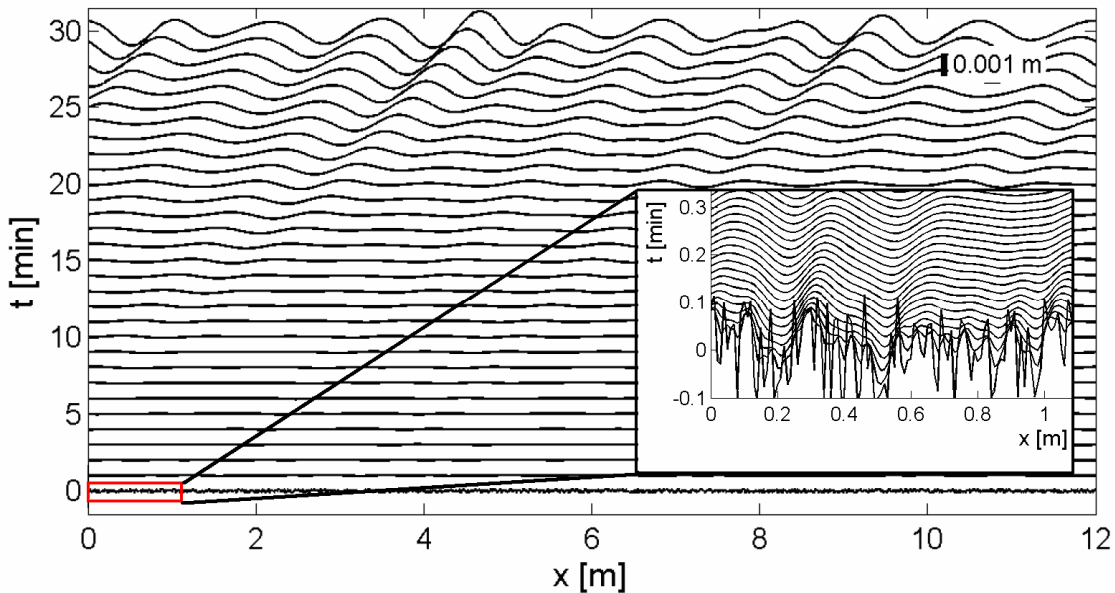

Figure 2.8: Initial model behaviour: diffusion until dune growth is reached (Domain length = 12 m)

Dune growth and asymmetry development

The DuDe model predicts fastest sinusoidal dune growth for dunes with a wavelength of approximately 1.2 m. Remarkable is the fact that the dunes remain sinusoidal for a long time in contrast to the development of asymmetry observed during flume experiments (Coleman & Melville, 1997). According to Coleman & Melville (1997) asymmetry occurs during the first stages of dune evolution.
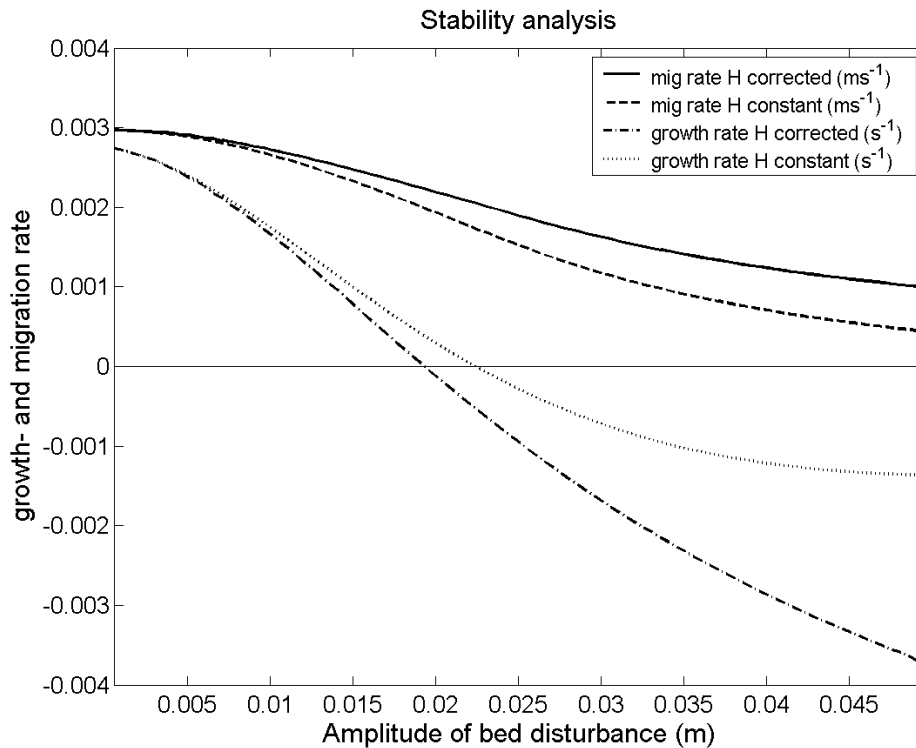

Figure 2.9 Linear behaviour, sensitivity of the growth and migration to the amplitude of a bed disturbance

The relative growth and migration rate of initial disturbances is determined for different amplitudes. Two situations are modelled: with the water level correction and without (H constant) to see if the initial behaviour would differ.
Figure 2.9 shows that the DuDe model is initially insensitive for variations in dune height, when the dune height does not occupy a significant portion of the water depth. This means that initially the wavelength determines the growth and migration of the dunes. If the migration rate is initially insensitive to the dune height, dunes remain symmetrical in this stage. Asymmetry is therefore a non-linear effect in the model.
The initial linear behaviour is also seen for the relative growth of river dunes. Initially the relative growth does not change when the wave height increases. The decrease in relative growth shows that the relative growth decreases with the amplitude of the bed disturbance as it reaches the equilibrium height belonging to the applied wavelength of the disturbance.
Dunes migrate at a celerity of approximately 4 m hour^{-1}. Differences in migration rates eventually lead to dune merging.
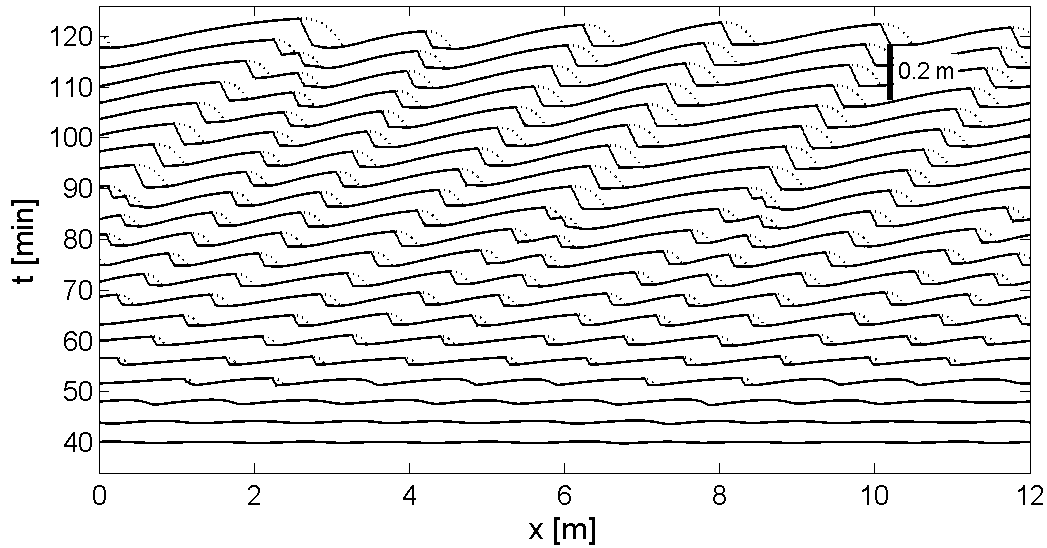
Figure 2.10: Asymmetry development and flow separation, flow separates after 50 minutes

Dune merging

Dune merging is described by several publications on flume and field experiments. Two dunes with different migration rates merge into a bigger bed form. (Leclair, 2000) uses the concept of 'catching up'. "Dunes that '*catch-up*' other dunes occur when the through elevation of a downstream dune is lower than that of an upstream, faster dune'. Before a dune is caught up, it decelerates markedly, as shown by Ditchfield & Best (1992) and may sometimes even cease to migrate. The 'caught-up' dune then suddenly increases in both height and length as the trough remains at the same elevation on the bed, The catching-up of dunes occurs at all flow velocities and aggradation rates, but is not frequent."

Field experiments also report on the merging of dunes, as described by Jerolmack and Mohrig (2005). "Large-scale bed features remained recognizable over the duration of their observations, while individual bed forms were observed to split into smaller features, merge to form larger features, spontaneously form on the stoss-side of larger features, and disappear in the lee slope of larger features." Merging of river dunes is seen during model simulations with the DuDe model, but initiation of new dunes or splitting of dunes does not occur during model simulations with the DuDe model. This means that dune height and length increase but do not decrease. Eventually this leads to unexpected high and long dunes (figure 2.11 & 2.12). Expected dune length and height (L ≈ 1m, Δ ≈ 0.05 m) are exceeded, because merging of dunes is a continuous process during these simulations.
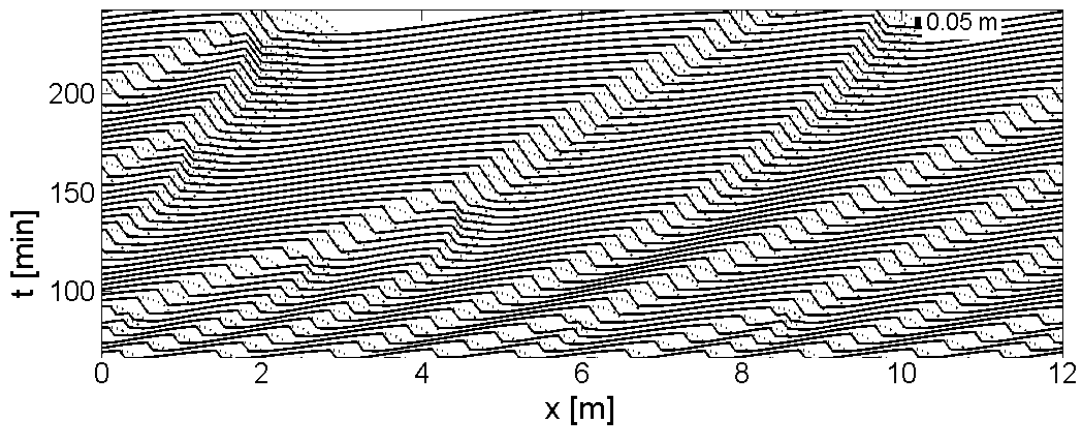
Figure 2.11: Model simulation (*H=0.15m d₅₀= 0.8mm, q= 0.076m²s⁻¹*); merging leads to unexpected long dune length and height
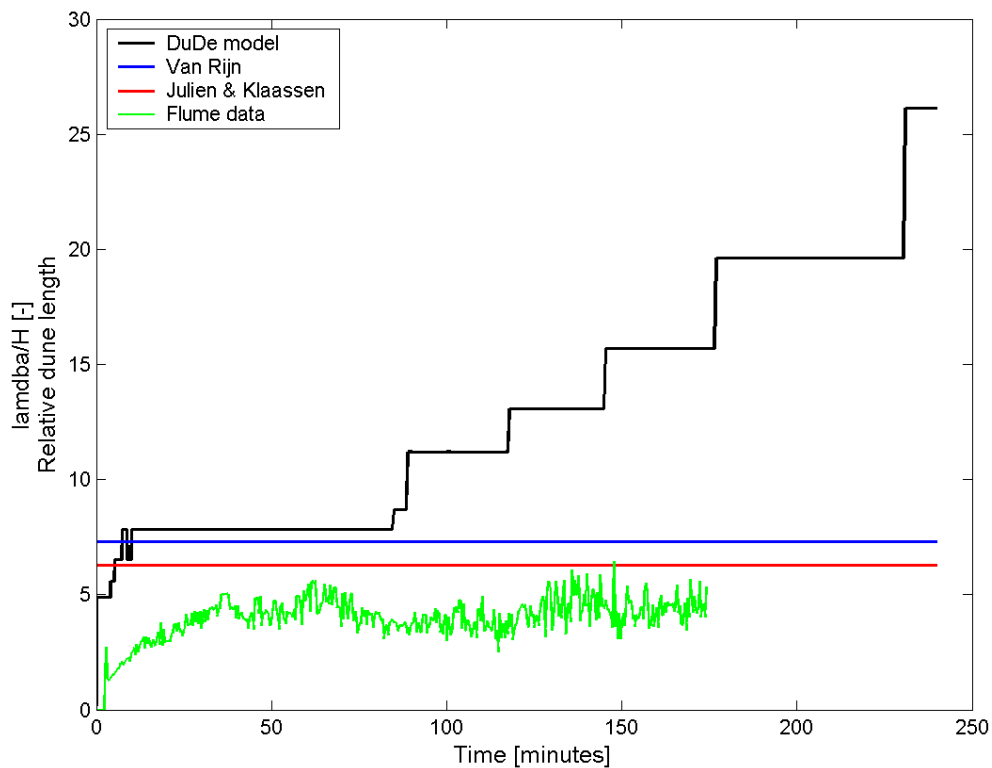
Figure 2.12: Dune length grows as a result of continuous merging and the lack of a splitting mechanism.

HIGHLIGHTS Chapter 2: Research background

- The DuDe model combines a 2DV flow solver with a sediment transport formula, flow separation is parameterized to avoid complex turbulence modelling.

- DuDe simulates dune growth and migration of dunes that become asymmetric with an angle of repose lee side and flow separation behind the crest.

- Asymmetry is observed as a non-linear effect in the model.

- The lack of a splitting mechanism makes that dunes keep merging and therefore growing in length and height.

3   Flume experiments

Flume experiments on the evolution of river dunes from flat bed are conducted under steady and unsteady conditions. The steady flow experiments are mainly used to investigate the stages of dune development and to compare the DuDe model with a controlled environment. Recent reports on experiments (Coleman & Melville, 1996; Coleman, 2005; Venditti et al., 2005) do not show the large detail, needed to determine dominant processes in the development of an equilibrium situation. Coleman (2005) focuses on the time to equilibrium and the equilibrium height and derives relations for these parameters, based on comparison of numerous flume experiments. They, however do not explain why this equilibrium is reached and do not qualitatively describe the observed behaviour. Venditti et al. (2005) mainly aim at the first stage of dune development; initiation from flat bed. Qualitative descriptions on the development of the initial dunes are incorporated, but the reason for finite dune lengths is not found in this publication.
The goal for the steady flow experiments is to investigate the equilibrium situation for river dunes and to find a mechanism for dune length and height stabilization. This knowledge can be used to improve the DuDe model.
The unsteady (flood-wave) experiments are conducted to investigate the influence of a flood wave on the development of river dunes and are described in Appendix 5.

3.1 Method and experimental set-up

The experiments are conducted in a 0.44 m wide, 12 m long, glass-sided flume. The flume, located at the University of Auckland is fully recirculating (both water and sediment) and tilting. The flume was filled with a 60mm thick layer of near-uniform coarse sediment with a median grain size d_{50} = 0.85 mm. See figure 3.1 for the result of the sieve analysis.
After distributing the sand evenly over the flume bed, the flume was carefully filled with water to the initial water depth (H). The bed was flattened before each run to make sure that all experiments started with the same initial bottom configuration. To obtain the desired bed slope, the flume was tilted.

Grading curve for course sand d_{50}=0.85-mm
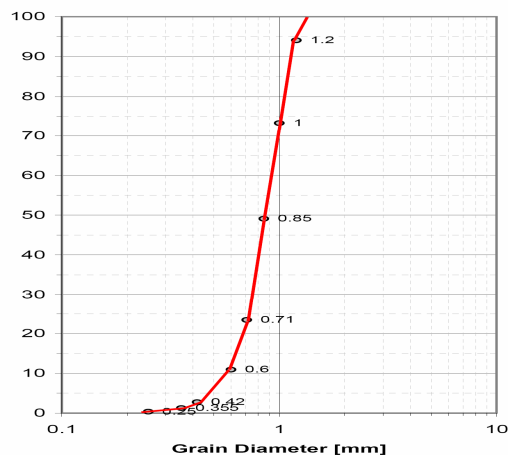

Figure 3.1: Near-uniform sediment mixture

At t=0, the pumps (sediment and water) were turned on simultaneously with the start of the bed profile measuring. The bed profile was measured with an automatic carriage system containing a depth sounding probe, which measured the bed elevation. The position of the carriage along the flume is determined by a potentiometer mounted on a wheel which is attached on the carriage and moved along the side of the flume. The carriage moved over a 6 m long test-section starting 4m downstream of the sand and water inlet. It was able to measure a centreline bed profile, roughly every 23 seconds with a spacing of approximately 2.5mm. According to Coleman & Melville (1997) the accuracy of bed-elevation measurements is ± 0.4mm. For visual support, a fixed video camera recorded dune evolution from the start over a section of 1.5 m during several experiments. A handheld camera was used to observe small scale processes. During the experiments the water

surface elevation was monitored to assure that the water surface slope was parallel to the bed slope. The downstream water level was adjusted by moving a tail gate at the downstream end of the flume when a discrepancy was observed. These adjustments have not been applied for earlier experiments (T2-T8, T11,T13-T15 & T17).
In these earlier experiments, a water level slope resulted in a bed slope change.
Water temperature, initial water level and bed slope were recorded before the start of an experiment. Depth-averaged mean flow velocity was estimated using Acoustic Doppler Velocimeter (ADV) measurements. A logarithmic profile was fitted through the ADV-data and the mean flow velocity was estimated as the velocity at 1/e of the height of the water column above the sand bed. Two shear velocities were calculated for each flow setting. $u_*^{(1)}$ was calculated as $(gHi_b)^{-1/2}$ (see explanation of symbols in table 3.1), whereas $u_*^{(2)}$ was determined based on the ADV measurements.
Experiments under steady flow conditions are performed for three different settings. The bed slope is kept constant at a value of 0.0015, but the pump settings and initial water
level are different:

- T22: H_0 = 150 mm, q = 0.10 m^2s^{-1}
- T23: H_0 = 125 mm, q = 0.08 m^2s^{-1}
- T24: H_0 = 100 mm, q = 0.06 m^2s^{-1}

The method to generate river dune characteristics from the highly detailed and extensive data-sets is developed by Dougal Clunie (University of Auckland) and has been improved by Andries Paarlberg. Outliers were filtered by a software tool called clean-up. Subsequently, a software tool *bedformer*, determines river dune dimensions (height, length and steepness) for every measured profile. The tool determines a lee side based on a certain number of points. These points need to form a line with a minimum lee face angle at a minimal horizontal distance from another lee side. Consequently, the tool looks upstream for a crest by determining a local maximum and downstream for the trough as a local minimum downstream. When crests and trough location and elevation are known, the dune dimensions can be determined. The sensitivity for the variability in four criteria to define a dune is determined. These criteria are:

- minimum dune height (default value: 0.005 m),
- minimum horizontal distance between identified lee-faces (default value: 0.045 m)
- minimum number of points taken into account to constitute a lee face (default value: 6)
- minimum angle of the lee-face slope (default value: 12º)

Friedrich et al. (in press.) show that the dune dimensions determined by bedformer are mainly sensitive to the minimum dune height. An increase in the minimum dune height means that small dunes are not recognized as dunes. This reduces the number of dunes and therefore increases the average dune length and height. Therefore the results (section 3.2) show only graphs with a dependency on minimum dune height. Friedrich et al. (2007) present an alternative method for determining dune dimensions because the discrete method is highly sensitive to this arbitrary minimum dune height that defines a dune (Friedrich et al., 2007).
Dune length, height and steepness during dune development are determined for three different flow strengths and time to equilibrium and other dune characteristics are compared with equilibrium predictors (Appendix 2). Dune geometries over time are also determined for unsteady flood wave conditions.

3.2 Results

Close visual observation and video capturing showed that the initial stages of bed form development from flat bed start with local pile ups of grains. These local pile ups organise within minutes into fairly straight crest lines, perpendicular to the flow direction with a preferred spacing (figure 3.2).

The mean initial spacing for the steady flow experiments (T22-T24) was approximately 0.20 m, which is slightly higher than expected, based on the method of Coleman & Melville (1996):

$$l = \frac{10^{2.5}}{R_{*c}^{0.2}} * d_{50} \text{ in which:} \qquad\qquad R_{*c} = \frac{d_{50}u_{*c}}{\nu} \qquad\qquad\qquad (3.2.1)$$
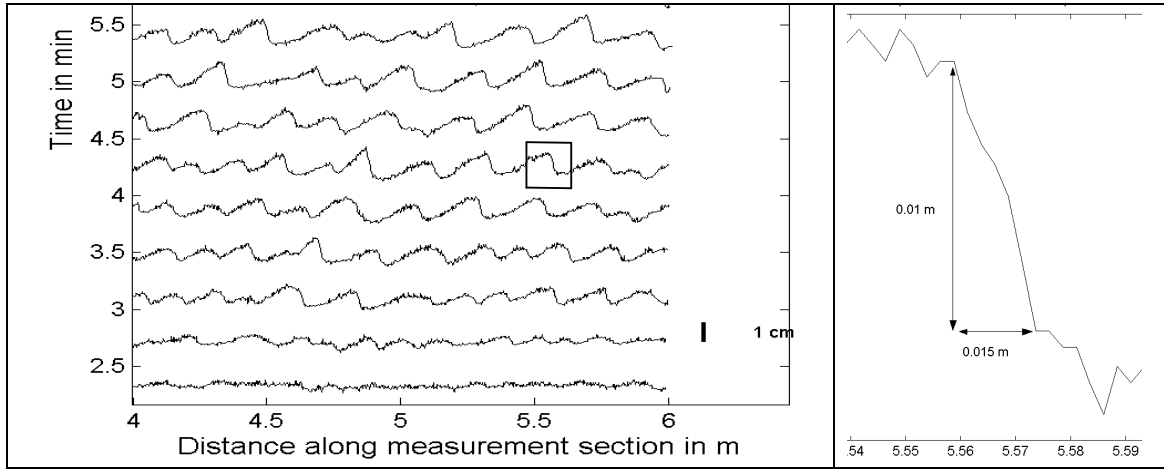
Figure 3.2: Dune initiation for experiment T22, showing a regular pattern of dunes with a spacing of approximately 0.20 m and a maximum lee side angle, equal to the angle of repose (≈ 30º) as seen in the right box.

Coleman & Melville (1996) predict an initial spacing of 0.15 m, based on the grain size and fluid properties. The initial spacing is a function of the critical grain Reynolds number and the mean grain diameter of the sediment (formula 3.2.2)

The critical grain Reynolds number is a function of the median grain size (d_{50}) and the critical shear velocity (u_{*c}). Using the method of Van Rijn (1993) the critical shear velocity can be determined based on the dimensionless grain size D_* and the viscosity and relative density (Δ):

$$D_* = d_{50}\left(\frac{\Delta g}{v^2}\right)^{1/3} \tag{3.2.2}$$

$$\theta_{cr} = 0.013 D_*^{0.29} \quad if \quad 20 < D_* \leq 150 \tag{3.2.3}$$

$$u_{*c} = \sqrt{\theta_{cr}(\Delta g d_{50})} \tag{3.2.4}$$

To determine whether the initial spacing is independent of flow characteristics, the initial spacing of experiment T22-T24 is combined with earlier flume experiments (T2-T8, T11,T13-T15 & T17). The initial spacing has been derived from the bed plots (Appendix 6) by calculating the mean spacing for the first noticeable dunes.

The measured initial spacing shows no correlation with flow parameters (Appendix 7). As expected, discharge (q), waterdepth (H) , bed shear velocity (u_*) and Froude number, do not correlate with the measured initial spacing.

The right box of figure 3.2 shows an important detail. The lee side of initial dunes immediately form an angle of repose. Grains avalanche down the angle of repose lee face of these already asymmetrical short dunes in the early stages of development. This makes the presence of a small separation zone inevitable, because flow can not follow these sharp angles of the bed. Recirculating flow inside the flow separation zone helps maintaining the angle of repose lee side and plays therefore already an essential role in the growth and development of initial dunes.

Dunes grow by trough scouring and lee side deposition, the lee side deposition results in crest accretion as well. Dune growth is observed over the total flume length (Appendix 6)

Subsequently, these small dunes grow and merge into longer and higher dunes as a result of varying migration rates (Appendix 6). Upstream dunes catch up, or merge with downstream dunes and travel downstream together at a migration rate lower than the upstream dune before merging, but not necessarily slower than the downstream dune. Dune height and length grow simultaneously until they eventually reach an equilibrium. The time to equilibrium can be estimated with an empirical formula, based on the median grain size (d_{50}), water depth (H) and the dimensionless shear stress (θ) and shear velocity (u_*) (Coleman et al. (2005):

$$t_e = 2.05 * 10^{-2} (d_{50}/H)^{-3.5} (\theta/\theta_c)^{-1.12} (d_{50}/u_*) \tag{3.2.5}$$

The expected time to equilibrium is given in table 3.3. To determine the observed time to equilibrium for the experiments, the moment where the dunes do not grow in length and height is visually estimated by drawing an imaginary asymptote for the graphs. The time to equilibrium is defined to be the time between the moment that 5% of the equilibrium height is reached until 95% of the equilibrium height is reached. The observed time to equilibrium for the flume experiments is of the same order as predicted by the Coleman et al. (2005) (formula 3.2.5). Based on analysis of figures similar to figure 3.3, the observed dune height and the measured equilibrium length are determined (table 3.4). The observed equilibrium height and length are slightly smaller than expected based on dune length estimators, but given the uncertainty of the method to determine dune length and height, it is in accordance with the expected values (table 3.3 & 3.4). However the trend in the time to equilibrium is different to what was expected. A higher flow strength and larger water depth leads to a shorter time to equilibrium, instead of longer, what was expected based on the method of Coleman et al. (2005)

The conditions of experiment test number 22 resemble the conditions for which the DuDe model has been calibrated and should therefore deliver results comparable to the model outcomes.

Flow Cond	Test Numbers	Flow parameters								
		PUMP setting	b [m]	Q [l/s]	q [m2/s]	H_0 [m]	b/H_0 0	i_0 0	U [m/s]	u_{*1} [m/s]	u_{*2} [m/s]
VII	22	20	0.44	43.74	0.0994	0.1500	2.93	0.0015	0.65	0.047	0.037
II	23	17	0.44	35.94	0.0817	0.1250	3.52	0.0015	0.62	0.043	0.036
IV	24	14	0.44	27.19	0.0618	0.1000	4.40	0.0015	0.58	0.038	0.035

Table 3.1:Flow parameters
(b = flume width, Q = discharge, q = specific discharge, H0 = initial water depth, i0 = initial water surface and bed slope
U = average flow velocity, u* = shear velocity, with u*1=sqrt(g*H0*i0), and u*2=based on ADV measurements (see exp. set up)
Note, for experiment T22,23,24, water depth is changed during experiment, such that w/s slope is equal to bed surface slope)

Flow Cond	Test Numbers	Non-dimensional parameters					
		Fr	Re_gr	Y	Y/Ycr	Us/Usc	Us/Usc from theta
VII	22	0.536	39.93	0.1604	4.64	1.709	2.153
II	23	0.561	36.45	0.1337	3.86	1.671	1.965
IV	24	0.583	32.61	0.1070	3.09	1.600	1.758

Table 3.2: Non dimensional parameters
(Fr = Froude number = U/sqrt(g*H0), Re_gr = grain Reynolds number = u*1*D50/visc, with D50 = average grain size and visc = 1*10^{-6}
Y = theta = Shields number, Us = u*, Usc = u*c = critical shear velocity (based on Shields number))

Flow Cond	Test Numbers	Coleman	Van Rijn (1993)		Julien&Klaassen (1995)		1/3H	6H
		time to eq. [s]	Δeq [m]	Leq [m]	Δeq [m]	Leq [m]	Δeq [m]	Leq [m]
VII	22	4859	0.063	1.095	0.079	0.942	0.050	0.900
II	23	3449	0.052	0.913	0.070	0.785	0.042	0.750
IV	24	2267	0.039	0.730	0.060	0.628	0.033	0.600

Table 3.3: Expected dune characteristics
(Coleman = Coleman et al. (2005), Δ= dune height, L = dune length)

Flow Cond	Test Numbers	Observed dune characteristics				
		time to eq. [s]	Heq [m]	Δeq [m]	Leq [m]	Δ/L eq [-]
VII	22	3000	0.190	0.050	0.75	0.066
II	23	7800	0.160	0.044	0.70	0.066
IV	24	7200	0.130	0.036	0.70	0.051

Table 3.4: Measured dune characteristics

Figure 3.3 shows a stacked plot of bed profiles which show the evolution of dunes from short initial dunes (which already show strong asymmetry) to dynamic equilibrium. Every line in this plot shows the measured bottom profile with a time spacing (in this case 4 minutes). The scale line can be used as a references to estimate dune heights. Dune migration rates can be visualized, because dunes can be tracked downstream, with the crest position on the x-axis and the expired time on the y-axis.

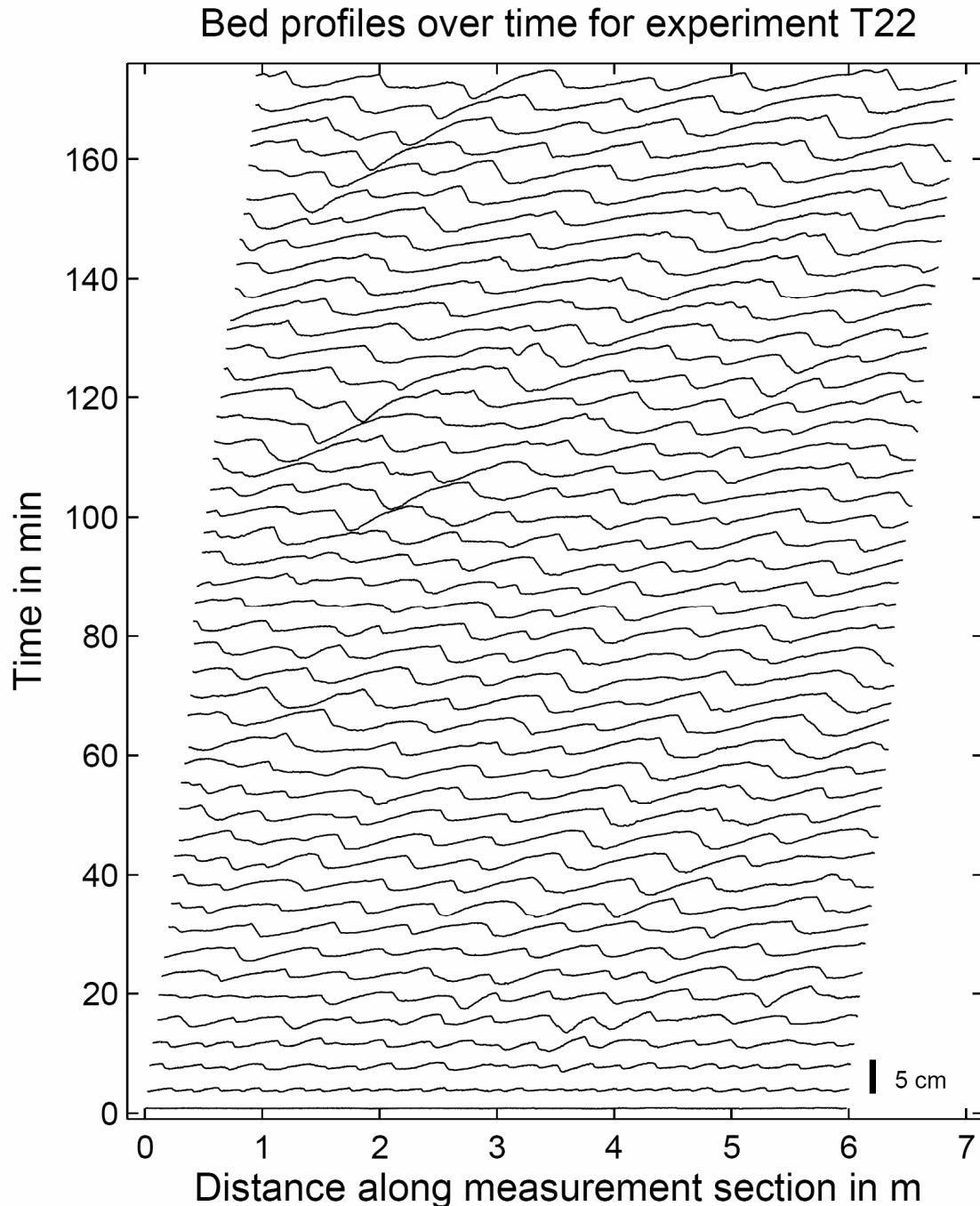## Bed profiles over time for experiment T22

Figure 3.3: Bed profile for experiment T22, see table 3.1 & 3.2 for flow characteristics.

A dynamic equilibrium occurs when two reversible processes occur at the same rate. Merging and splitting are reversible, because they change the mean dune length oppositely. The regular pattern, observed during the first minutes changes after more than an hour in a more dynamic display of dunes where merging and splitting occurs.

Figure 3.4 shows a picture of splitting and merging (See Appendix 8 for more detail). Merging occurs when dunes with different migration rates collide. Splitting is observed on the downstream part of relative long stoss sides (>1.20 m), when superposed wavelets occur on the upper half of the stoss side.
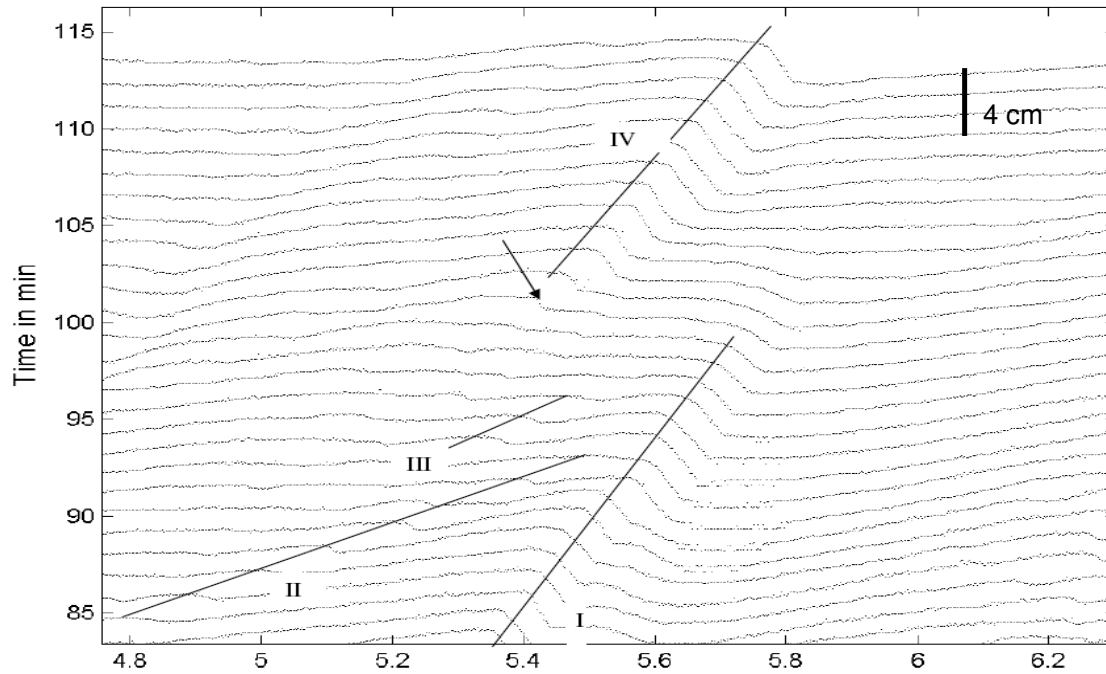
Figure 3.4: Superposed wavelets split the stoss side of a big dune (Appendix 8).

The sediment transport changes at that location from Type I transport, which is standard bed load transport into Type II transport, which is transport of sediment by superposed wavelets that migrate until they reach the crest of the underlying dune, thereby filling the lee side of the underlying dune (figure 3.5). This type II transport continues until one of the superposed wavelets grows in height and slows down and forms a flow separation zone with recirculating flow itself. Appendix 8 shows that a superposed wavelet can decrease the sand supply to the crest of the underlying dune thereby, scouring the crest of the underlying dune. This results ultimately in shorter dunes and in combination with merging leads to equilibrium length and height.
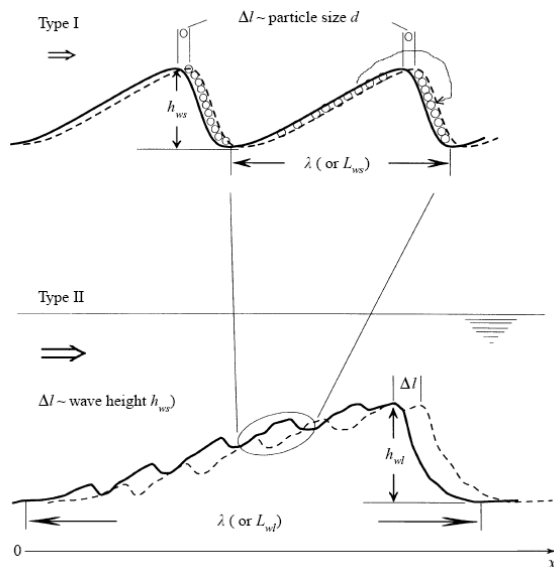

Figure 3.5 Two types of sand wave movement (Nikora et al. 1997)

Dune length and height grow exponentially at the same pace, resulting in a constant steepness during dune growth (figure 3.6). See Appendix 6 for the bed profiles of experiment T23 and T24. The observed equilibrium dune dimensions are obtained by estimating the asymptote for the dune

dimension plots (figure 3.5). The three lines show that dune dimensions depend on the definition of dune. When dunes smaller than 0.025 m are filtered out, obviously the number of dunes is smaller than for a threshold dune height of 0.005. This results consequently in higher mean dune lengths and heights because the smallest (lower and shorter) are filtered out. The mean dune dimensions agree nevertheless with the expected dune dimensions as seen in table 3.3 and 3.4.
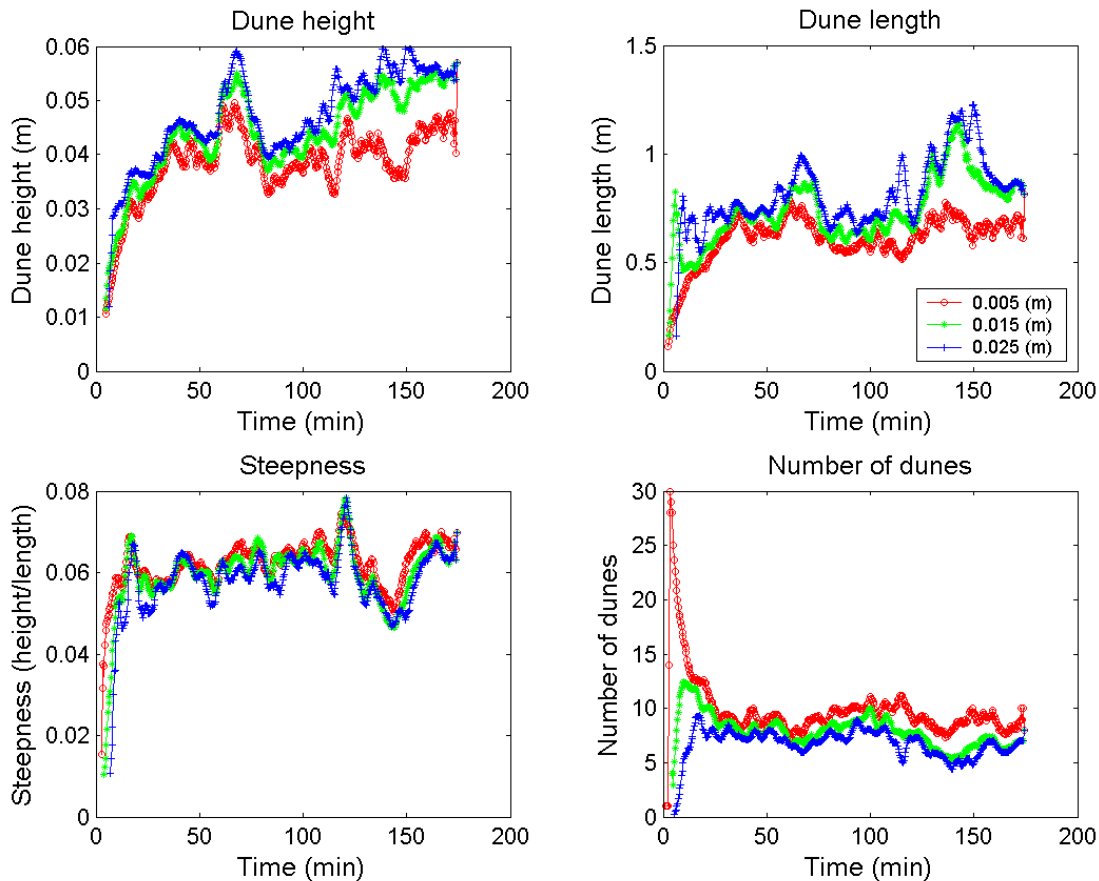

Figure 3.6: Dune dimensions (height, length, steepness and number of dunes) during dune development (T22, flow depth 150 mm d₅₀ = 0.85 mm) for different minimum dune heights (red = 0.005, green = 0.015 and blue = 0.025)

Dune length is not constant during the various stages of dune development, but increases over time. As a result of dune development, roughness of the bed increases. Because the discharge is kept at a constant value, water levels increase during dune growth. This effect can be seen in figure 3.7.
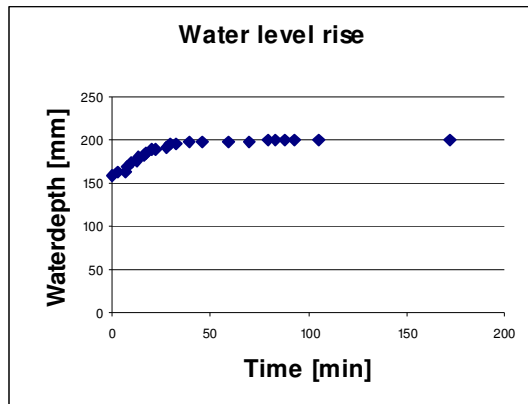

Figure 3.7: Water depth increase during dune growth

Starting with a water depth of 0.15 m, the water depth increases to an equilibrium value of 0.20 m. Dune heights stabilize at a value of 0.05 m (figure 3.6) with a dune length of 0.75 m, resulting in an aspect ratio, or steepness(Δ/L) of 1/17. The corresponding water level rise is 5 cm which is an increase of 30%.

3.3 Possible dune splitting mechanisms

The observation of equilibrium dune dimensions experiments show a dynamic equilibrium because splitting and merging both take place. The cause for dune splitting is not obvious, but the observations have lead to possible dune splitting mechanisms:

Random pile ups by turbulence bursting

Turbulent bursting is observed to create pile-ups superimposed on stoss sides. These pile-ups can develop into small dunes and develop a lee side. It is unknown why some disturbances survive and other disappear almost instantaneous. They migrate at high celerities in downstream direction, filling the lee side of the underlying dune or creating their own flow separation zone. The random initiation of superimposed wavelets seems to be one of the main mechanism for dune splitting

Suspended sediment transport

Suspended sediment transport over a crest is observed during the experiments. In contrast to the DuDe model, this means that not all sediment is used to migrate the lee side. A part of the sediment is deposited on the stoss side of a downstream dune. This effect is stronger when dunes become higher. This could be a trigger for new dune initiation and therewith for dune splitting.

HIGHLIGHTS Chapter 3: Flume experiments

- Flume experiments show the existence of a dynamic equilibrium where dunes split and merge continuously.

- During the initiation of dunes, asymmetry and flow separation appear within the first minute of dune development from flat bed.

- Superposed sand wavelets split long stoss sides (>1.20m) and decrease the migration rate of underlying dunes.

- Random initiation as a result of turbulence bursting and the deposition of suspended sediment on downstream stoss sides leads to the development of sand wavelets.

---

4   Implementing dune splitting

Section 2.4 shows the output of model simulations performed with the DuDe model to investigate the current behaviour of the model. The initial behaviour differs from the observed initial behaviour in the experiments. Dunes grow and migrate as a result of the coupled system of flow equations and sediment transport formula. The migration rate of dunes in the DuDe model corresponds to the values found during the experiments ($\approx$4mhour^{-1}). Dunes become asymmetric as observed during the experiments (chapter 3). Asymmetry development differs slightly because, in the model it seems to occur as a non-linear effect of the acceleration of water flow over the dunes. This is in contrast to the flume experiments where asymmetry is observed instantaneous.
The presence of merging dunes with varying celerities as observed in model simulations is confirmed by the flume experiments. Dunes overtake and migrate together at a lower celerity. The reason for dune lengths to grow infinite in the model simulations is the lack of a splitting mechanism in the DuDe model. Equilibrium dimensions perceived during the experiments which can be estimated by equilibrium predictors are not observed during model simulations. This chapter will evaluate the model behaviour and

4.1 Model behaviour

Influence of periodic boundaries

To investigate whether the non-linear effect of parameterization of flow separation causes continuous merging of dunes, and therefore prevents dunes from splitting or reaching equilibrium dimensions, model simulations have been conducted without the parameterization of flow separation. These model simulations show interesting results. Figure 4.1 shows that even without the occurrence of a flow separation zone large dunes do overtake or dissolve smaller dunes.
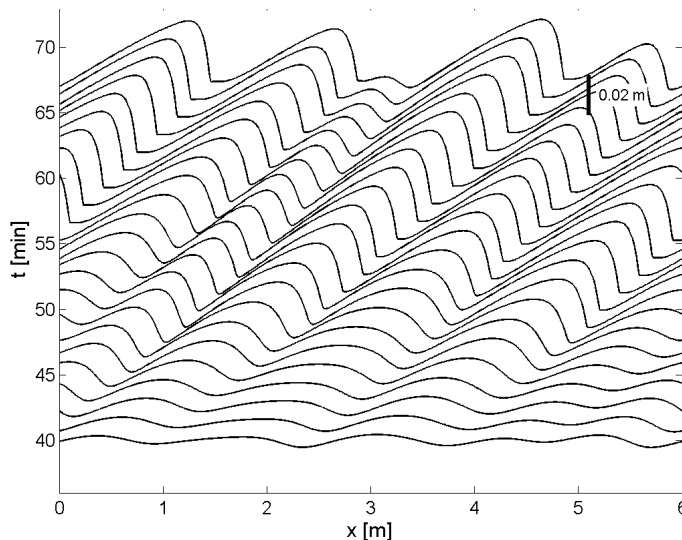

Figure 4.1: Periodic boundaries causing dunes to merge.

The dune that "enters" the domain around the 45th minute completely fades away in the shadow of the upstream dune. When we track this dune back to t = 40 minutes, the dune height and length of the overtaking dune are both smaller than the dune that becomes overtaken. So, dune height and length are not the explanation for this behaviour.
A few minutes later the overtaking of dunes during the absence of parameterization of flow separation becomes even more obvious. Only three dunes remain after 80 minutes.
This process would have continued if the model has not become unstable after this moment, due to numerical difficulties. The chosen periodic boundaries of this model have an impact on the prediction of equilibrium dimensions. The periodic boundaries limit the possibilities of dunes to grow in length without merging. Besides that, these boundaries are responsible for the existence of a false equilibrium, perceived when the dune length reaches the length of the domain.

'False' equilibrium

Paarlberg et al. (2006) describe that after sufficiently long time the dune height stabilizes and dunes do not grow, but only migrate. They refer to this phenomenon as a dynamic equilibrium. However, this equilibrium does not contain dynamics as observed in equilibrium during flume experiments. An equilibrium perceived during flume experiments or field studies is dynamic because dunes merge, split, overtake and dissolve, while the mean dimensions remain fairly constant.
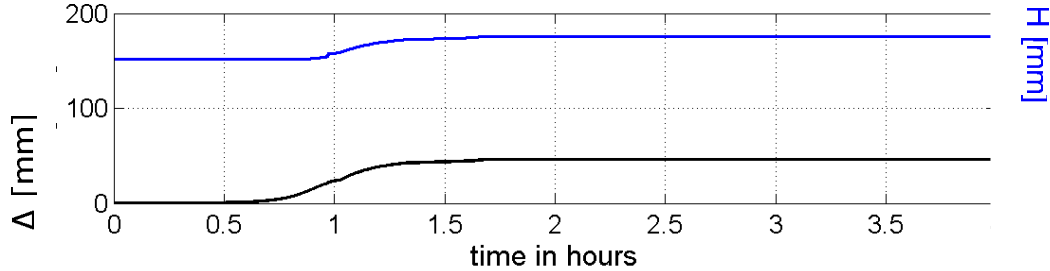

Figure 4.2: Development of a false equilibrium (H=0.15 d_{50} = 0.85*10^{-3})

Model simulations lead to an equilibrium dune height after a sufficiently long time (figure 4.2). The dune height stabilizes and the water level elevation as a result of increased roughness also reaches an equilibrium. This result is in accordance with the outcomes of the dune experiments described in section 3.2, where a water level rise of 30% is perceived, shown in figure 2.4. The modelled equilibrium however, has a different cause. A visualization of the equilibrium state of this model simulation (Figure 4.3) shows that it is a rather static equilibrium. The equilibrium length is forced by the length of the domain with periodic boundaries. The equilibrium height is observed, because dune length and height are interrelated. The dune length reaches a maximum *(L = 1 m).* The dune height will not grow to infinity but also reaches an equilibrium *(Δ = 0.046 m)* when the dune length reaches the length of the periodic model domain.
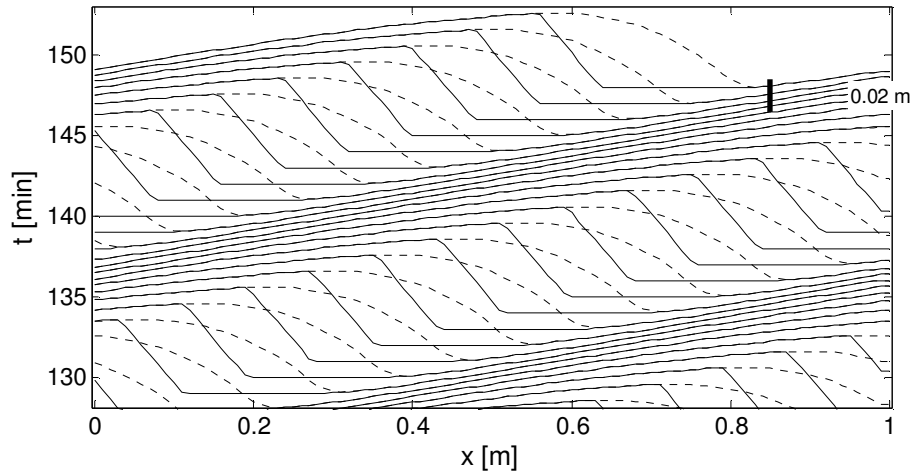

Figure 4.3: A dune has reached maximum dimensions for this domain length

The expected aspect ratio (Δ/L) based on the method of Van Rijn (1993), varies between 0.04 and 0.06 (1/25 - 1/17), for Julien & Klaassen (1995) this ratio varies between 0.085 and 0.095 (1/12 - 1/10). The model is therefore, with an equilibrium aspect ratio (Δ/L = 1/22) in reasonable agreement with these predictors.
The modelled height, however, does not reach an equilibrium as a result of a physical balance, but is limited by the periodic boundaries.
This makes the equilibrium dimensions highly dependent of the chosen domain length. The aspect ratio as predicted by the DuDe model is not constant. The equilibrium height of dunes is, given the absence of a splitting mechanism, only limited by the domain length.
Figure 4.4 shows the influence of the domain length on the equilibrium dune height predicted by the DuDe model.

19/06/2007   Modelling river dune splitting
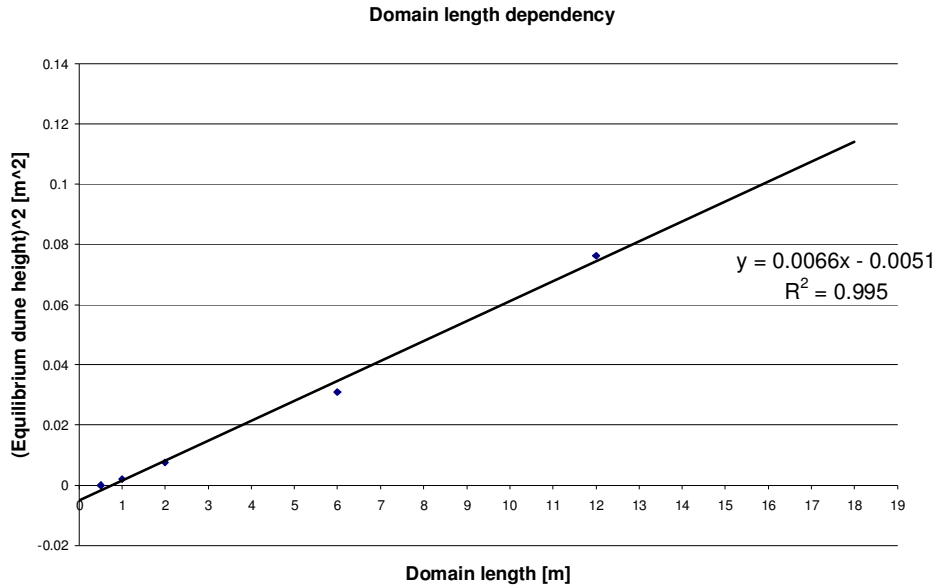
Domain length dependency

Figure 4.4: 'False equilibrium'; Equilibrium dimensions are a function of the chosen domain length

The predicted equilibrium height of a dune can be described as a function of the domain length.
$\Delta = (0.0066\Lambda - 0.0051)^{1/2}$ (Δ = equilibrium height [m], Λ = domain length [m]).
More important however is the clear depency of the domain length. Because this limits the applicability of the model for larger domains. This leads to the first attempt to the improve the model by inducing splitting by a random disturbance.

4.2 Random disturbance

As described by Leclair (2002) new dunes initially grow by accretion of sediment. After the formation of a new dune, the underlying (parent) dune could develop, but destruction is very common (as decaying dune). Close observation and movie capturing during experiments in New Zealand (section 3.3 and Appendix 8) show that dunes initiate on long stoss sides in the same manner as they do from flat bed. However, dune initiation from flat bed is a result of the interaction of the flow and sediment equations. This, however, cannot take place from a theoretical perfect flat bed. Initially this model needs bed gradients ($h_x \neq 0$). The initiation of new/superposed dunes also needs an irregularity in the bed profile. The type of disturbance and the results of these model changes are described in this section.
As a result of the simplified flow equations, random pile ups of grains or turbulence bursts do not occur in the model simulations. Raudkivi (2006) states that, the knowledge of these flow structures is still insufficient to enable rigorous analytical modelling of the processes at the sand-water interface. Therefore the attempt is made to initiate new dunes by introducing a random disturbance signal every 10th time step, to imitate the influence of turbulent flow structures on the bed. The random signal is applied under the condition that no flow separation was present to avoid numerical difficulties in determining the parameterized bed over a disturbed bed. The maximum value of this disturbance was set to two grain diameters ($2*d_{50}$). The spacing (Δx) has the same value as the spacing in the calculation ($\Delta x = 0.01m$) As seen in figure 4.1 the disturbance is added every 10th time step. When the frequency of the disturbance is increased (e.g. every time step) dune development depends too strong on the disturbance. The bed then becomes an accumulation of disturbances instead of an outcome of the model equations.
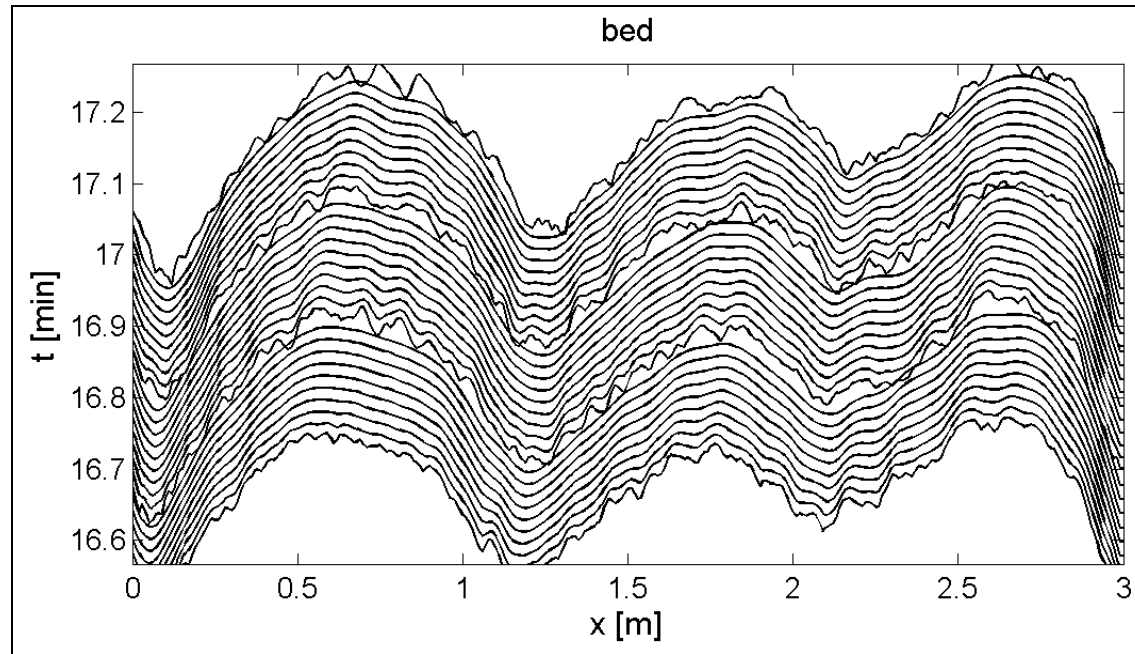
4 IMPLEMENTING DUNE SPLITTING   37

Figure 4.5 Diffusion of the superposed signal

Figure 4.5 shows the strong diffusion of the applied disturbance and growth of the applied disturbance or scouring of the underlying dune is not perceived. This rises the question whether a domain-filling random disturbance can initiate new dunes. For a random signal to grow and develop into a new dune on top of the parent dune, a wavelength smaller than the wavelength of the parent dune has to show growth. To investigate whether a wavelength exists that grows given the physics incorporated in the model a simple numerical stability analysis is performed.

Several attempts to implement a continuous disturbance did not lead to growth of superposed bed forms, let alone the splitting of long dunes. The success of new dune initiation as a mechanism to inhibit the dune length growth in the DuDe model depends on the possibility of these new dunes to develop. In order to obtain a successful splitting mechanism, growth of new dunes has to be supported by the initial behaviour of the model. Therefore a stability analysis is conducted to examine the growth of superposed bed forms with various wavelengths on top of an existing bed profile (Appendix 9).
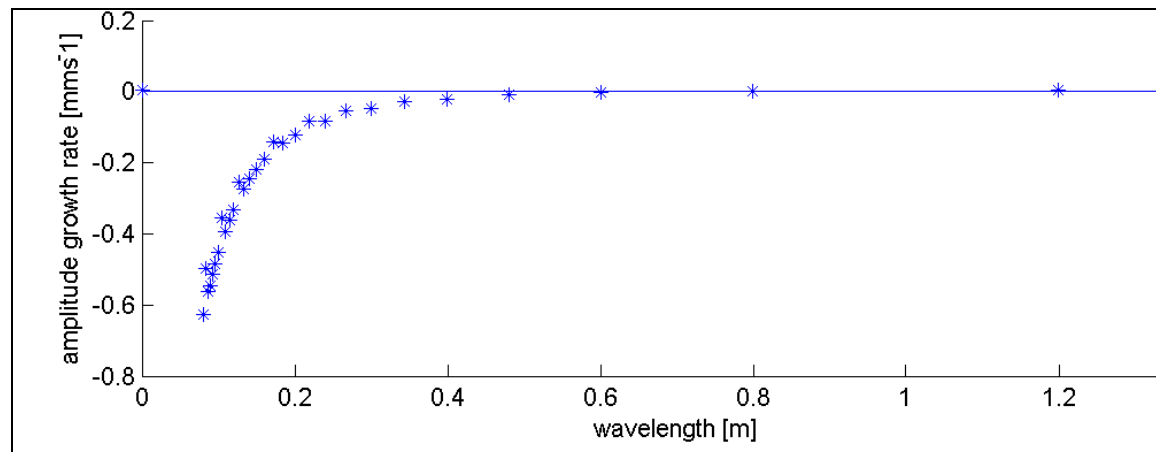

Figure 4.6: Numerical stability analysis for sinusoidal bed disturbances with differing wavelengths

This stability plot (figure 4.6) shows negative growth for superposed bed features with wavelengths smaller than 80 cm. This implies that the method of initiation of dune splitting by disturbing the bed under the given model settings is not promising.

4.3 Stabilizing effect of slope terms

The stability analysis for the current model settings has lead to the conclusion that the fastest growing wavelength is in accordance with the equilibrium predictors but differs from the initial dunes observed during the flume experiments. New dunes do not grow, because only large dunes perceive growth. The model contains several parameters that can influence the fastest growing wavelength and therefore can change the possible success of a random disturbance on the equilibrium dune dimensions. Two of these parameters are the slope terms λ_1 and λ_2. The growth of river dunes is said to be driven by the phase lag between the bed configuration and the bed shear stress. The slope effects as described in section 2.2 have an important role in the stability of a certain wavelength. To investigate whether the slope terms, influence the fastest growing wavelength, the stability analysis conducted in the previous section is repeated for different slope parameters.

The bed slope parameters λ_1 and λ_2 change the local flux based on the bed gradient. The only model parameter that could be changed to investigate the sensitivity of the model to these parameters is the angle of repose ϕ_s.

$$q_s = \alpha(\tau_b - \lambda_1 \tau_{cr,0})^\beta \lambda_2 \qquad \lambda_1 = \frac{1 + h_x / \tan \phi_s}{\sqrt{1 + (h_x)^2}}$$

$$\tau_{cr,0} = \theta_{cr} g \Delta d_{50} \qquad \lambda_2 = \frac{1}{1 + h_x / \tan \phi_s}$$

$$(4.3.1)$$

ϕ_s changes both slope effects. An increase of the angle of repose makes that the indirect slope effect λ_1 increases the influence of the local bed slope (h_x) . This should result in steeper and therefore shorter wavelengths. λ_2 has a direct influence on the local flux and with a larger value for ϕ_s increasingly increases the flux downslope and decreases the sediment flux upslope.

These qualitative hypotheses are also seen in the numerical stability analyses. The next page shows the stability plots for several values ϕ_s. See table 4.1 for the corresponding lambda value.

Angle of repose (ϕ_s)	1 / (tan ϕ_s)
30	1.73
31.5	1.63
45	1
63	0.5
90	0

Table 4.1: Conversion table

The influence of these slope parameters is clear (figure 4.7). The fastest growing mode for an angle of repose of 63º, is approximately 0.3 m, in contrast to 1.2 m for a natural angle of repose. However, this is not a realistic value for the angle of repose, which ranges naturally between 25º and 35º depending on sediment properties (Simons, 1957 in: Chang,, 1988). Model simulations with the sediment transport formula using ϕ_s =63º show that, despite the smaller fastest growing mode, dunes merge (Appendix 10). Initially they grow faster and steeper. After 15 minutes, dunes start to merge and the wavelength and wave height increase. The steepness or aspect ratio (H/L) is much bigger (1/10) compared to the situation with an angle of repose of 30º (approx. 1/40). The slope terms have influence on both the initial behavior of bed evolution and influence the aspect ratio of bed forms, but do not influence the overall pattern of merging dunes. regardless of the fastest growing wavelength, dunes merge when flow separation is parameterized. Without the inhibition of the migration rate of high and long dunes, or incorporation of dune splitting, it is not possible to simulate dune development obtaining an equilibrium dune length.
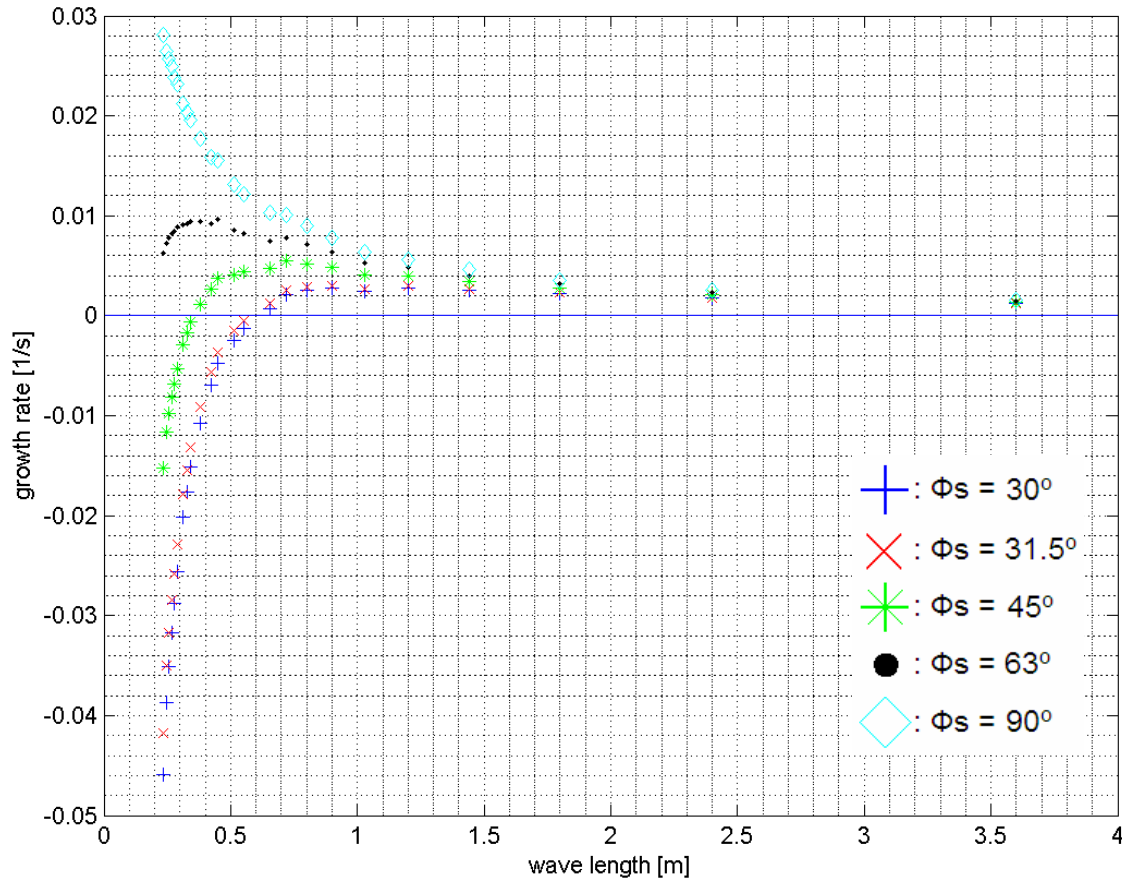
Figure 4.7: Growth rate plots for superposed disturbances with an angle of repose of: 30º, 31.5º, 45º, 63º and 90º

4.4 Superposed wavelets

Next to the ability to grow, the migration rate of dunes is critical in the search for a dynamic equilibrium. As seen in the early model simulations in section 2.4 (figure 2.7), larger dunes migrate faster and overtake smaller dunes as a result of a higher flux due to acceleration of flow over the dune crests. This, however is in contrast to what is assumed by (Exner, 1920).
The migration rate of dunes can roughly be described as the sediment flux over the crest of the dune divided by the height of the dune:

$$c = q_c / \Delta \tag{4.4.1}$$

The assumption of a constant sediment flux would imply that dunes migrate with celerities inversely proportional to their heights (Exner, 1920). But this assumption is false. Sediment flux is a function of bed shear stress and this depends on the present flow conditions and mainly depends on the local bed elevation. Flow accelerates over a dune crest, resulting in a higher shear stress at the bed. Larger dunes (both in length and in height), therefore, can only migrate faster than smaller dunes when the flux over the crest of a dune divided by the height of the dune is bigger than that of the smaller dune. This is an important nuance difference. The possibility of smaller dunes to migrate faster than large dunes opens the possibility for a dynamic equilibrium without larger dunes overtaking the small.
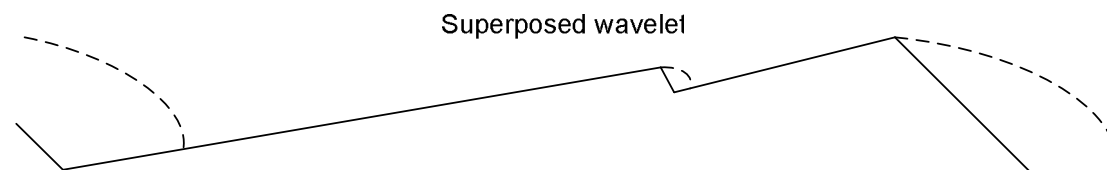

Figure 4.8: Schematisation of a superposed sand wavelet with flow separation

The survival of superposed sand wavelets is possible and could inhibit dune growth. Superposed sand wavelets experience a relative high shear stress compared to their height, because they are located higher in the water column and should therefore migrate much faster than the dunes on which they are located. These superposed bed forms are responsible for deceleration or even ceased migration of the bigger underlying dune, as seen in figure 3.4.

Namely, the arrow in figure 3.4 shows a dune with a developed angle of repose that grows out to be the crest of the dune upon which it was superposed. Earlier superposed wavelets (II & III) did not break down the underlying dune, but transported sediment to the dune crest. The absence of flow separation behind the disturbances during the model simulations described in section 4.2 is found to be the reason for the negative growth of these small features. The analysis of the growing wavelength (section 4.2) shows that superposed lumps with a short wavelength will dissolve, because of their negative growth rate. When flow separation occurs behind the superposed sand wavelets all sediment transported over its crest is deposited behind the crest. This assures that they do not dissolve/diffuse. The flume experiments give reason to believe that early flow separation, when bed features are several grain sizes in height is a natural phenomenon. The observed asymmetry of the initial bed forms is high and visual observations reported also the built up of an angle of repose lee side from the start of dune development (section 3.2).

Superposed bed features are observed in numerous flume and field experiments, an extensive reference of superposed bed forms is found in Venditti et al. (2005)

Despite classification difficulties, the existence of these features is not challenged. Venditti et al. (2005) give a detailed description of, what they call, sand sheets: "Over equilibrium dunes, three to four sand sheets were observed per 100s. Sheet thickness was 10% of the height of the dune upon which they where superposed; they migrated at 8 to 10 times the dune rate; they had nearly constant lengths over the full range of dune lengths and flow conditions and they had aspect ratios of approximately 1:40." They resemble the features that we call wavelets.

Besides the shape of these so called sand sheets, the location where they occur is important. Development of the sand sheets, observed by Venditti et al. (2005) appeared to be related to a minimum distance from the crest of the upstream dune. Not the distance to the downstream dune shows to be important, but the distance from the crest of the upstream dune (x_{rear}). Logically the sheets form downstream of the flow reattachment point of the upstream dune. A value of 0.5m for x_{rear} is necessary for the sheets to form (Venditti et al., 2005). Furthermore, when the underlying dune has a wavelength L in the range [0.5 – 1], $x_{rear} \approx 3 L_{st}$ (L_{st} is the length of the separation zone).

The fact that these superposed features develop a certain distance downstream of the flow re-attachment point is linked to the regrowing internal boundary layer, and increasing shear stress downstream of the flow reattachment point. Direct downstream of the flow reattachment point the bed shear stress does not exceed the threshold for sediment movement.
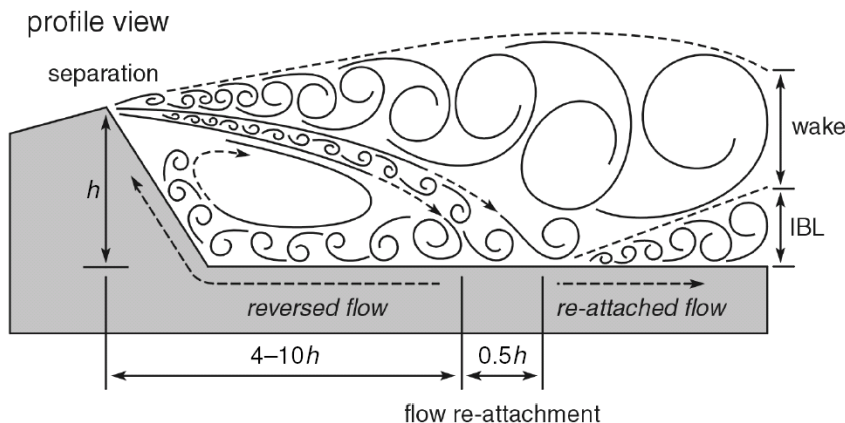

Figure 4.9: Flow reattachment and development of the internal boundary layer (IBL). [Walker & Nickling, 2002]

The internal boundary layer (IBL) regrows, in the same way as the boundary over a flat bed develops, therefore a long stoss side acts like a flat bed. New dunes or wavelets occur in a similar way as initiation from flat bed. To test the hypothesis of faster migration of superposed wavelets, a model simulation over a created profile is performed. The initial bed consists of a dune on which the wavelet is superposed. The profile has a wavelength of 1m, an aspect ratio of 1/40, a dune height of approximately 0.045m and an angle of repose of -30 º. The crest of the superposed sheet has the same bed elevation as the crest of the dune upon which it is located. The height of

the superposed dune itself is 0.015 cm. According to the formula of Exner (formula 4.4.1) the celerity of the superposed feature should be three times the celerity of the underlying dune, because the bed shear stress and therewith the flux at the crest of the superposed feature is equal to the bed shear stress and flux at the crest of the underlying dune and the dune height is approximately three times smaller.

A model simulation has been performed with the initial bed configuration as seen in figure 4.10.
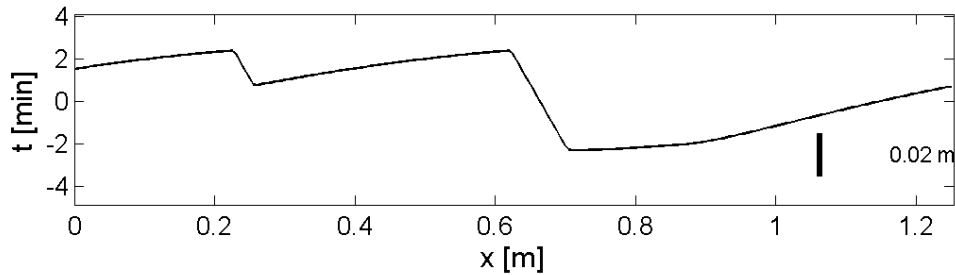

Figure 4.10: Initial bed configuration to test the effect of a superposed dune.

to obtain knowledge on the possible 'stabilizing' effect of superposed bed forms on the wavelength of underlying dunes.
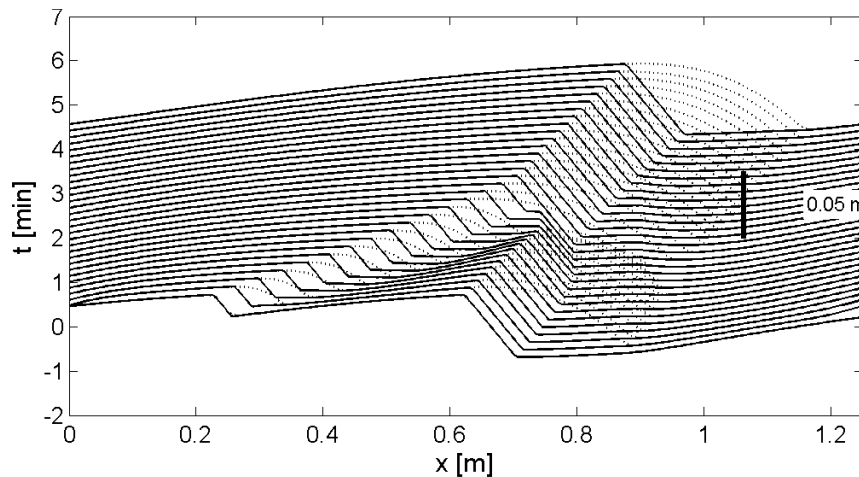

Figure 4.11 Upstream movement of a dune crest subject to superposition.

Figure 4.11 shows the results of this model simulation. The crest of the underlying dune has moved upstream as a result of overtaking process of the superposed bed feature in a similar way as seen during flume experiments (figure 3.4).

The superposed bed form approaches the underlying dune crest at a celerity which is, as expected, three times the celerity at which the underlying dune traverses downstream
(9 mhour^{-1} instead of 3 mhour^{-1}). Just before the two crests merge, the flow separation zone of the superposed bed form overtakes the underlying flow separation zone, which means that the migration of the underlying dune holds. There is no flux inside the flow separation zone and all sediment is used to migrate the superposed feature until the two dunes merge and migrate as one. The decelerating effect of superposed bed forms on the migration of dunes is hereby shown. The next step is to implement superposition as a process into the existing DuDe model. This subject is dealt with in the next section.

4.5 Continuous application of dune splitting.

The finite applicability of the DuDe model and the positive result of the exploration of a superposed wavelet opens the way for a new parameterization. Since dune merging is an effect that occurs with various model settings and in at a, for river dune modelling, relative short timescale, a parameterization of splitting is the only solution to extend the applicability of the DuDe model.

The choice of the form of the superposed sand wavelet is based on five criteria:
- Relative small height in respect to the underlying dune
- Angle of repose to assure flow separation behind the crest
- No net sediment accretion or erosion to assure sediment continuity
- Smooth connection to the existing bottom to prevent numerical difficulties
- Applied on the upper half of the stoss side of long dunes, as observed

To match these criteria, a double triangle as seen in figure 4.13 is developed.
Because the wavelet is modelled as a double triangle, both above and under the bed level of the stoss side on which it is superposed, sediment continuity is guaranteed.
The lee side has an angle of repose and the head and tail of the disturbance smoothly connect to the original bed. It ranges from the reattachment point of the upstream dune to the crest of the downstream dune to make sure it migrates over the upper half of the stoss side.
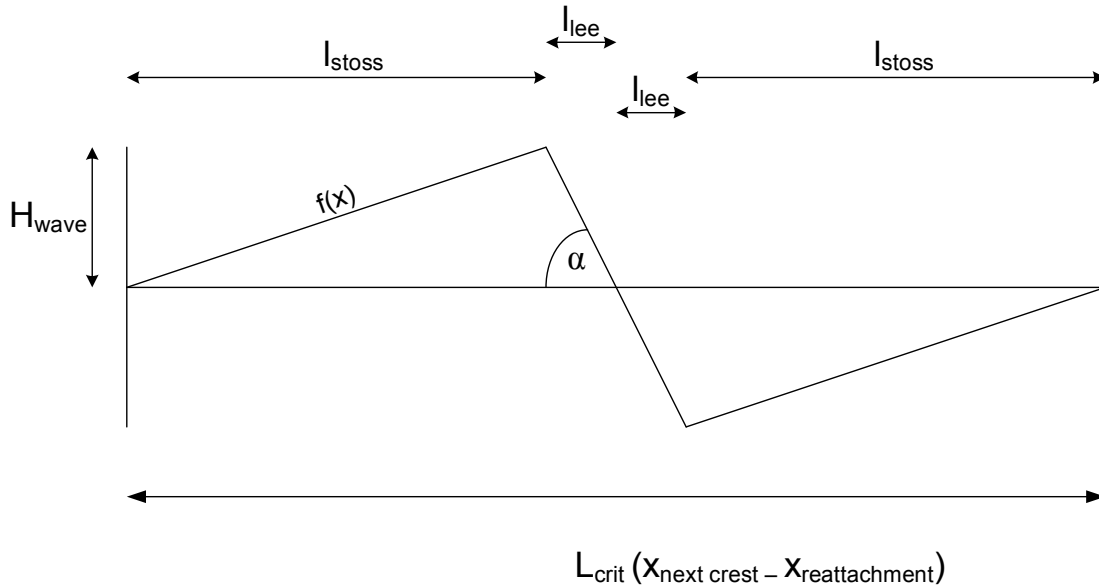

Figure 4.13 Schematization of the superposed wavelet

The wavelet is superposed when the length of a stoss side exceeds a critical length of the stoss-side L_{crit} (L_{crit} = $x_{next\ crest}$ - $x_{reattachment}$; i.e. the distance between the reattachment point of the upstream dune and the crest of the downstream dune)
The value of L_{crit} is set at 1.0 m and is based on the stability analysis and the results of the experiments where superposed wavelets occurred. This critical length is determined so that when it is split in half the wavelet has the minimal wavelength for which growth is perceived based on the numerical stability analysis (0.5 m, see figure 4.4). The experiments show superposed wavelets on dunes with dune lengths ranging from 1 m to 1.4 m.
The wavelet is created with a predetermined height (H_{wave}) and an angle of repose (α = -30º) for the skewness of the wavelet's lee side. H_{wave} is initially set to 6 mm to create a substantial flow separation zone. The numerical implementation of the wavelet is described in Appendix 11.

4.6 Results of the implementation of dune splitting

Model simulations of the superposed wavelets (figure 4.13) show the effect of upstream movement of the dune crest. When the dune length exceeds the critical length L_{crit} a wavelet is superposed. It grows instantaneously until it reaches the crest of the underlying dune. When it reaches this crest it limits the sediment transport to the crest. The underlying crest slows down and dissolves, when the flow separation zone of the superposed dune grows and overtakes the dune crest of the underlying dune.
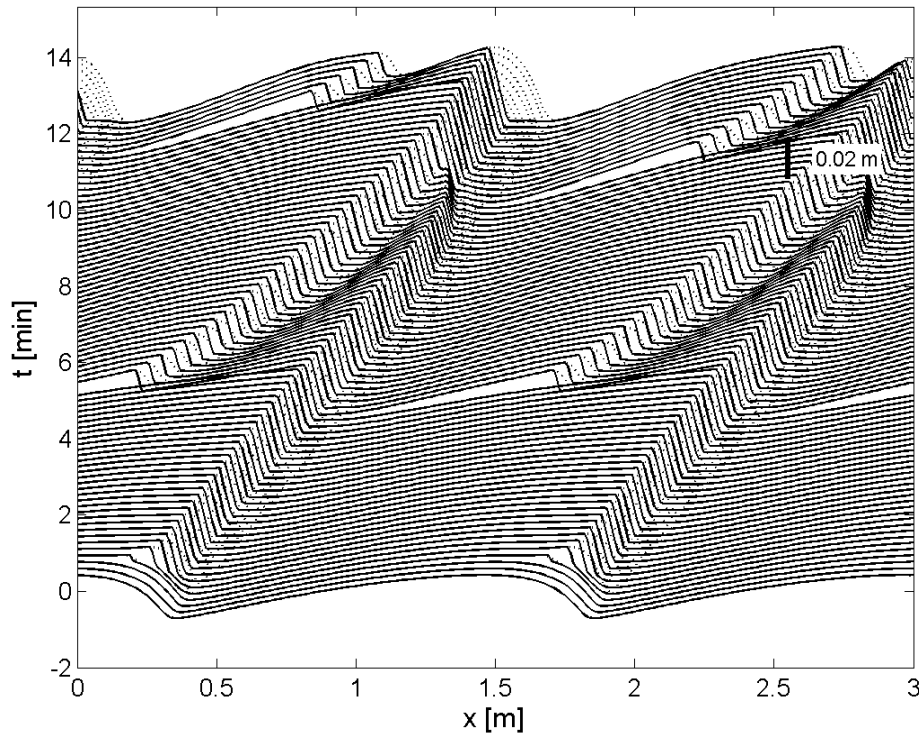

Figure 4.13 Superposed wavelets decreasing the migration of underlying dunes

A superposed wavelet has the ability to place the dune crest of the underlying dune upstream. When the superposed wavelet has overtaken the dune completely and a stoss side becomes too long again, the process repeats itself.

Model simulations over a longer time are performed with the following conditions:

- Domain length = 4m
- H_{wave} = 0.006m
- L_{crit} = 1.0m
- Npx = 400
- Npz = 15

The results of this simulation are analyzed with the *bedformer* software tool (section 2.2). Dune height, length, steepness and number of dunes are standard output. The migration rate is added in the fourth plot. The threshold dune height for *bedformer* is set to 0.1 mm, to make sure that all dunes are distinguished. Because the DuDe model always delivers a smooth signal, this threshold value will not lead to an overestimation of the number of dunes and an underestimation of the dune length or height.
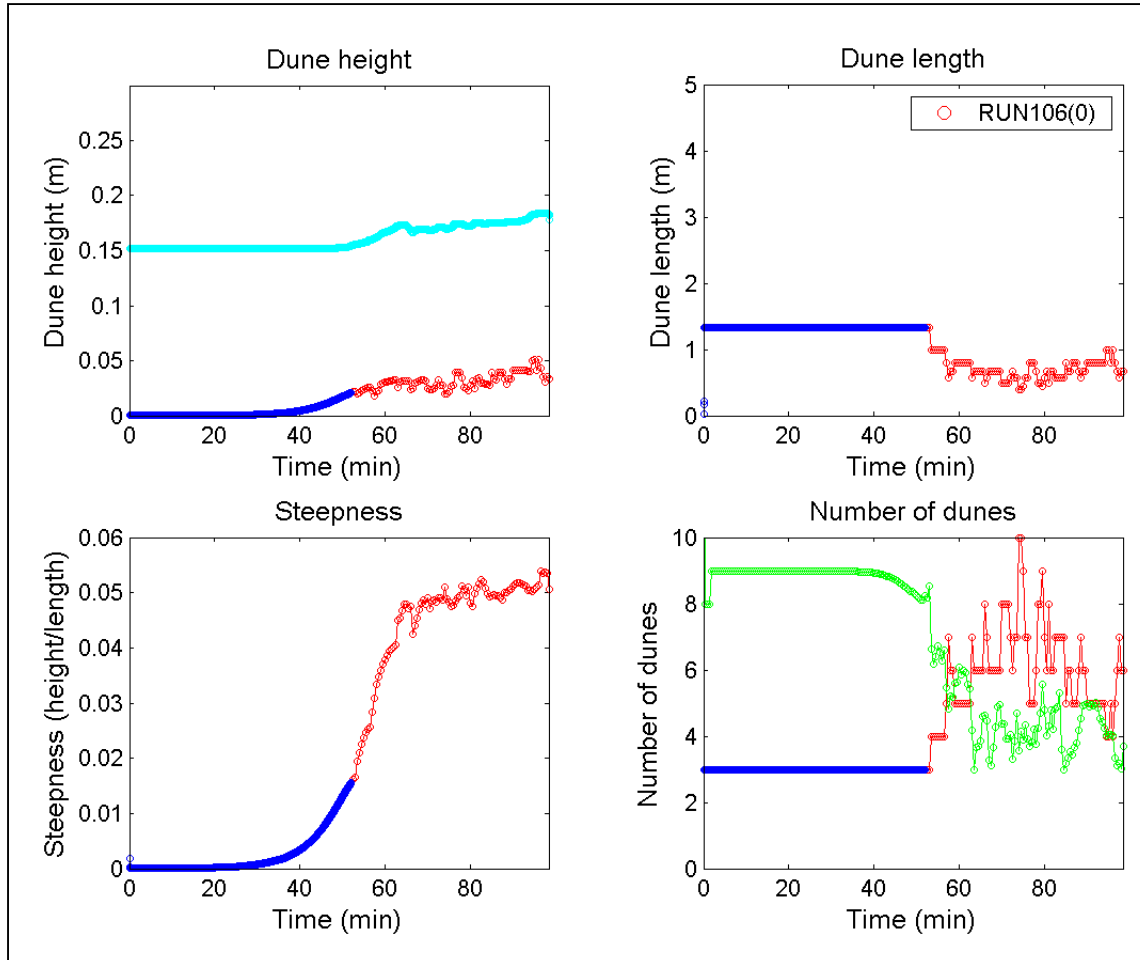

Figure 4.14 Dune dimension predicted by the improved DuDe model a) Dune height and water depth b) Dune length c) Steepness/aspect ratio d) Number of dunes and migration rate
(**Blue** = dependent variable, no parameterization of flow separation. Red = dependent variable, flow separation is parameterized Turquoise = Mean water depth (H), Green = migration rate based on Fourier analysis[m/hour].)

When the improved DuDe model is used to predict dune dimensions for dune development from flat bed using a random disturbed initial bed profile, dune dimensions reach an equilibrium. As seen in figure 4.14:

- equilibrium dune height is approximately 0.04 m,
- dune length is 0.7 m
- with an aspect ratio of 1/20
- water level rise due to increased roughness is 0.03 m (18%)
- time to equilibrium is 70 minutes
- migration rate is approximately $4mhour^{-1}$

The plot of the bed evolution shows that dune merging and splitting occur as expected based on the experiments described in chapter 2. The superposed wavelets migrate at a higher celerity than the underlying dune as expected and decrease the migration of the long dunes. This behaviour of the model extends the applicability of the improved DuDe model and proves that a mechanism of splitting is indeed responsible and therefore needed for a continuous dune development model.
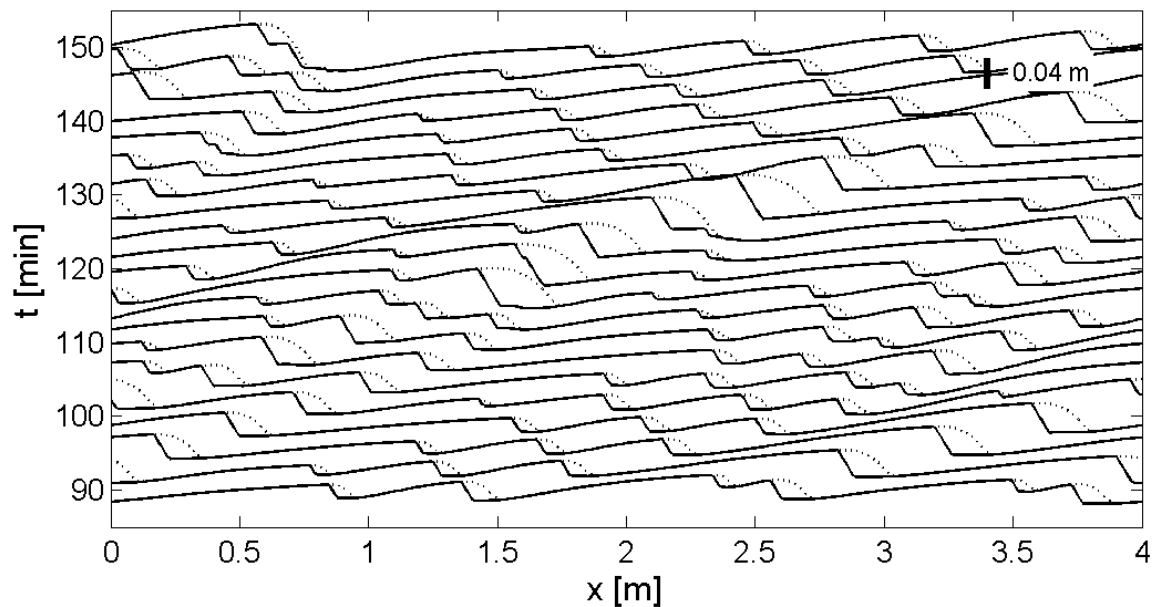

Figure 4.15: Dune evolution with superposed wavelets initiating on the stoss sides of long dunes in a dynamic equilibrium (L_{crit} = 0.100m ; H_{wave}= 0.006 m).

Equilibrium dune dimensions are reached and a dynamic equilibrium with splitting and merging of dunes is observed (figure 4.14 & 4.15). Dune with different heights are seen and the display of dunes with average lengths of 0.7 m forms much more resembles the observed behaviour in figure 3.3. This increased dynamics is promising for future applicability of the model.

4.7 Evaluation of equilibrium characteristics

By implementing superposed wavelets the migration rate of big dunes has decreased and long stoss sides are split in two when they exceed the critical length (L_{crit}). This implementation extends the applicability of the DuDe model. The next model simulations show the behaviour of the DuDe model without without splitting, the improved model (DuDe +) and the experiments T22.
The conditions of the model simulations have been matched with the experimental conditions. These conditions can be found in table 5.1.

Flow and sediment characteristics	DuDe	DuDe +	Experiment (T22)
Waterdepth (H) [m]	0.150 m	0.150 m	0.150 m
Grain size (d_{50}) [m]	$0.85 * 10^{-3}$ m	$0.85 * 10^{-3}$ m	$0.85*10^{-3}$ m
Bed slope (i_b)	$15 * 10^{-4}$	$15 * 10^{-4}$	$15 * 10^{-4}$
Discharge per unit width q [$m^2 s^{-1}$]	0.099 $m^2 s^{-1}$	0.099$m^2 s^{-1}$	0.099 $m^2 s^{-1}$
Numerical properties			
Horizontal grid size (dx)	0.01 m	0.01 m	n/a
Number of vertical points (Npz)	15	15	n/a
Domain length	4	4	n/a

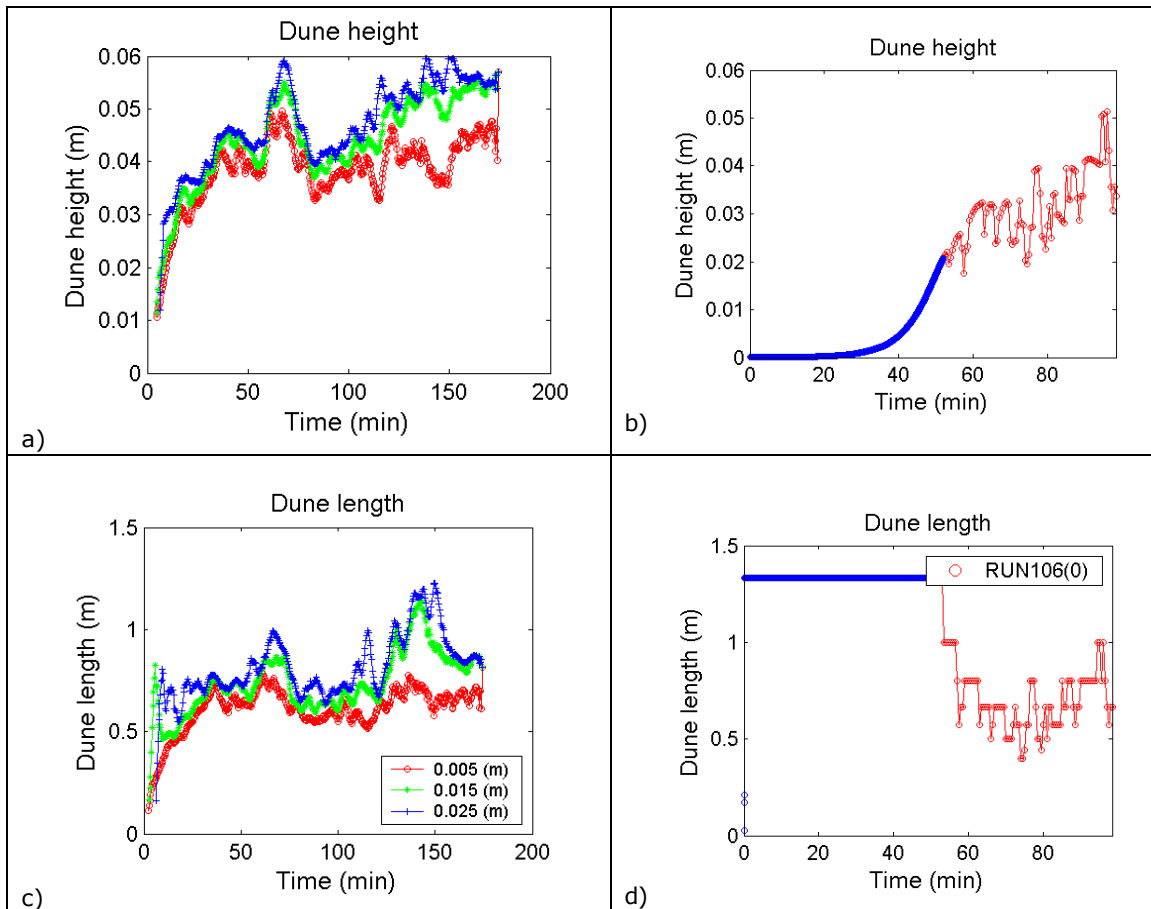**Table 4.2: Model and experimental conditions**

Figure 4.16: Dune height and length comparison between flume experiments (a&c) and model simulations including splitting (b&d)

Dune height and length are of the same order, when splitting is implemented in the model.
The initial phase of the dune height development during the model simulation (figure 4.16b) is remarkably different from the initial dune height development during the experiments (figure

4.16a). This is a result of the different dune initiation principle, described in section 2.4 (see initial model behaviour).

Equilbrium characteristics	DuDe	DuDe+	Experiment (T22)
Dune height Δ [m]	0.146[*]	0.04	0.05
Dune length λ [m]	4	0.7	0.75
Water depth H [m]	0.23[*]	0.180	0.190
Time to equilibrium	180 min	65 min	55 min
Migration rate [mhour^{-1}]	3mhour^{-1}	4 mhour^{-1}	4 mhour^{-1}

Table 4.3 Comparison between equilibrium dimensions in the experiments, predictors and model simulations before and after the implementation of the superposed wavelets (* 'false' equilibrium).

For a wavelet height H_{wave} of 6mm and a critical stoss side length L_{crit} of 1.0 m the improved model (DuDe+) reaches an equilibrium stage which is in accordance with the flume experiments. See table 4.3. Because the model depends on the parameters in the numerical code to implement splitting, a sensitivity analysis needs to deliver knowledge, how strong equilibrium dimensions depend on these parameters.

HIGHLIGHTS Chapter 4: Implementing dune splitting

- A random disturbance does not lead to dune splitting because the growth rate of wavelengths smaller than 0.5 m is negative.

- Model simulations with the improved model show that superposed wavelets decrease the migration rate of underlying dunes.

- The implementation of splitting results in equilibrium dimensions.

- The improved model successfully describes dune development from flat bed to equilibrium as a result of continuous splitting and merging of dunes.

5   Sensitivity analysis

5.1 Sensitivity analysis of the sediment transport formula

The initial diffusive stage in the model, where the initial signal disappears and deforms until dunes reach wave lengths that are able to grow (>0.8m), takes too long.
To see whether the sediment transport equation can be changed to solve this problem, a sensitivity analysis for this formula is conducted.
The sediment transport formula (5.1.1) contains two parameters, see section 3.2. The parameter α is a proportionality constant = 0.5 s^2m^{-1} and β = 1.5 is a nonlinearity parameter.

$$q_s = \alpha(\tau_b - \lambda_1 \tau_{cr,0})^\beta \lambda \qquad\qquad\qquad (5.1.1)$$

Because the dune evolution is based on the changes in bed elevation and therefore directly subject to the parameters in the sediment transport formula (formula 3.2.6) this formula is subject to a sensitivity analysis. α is a proportionality constant and has only a linear relation with the sediment transport. This parameter is therefore not interesting in the search for equilibrium dimensions. β is a non-linearity parameter, by performing model simulations with four different values for this parameter, the sensitivity of this model to this parameter is determined.
A fixed domain length of 1 m is used with an initial sinusoidal bed profile. All simulations end with one dune (length = 1m).

β	Migration rate	Time to equilibrium	Equilbrium dune height (Δ [m])
1.25	38 mhour^{-1}	10 min	0.049
1.5	10 mhour^{-1}	40 min	0.042
1.75	2 mhour^{-1}	120 min	0.038
2.0	0.7 mhour^{-1}	600	0.037

Table 5.1: Equilbrium characteristics for different β values (Appendix 12)

Table 5.1 shows that β strongly affects the migration rate of the dunes. As a result of the fact that bed shear stresses are always smaller than 1.0, the sediment transport decreases for increasing β values. The time to equilibrium depends on the migration rate (inversely proportional to the migration rate).
The equilibrium dune height is not strongly influenced by the change in β and the observed dune development as shown in Appendix 12 is not essentially different. Changes in β determine the speed of the processes in dune development rather than the process itself.

5.2 Sensitivity analysis for the wavelet parameters H_{wave} and L_{crit}

The implementation of dune splitting by superposing uses two parameters that are
The critical length L_{crit}, which is the threshold for dune splitting is the first. When a stoss side exceeds L_{crit}, a superposed wavelet is created.
The second parameter is H_{wave}, which stands for the amplitude of the superposed wavelet. Both parameters are shown in figure 5.1.
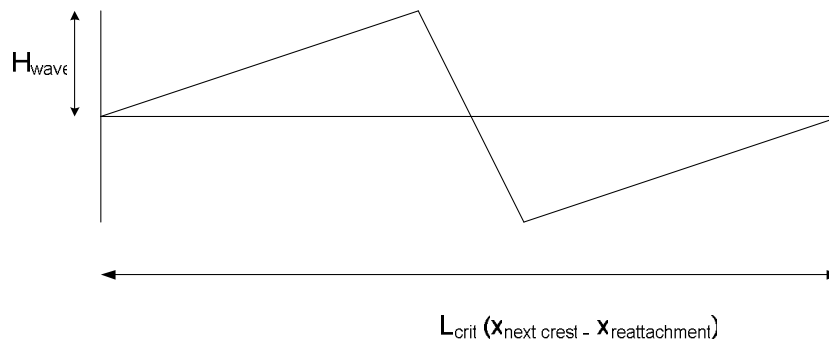

$$L_{crit}\ (x_{next\ crest} - x_{reattachment})$$

Figure 5.1: Two wavelet parameters H_{wave} and L_{crit}

A sensitivity analysis for these parameters has been performed in a domain with a length of 4 m. Dunes are random initiated and grow in length and height until superposition occurs.
Appendix 13 shows the results per experiment of this sensitivity analysis. The main results are given in table 5.2.

H_{wave} [m]	L_{crit} [m]	Δ [m]	λ [m]	Time to eq.	Mig. Rate [mhour^{-1}]
0.003	1	0.03	0.6	80 min	4
0.006	1	0.04	0.7	65 min	4
0.012	1	0.05	0.7	120 min	2
0.006	1.25	0.05	0.8	120 min	2
0.006	1.5	0.07	1.0	120 min	1.5
0.006	1.75	0.10	1.33	130 min	1
0.006	2	0.11	1.33	200 min	0.8

Table 5.2: Sensitivity of the equilibrium characteristics to the wavelet parameters H_{wave} and L_{crit}

The results of this sensitivity analysis show that the equilibrium dune height increases when H_{wave} increases but the equilibrium dune length remains almost the same. We observe in the bed plots of these model simulations that the dunes are initiated as smaller dunes when the H_{wave} is small, but they grow fast and have the same effect on the migration rate of the underlying dune.
L_{crit} has a much bigger effect on the equilibrium characteristics, because the critical length limits the equilibrium dune length, as seen in table 5.2. Therefore it also limits the growth of the dune height. For a large critical stoss side length (L_{crit}= 2), the equilibrium dune height is almost three times the value reached when the critical dune length is small (L_{crit} = 1). The time to equilibrium increases with increasing equilibrium dune heights, because the dunes migrate slower (larger lee side to fill).

<div style="border:1px solid">

HIGHLIGHTS Chapter 5: Sensitivity analysis

- The nonlinearity parameter β in the sediment transport formula determines the speed of the processes in dune development rather than the process itself.

- The implemented parameterization of splitting is highly sensitive to the critical stoss side length.

- The initial height of the superposed wavelet has only a small influence on the equilibrium dimensions of dunes.

</div>

6   Discussion

6.1 Experiments

The flow field during the experiments was practically two-dimensional. The minimum width/ depth ratio is just under 3 (for experiment T22). Vanoni & Brooks (1975) expect side wall effects when the width depth ratio is smaller than 5. So, bed shear stresses could be slightly overestimated because this correction is not applied for these experiments. This small width depth ratio limited the lateral component (three-dimensionality) of the flow, so centreline profiles can be regarded as recording regular 2D dunes formed under interaction with 2D flow.
The measurement section is only 6 m in length and the total length of the flume is 12 m. This implies that average dune dimensions are strongly influenced by dunes of different sizes migrating in and out of the measurement section. More important, as a result of this short flume length, dunes might also not be able to reach their potential size over the length of this flume, before sediment recirculates. However, dune height and length at the upstream end of the test section did not significantly differ from the dunes at the downstream end, what implies that dunes will not grow much higher when a larger flume is provided.

6.2 Bedformer

The obtained dune dimensions as presented with the bedformer tool are subject to definitions of a dune. Slight variations of the thresholds for minimum dune height varies the dune geometries significantly, although the general trend of exponential growth from initial bed features to equilibrium dunes is visible for all experiments. Friedrich et al. (2007) present a continuous approach that results in unambiguous statistical characterisation of the growth of dunes, but is still in development in order to find the relation between these characterisations and the discrete dune geometries.

6.3 Critical stoss side length (L_{crit})

The critical stoss side length for implementation of the splitting mechanism is subject of discussion. Venditti (2005) links the occurrence of superposed wavelets to the distance between the reattachment point and the crest of the upstream dune (x_{rear}). The experiments show that superposition does not occur behind high dunes, but on the stoss side of long dunes. Therefore we do not use the same criterion as suggested by Venditti (2005). However, given a situation with dunes of 0.04 m high and 1.3 m long, the criterion of a stoss side of 1m splits a dune with a length of 1m plus the length of the separation zone. This would mean that the dune length of the splitted dune is approximately 1.25 m (length of the separation zone $\approx 6\Delta \approx 0.25$). According to Venditti, superposition occurs 0.5 m behind the crest of the upstream dune, over a length of three times the separation zone length. This would mean that the length of a splitted dune is also 1.25 m. Both methods predict superposition for the same dune length.
The model is highly sensitive to the critical stoss side length. The critical stoss side length (L_{crit}) is fixed, based on the first wavelength that grows given the stability analysis for the model settings used. This length will not vary when the flow or sediment conditions change. The fixed L_{crit} makes that no variability is built in. This will ultimately result in equal equilibrium dune dimensions regardless of flow conditions. The possibility to determine the critical stoss side length internally in the model by stability analysis is one of the recommendations for future research.

6.4 The existence of a dynamic equilibrium

A main question that has risen during this research project is:
'Do equilibrium dimensions really exist?'
Is the assumption that dunes reach equilibrium heights under steady flow conditions correct? Flume studies are maybe not the right experimental setting, because recirculation of sediment does not mean recirculation of dunes, as seen with a model with periodic boundaries. The dunes that migrate out of the test section do not enter the domain as dunes. Equilibrium predictors based on field studies predict much larger dunes (as a result of a higher water depth), but also predict an equilibrium. The reason for this equilibrium could be that the flow is not unidirectional and more important, flow conditions might never be steady long enough, to investigate whether dune dimensions reach an equilibrium under steady flow conditions.

7   Conclusion & Recommendations

7.1 Conclusions

The goal of this research project is:

Improving the prediction of equilibrium river dune dimensions, by incorporating splitting in the DuDe model for bed form evolution.

The conclusion is based on four research questions are:

I What are the strengths and weaknesses of the DuDe model ?

The model simulates dune growth and migration as expected based on flume experiments. Dunes become asymmetric and develop angle of repose slip faces. Flow separation is parameterized and merging of river dunes is realistically simulated.
Initial model behaviour differs from the initial stage observed in flume experiments. The initial spacing expected and observed of approximately 0.2m, is not observed during model simulations.
Asymmetry develops over an hour time during model simulations in contrast to only minutes during the experiments. Flow separation is not perceived until the dunes reach near equilibrium dimensions, where flow separation is observed during the first minutes of dune development in the flume.
Splitting of river dunes is not observed. A dynamic equilibrium as predicted by numerous researchers and as seen in flume experiments is not obtained by the model. Dune length is only limited by the periodic domain boundary and depends therefore on the chosen domain length. A 'false' equilibrium is created when the equilibrium dune height reaches the boundaries of the periodic domain.

II What processes are observed during flume experiments that explain the existence of equilibrium dune dimensions?

Experiments show that dunes develop from flat bed with an initial spacing, as described by Coleman et al. (2005). Dunes grow exponentially and reach a dynamic equilibrium, under steady flow conditions, where splitting and merging of dunes is perceived and and dune height and length reach an equilibrium.
The reason for this equilibrium is the occurrence of splitting of river dunes. Dunes with a long stoss side become superposed by sand wavelets and therefore decrease in length.
Detailed observation of sediment transport and river dune development show the origination of superposed wavelets on the back of long stoss sides. The dune length of dunes that become superposed has a mean value of 1.3m. These superposed dunes resemble the initial dunes during the first stages of dune development from flat bed. Random disturbances as a result of turbulent bursting or suspended sediment transport are the trigger for dune splitting.

III How can splitting of river dunes be implemented in the DuDe model?

The DuDe model uses an initially disturbed bed at the start of a simulation (t_0). Due to a simplified pressure distribution and approximated turbulence structure, the model lacks a certain degree of randomness. A disturbance is therefore needed to initiate superposed wavelets because random pile ups due to turbulent streaks do not occur.
The implementation of a random disturbance superposed on existing dunes does not lead to growth or new dune development when dunes are already present, because growth is only perceived for wavelengths larger than 0.5m.
Inspired by the observations during flume experiments a parameterization of splitting has been developed. When the stoss side of a dune exceeds a certain threshold length (L_{crit}) a sand wavelet is superposed. L_{crit} is based on the wavelength that is found to grow based on a stability analysis. This wavelet is numerically implemented as a triangular disturbance on the stoss side of the underlying dune. The wavelet has an angle of repose to assure flow separation and a has a smooth connection to the underlying dune.
The length of the stoss side of a dune that becomes superposed (L_{crit}) is determined at 1.0 m based on flume conditions. These superposed wavelets are created with an initial height H_{wave} = 0.006m.

IV Does the implementation of splitting lead to the prediction of equilibrium dune dimensions?

The implementation of dune splitting by superposing wavelets on the stoss side of long dunes has lead to equilibrium dune dimensions which are in accordance with flume experiments. The time to equilibrium is also similar to the observed time to equilibrium. The model now predicts dune development from flat bed to equilibrium under steady conditions.

Sensitivity analysis, shows that the β parameter changes the speed at which the processes in the model take place, not the processes itself.

Besides that it shows that the implemented parameterization of splitting is highly sensitive to the critical stoss side length (L_{crit}). An increase in the critical stoss side length L_{crit}, logically delivers longer dunes and therefore higher dunes.

The initial height of the superposed wavelet (H_{wave}) has less influence because smaller waves grow fast.

In sum, the model changes do lead to the correct prediction of equilibrium dune dimensions, because the model shows besides merging also continuous splitting of river dunes.

7.2 Recommendations

The critical length (L_{crit}) should depend on the flow conditions to make this model applicable for unsteady flood wave conditions. When water levels increase, the critical stoss side length superpose wavelets increases as well. By performing a stability analysis for the existing bed profile during a simulation the L_{crit} can be changed based on physical grounds. This first step would make the model applicable for unsteady flood wave conditions. The model will be used for river branches eventually and dune dimensions in rivers are much larger. Future research should focus on the extrapolation of the model simulations to river circumstances and eventually to incorporate the method in existing flood prediction models.

The discrepancy between the initial model behaviour and the perceived initial stage of dune development during the flume experiments, leads to the hypothesis that the sediment transport formula does not describe all complexity of the initial stage yet. Other dune models use sediment pick-up-deposition functions to describe sediment transport instead of a bed load formula. I would recommend trying a sediment pick-up-deposition or suspended load formula in addition to the bed load formula that is used at the moment. The sediment transport over the crest should not only be deposited at the lee side of the dune. This could trigger the initiation of wavelets without a parameterization of splitting.

One difficulty when this model is applied for field conditions is the translation between 2DV modelling and 3D field conditions, with bend flow and other lateral variability. I suspect a large influence of three dimensionality on the equilibrium dimensions of river dunes. Not only the streamwise component of flow influences the dune length, also the crest line curvature determined by the lateral component of flow has its influence on dune length and height. It would increase the computational effort needed to gain solutions with a three-dimensional model, but the developments in this area of the market are promising. Future models should definitely include more sophisticated methods to described turbulence and three dimensional flow.

References

Allen, J.R.L. (1968), Current Ripples, *Elsevier, New York*.

Anderson, A.G. (1953), The characteristics of sediment waves formed on open channels, *3rd Mid-western Conference on Fluid Mechanics, University of Missouri, Missoula.*

Bagnold, R.A. (1956), The flow of cohesionless grains in fluids. *Proc. R. Soc. Lond. A 249, 235-279.*

Best, J. (2005), The fluid dynamics of river dunes: A review and some future research directions, *Journal of geophysical research, Vol. 110, F04S02, doi:10.1029/2004JF000218.*

Blondeaux, P. (1990), Sand ripples under sea waves, part I. Ripple formation, *Journal of Fluid Mechanics, 218, 1-17.*

Chang, H.H. (1988), Fluvial processes in river engineering, *John Wiley & Sons, Inc., New York, N.Y.*

Charru, F. and E.J. Hinch (2006), Ripple formation on a particle bed sheared by a viscous liquid. Part I. Steady flow*, Journal of Fluid Mechanics. 550, 123-137.*

Coleman, S. E., and B. Eling (2000), Sand wavelets in laminar open channel flows, *Journal of Hydraulic Research, 38(5), 331–338.*

Coleman, S.E. and B.W. Melville (1996), Initiation of bed forms on a flat sand bed, *Journal of Hydraulic Engineering, 122, 6, pp. 301-310.*

Coleman, S.E., and B. W. Melville (1997), Ultrasonic measurement of sediment bed profiles, *27th Congress of the International Association for Hydraulic Research, San Francisco, California, U.S.A., B221-B226*

Coleman, S.E., M.H. Zhang and T.M. Clunie (2005), Sediment-wave development in subcritical water flow, *Journal of Hydraulic Engineering., 131, 106-111.*

Colombini M. (2004), Revisiting the linear theory of sand dune formation, *Journal of Fluid Mechanics, 502, 1-16, doi: 10.1017/S20022112003007201.*

Ditchfield, R. and J.L. Best (1992), Development of bed features, discussion, *Journal of Hydraulic Engineering, 118, 647-650.*

Dronkers, J.J. (2005), Dynamics of coastal systems. *Advanced Series on Ocean Engineering, Vol. 25. World Scientific, Singapore.*

Engel, P. (1981), Length of flow separation over dunes, *J. Hydraul. Div. Am. Soc. Civ. Eng., 107, 1133–1143.*

Exner, F.M. (1920), Zur Physik der Dünen, *Sitzungsberichte der Akademie der Wissenschaften in Wien, Abteilung IIa, Band 129.*

Fox, R.W. and A.T. McDonald (1985), Introduction to fluid mechanics, *Wiley, New York.*

Fredsoe, J. and R. Deigaard (1992), *Mechanics of Coastal Sediment Transport, pp. 260-289. World Scientific.*

Friedrich, H., A.J. Paarlberg and J. Lansink (2007), Evaluation of statistical properties of dune profiles, *Accepted for: Proceedings of the 5th IAHR Symposium on River, Coastal and Estuarine Morphodynamics, University of Twente, Enschede.*

Führböter, A. (1983), Zur Bildung von makroskopischhen Ordnungsstrukturen (Stömungsriffel und Dünen) aus sehr kleinen Zufallsstöhrungen, *Mitt. Leichtweiss Inst. Tech. Univ. Braunschweig, 79, 1-51.*

Giri, S. and Y. Shimizu (2006), computation of sand dune migration with free surface flow, *Water Resources Research, 42, W10422, doi: 10.1029/2005WR004588.*

Haken, H.(1978), Synergetics – An Introduction, *Springer-Verlag Berlin, Heidelberg, New York, (2nd edition).*

Hulscher, S.J.M.H., H.E. De Swart and H.J. De Vriend (1993), Generation of offshore tidal sand banks and sand waves, *Cont. Shelf. Res. 13, 1183-1204.*

Hulscher, S.J.M.H. (1996), Tidal-induced large-scale regular bed form patterns in a three-dimensional shallow water model, *Journal of Geophysical Research 101, 20727-20744*

Jerolmack, D.J. and D. Mohrig (2005), A unified model for subaqueous bed form dynamics, *Water Resources Research, 41, W12421, doi:10.1029/2005WR004329.*

Julien, P.Y. and G.J. Klaassen (1995), Sand dune geometry of large rivers during floods, *Journal of Hydraulic Engineering, 121 (9), pp.15-25.*

Kennedy, J.F. (1969), The formation of sediment ripples, dunes and antidunes, *Annu. Rev. Fluid Mech., 1, 147–168.*

Komarova, N. and S. Hulscher (2000), Linear instability mechanisms for sand wave formation, *Journal of Fluid Mechanics 413, 219-246.*

Kostachuk, R.A. and P.V. Villard (1996), Flow and sediment transport over large subaqueous dunes: Fraser River, Canada, *Sedimentology, 43, 849–863.*

Kroy, K., G. Sauermann and H.J. Hermann (2002), Minimal model for aeolian sand dunes, *Physical Review E 66(3).*

Leclair, S.F. (2002), Preservation of cross-strata due to migration of subaqueous dunes: an experimental investigation, *Sedimentology, 49, 1157–1180.*

McLean, S.R. (1990), The stability of ripples and dunes, *Earth-science Reviews, 29, 131- 144.*

Meyer-Peter, E. and R. Müller (1948), Formulas for bed-load transport, *Proceedings of the 2nd Meeting of the International Association for Hydraulic Structures Research, pp. 39-64, Int. Assoc. for Hydraul. Res., Madrid.*

Nelson, J.M., S.R. McLean and S.R. Wolfe (1993), Mean flow and turbulence fields over two dimensional bed forms, *Water resources research, 29, 12, Pages 3935-3953.*

Nikora V.I., A.N. Sukhodolov and P.M. Rowinski (1997), Statistical sand wave dynamics in one-directional water flows, *Journal of Fluid Mechanics 351: 17–39.*

Nino, Y., A. Atala, M. Barahona and D. Aracena (2002). Discrete particle model for analysing bedform development. *J. Hydraul. Eng., 128(4), 381–389.*

Paarlberg, A.J. (2006) Modelling dune development with Komarova & Hulscher's sediment transport equation*, internal document, Faculty of Engineering Technology, University of Twente, Enschede.*

Paarlberg, A.J. (2007), Modelnauwkeurigheid en onzekerheden van in Nederland toegepaste hydraulische modellen, verslag van interviews met waterbeheerders en modelexperts, *CE&M research report 2007R-001 / WEM-001.*

Paarlberg, A.J., C.M. Dohmen-Janssen, S.J.M.H Hulscher, J. van den Berg and A.P.P. Termes (2005), A parameterization of flow separation in a river dune development model, *in: G. Parker and M.H. Garcia (Eds.), Proceedings of the 4th River, Coastal and Estuarine Morphodynamics conference, Urbana, Illinois, USA, Volume 2, pp. 883-895. Taylor and Francis Group, London.*

Paarlberg, A.J., C.M. Dohmen-Janssen, S.J.M.H Hulscher, J. van den Berg and A.P.P. Termes (2006), Modelling morphodynamic evolution of river dunes. *Proceedings River flow 2006, Lisboa, Portugal.*

Paarlberg, A.J., C.M. Dohmen-Janssen, S.J.M.H Hulscher and A.P.P. Termes (2007), A parameterization of flow separation over subaqueous dunes, *accepted for: Water Resources Research.*

Raudkivi A.J. (1966), Bed forms in alluvial channels, *Journal of Fluid Mechanics, 26, 507-514.*

Raudkivi, A.J. and H.H. Witte (1990), Development of bed features, *Journal of Hydraulic Engineering, 116, 1063–1079.*

Raudkivi, A.J. (2006), Transition from ripples to dunes, *Journal of Hydraulic Engineering, ASCE.*

Shields, A. (1936), Anwendung der Aenlichkeitsmechanik and der Turbulenzforschung auf die Geshienbebewegung: *Mitteilungen der Preussischen Versuchsanstalt fur Wasserbau and Schiffsbau, Berlin, Heft 26, 26 p.*

Shimizu, Y. M.W. Schmeeckle and J.M. Nelson (2001), Direct numerical simulations of turbulence over two-dimensional dunes using CIP methods, Journal *of Hydrosci Hydraul. Eng., 19(2), 85-92.*

Simons, D.B., and E.V. Richardson (1966), Resistance to flow in alluvial channels, *U.S. Geological Survey Professional Paper 422-J.*

Soulsby, R.L. (1990), Tidal-current boundary layers, *in: B. Le Mehaute and D. Hanes (eds.), The Sea, Vol. 9 Ocean Engineering Science, 523-566*

Tsuchiya, A. and K. Ishizaki (1967), The mechanics of dune formation in erodible-bed channels, *in: Proceedings of the 12th Congress of the International Association of Hydraulic Research, 1, pp.479-486.*

TenBrinke, W.B.M., A.W.E. Wilbers and C. Wesseling (1999), Dune growth, decay and migration rates during large magnitude flood at a sand and mixed sand-gravel bed in the Dutch Rhine river system*, in: Fluvial Sedimentology VI (Eds N.D. Smith and J. Rogers), Int. Assoc. Sedimentol. Spec. Publ., 28, 15-32.*

Van den Berg, J. and Van Damme, R. (2005), Sand wave simulation on large domains, *in: Proceedings of the 4th conference on River, Coastal and Estuarine Morphodynamics, Urbana, Illinois, USA, Parker, G. and M.H. Garcia (eds), vol. 2, pp 991-997, Taylor and Francis Group, London.*

Vanoni, V.A., and N.H. Brooks, (1957), Laboratory studies of the roughness and suspended load of alluvial streams. *Sedimentation Laboratory, California Institute of Technology, Pasadena, Calif.*

Van Rijn, L.C. (1984), Sediment transport part III: Bed forms and alluvial roughness, *Journal of Hydraulic Engineering. ASCE, 110(12), pp 1733-1754*

Van Rijn, L.C. (1993), Principles of sediment transport in rivers, estuaries and coastal seas, *Aqua, Amsterdam.*

Venditti J.G., M.A. Church and S.J. Bennett (2005), Morphodynamics of small-scale superposed sand waves over migrating dune bed forms, *Water Resources Research, W10423, DOI: 10.1029/2004WR003461*

Villard, P.V. and M. Church (2003), Dunes and associated sand transport in a tidally influenced sand-bed channel: Fraser River, British Columbia, *Canadian Journal of Earth Science, 40: 115-130.*

Walker, IJ. and W.G. Nickling (2002), Dynamics of secondary airflow and sediment transport over and in the lee of transverse dunes. *Progress in Physical Geography 26: 47-75.*

Whitehouse, R. (1995), The transport of sandy sediments over sloping beds, *in: Advances in coastal morphology MAST report, Delft Hydraulics, Delft, the Netherlands.*

Wilbers, A.W.E. and W.B.M. ten Brinke (2003), The response of subaqueous dunes to floods in sand and gravel bed reaches of the Dutch Rhine. *Sedimentology, 50: 1013-1034.*

Wilbers, A.W.E. (2004), The development and hydraulic roughness of subaqueous dunes, *Ph.D. thesis, 224 pp., Fac. of Geosci., Utrecht Univ., Utrecht, Netherlands.*

Appendices

Appendix 1 Classification of bed forms

River dunes are not the only subaqueous river bed forms. In this appendix the types of current-generated bed features are discussed. Classification of bed forms, conditions under which they develop and field observations will be discussed.

Ripples are small bed features whose height and wavelength are small compared to the water depth and are not related to the water depth, but depend on the grain size of the bed material. They form on sandy beds with grain sizes up to about 0.8 mm (Chang,1988). River dunes are much larger current generated bed forms.
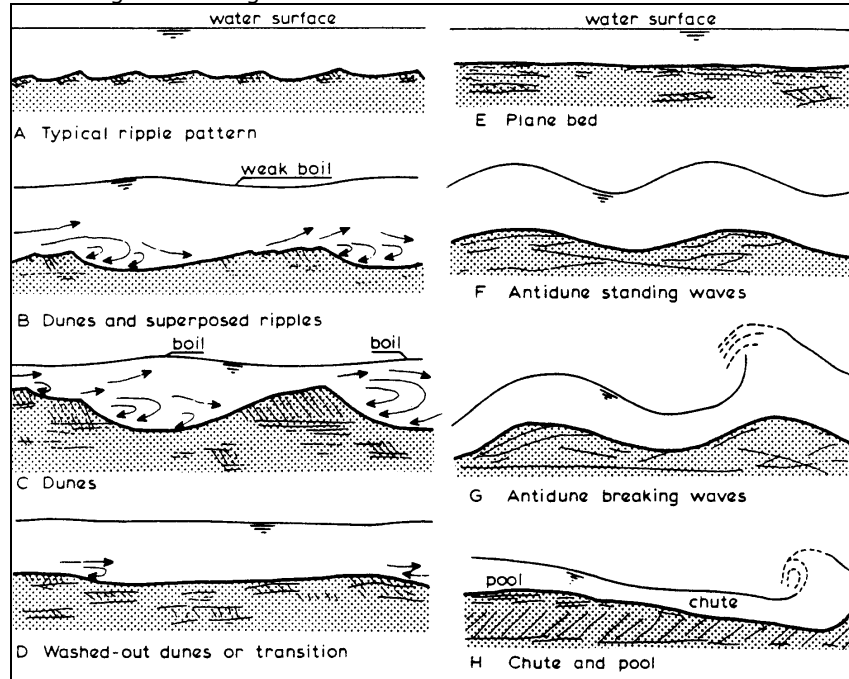
Figure A1.1 Classification of bed forms by Simons & Richardson (1966)

A classification by Simons & Richardson (1966) distinguishes eight stages of river bed forms, see figure 1. This classification is not a series of consecutive stages but is based on flow as well as on sediment properties. Stages A, B, C and E develop in a lower regime. The transition between lower and upper regime results in a washed out dunes (D).In the upper flow regime E to H can develop.

A lower regime is characterized by a small Froude number (formula A.1.1). In figure 1 B and C we see that during this regime, bed forms are out of phase with the water surface (water surface profile is lower over dune crests and higher above troughs)(Chang, 1988).

The Froude number is a function of mean stream velocity (u), the gravitational acceleration (g) and, in case of open-channel flow, the water depth (h) (Fox & McDonald, 1985)

Froude number: $Fr = \dfrac{u}{\sqrt{gh}}$ (A.1.1)
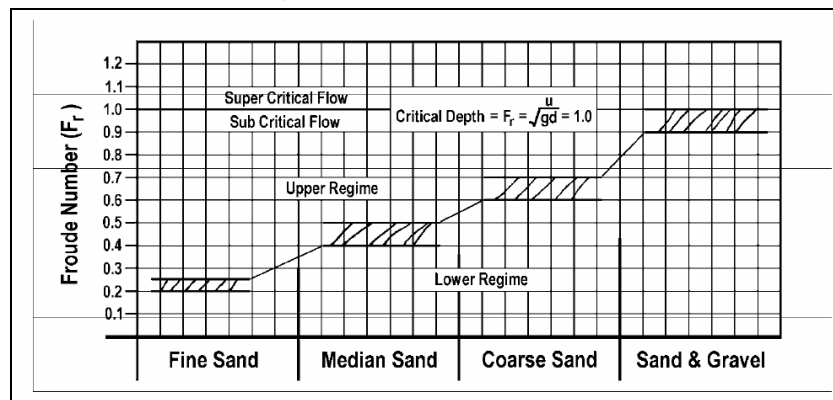
Figure A1.2 Flow regimes depending on Froude number and sediment grain size[1] (Simons, 1957, in: Chang 1988)

Bed forms in an upper flow regime develop in phase with the water surface.
The transition between lower and upper flow regime depends both on the Froude number and sediment grain size (figure A1.2).
Chang (1988) states: "In the lower flow regime, the bed roughness is ripples or dunes or both. Most of the movement is close to the bed over the backs of ripples and dunes. At the crest of these roughness elements, some of the sediment particles avalanche down the lee sides of the crest into the trough, where they are temporarily at rest. Therefore, the movement of particles follows discrete steps while the waves move slowly downstream. The resistance to flow is large in the lower regime, with form roughness predominant. In the upper flow regime of plane bed, anti-dunes and chutes and pools, the bed material transport is relatively large and is nearly continuous in motion. As the particles may move downstream on the surface of the sinusoidal wave, the wave itself may travel upstream (anti-dunes). The resistance to flow is small, with grain roughness predominant, see table A1.1"(Chang, 1988).

Flow regime	Bed form	Bed material concentration [ppm]	Mode of sediment transport	Dominant roughness type
Lower regime	Ripples	10-200	Discrete steps	Form roughness
	Ripples on dunes	100-1200		
	Dunes	200-2000		
Transition regime	Washed out dunes	1000-3000		Variable
Upper regime	Plane bed	2000-6000	Continuous	Grain roughness
	Anti-dunes	2000+		
	Chutes and pools	2000+		

Table A1.1 Bed form classification (Simons & Richardson, 1966)

---

[1] The American Geographical Union defines fine sand (125 – 250 µm) , median sand (250 – 500 µm), coarse sand (500 – 1000 µm) and gravel (2000 – 64000 µm)
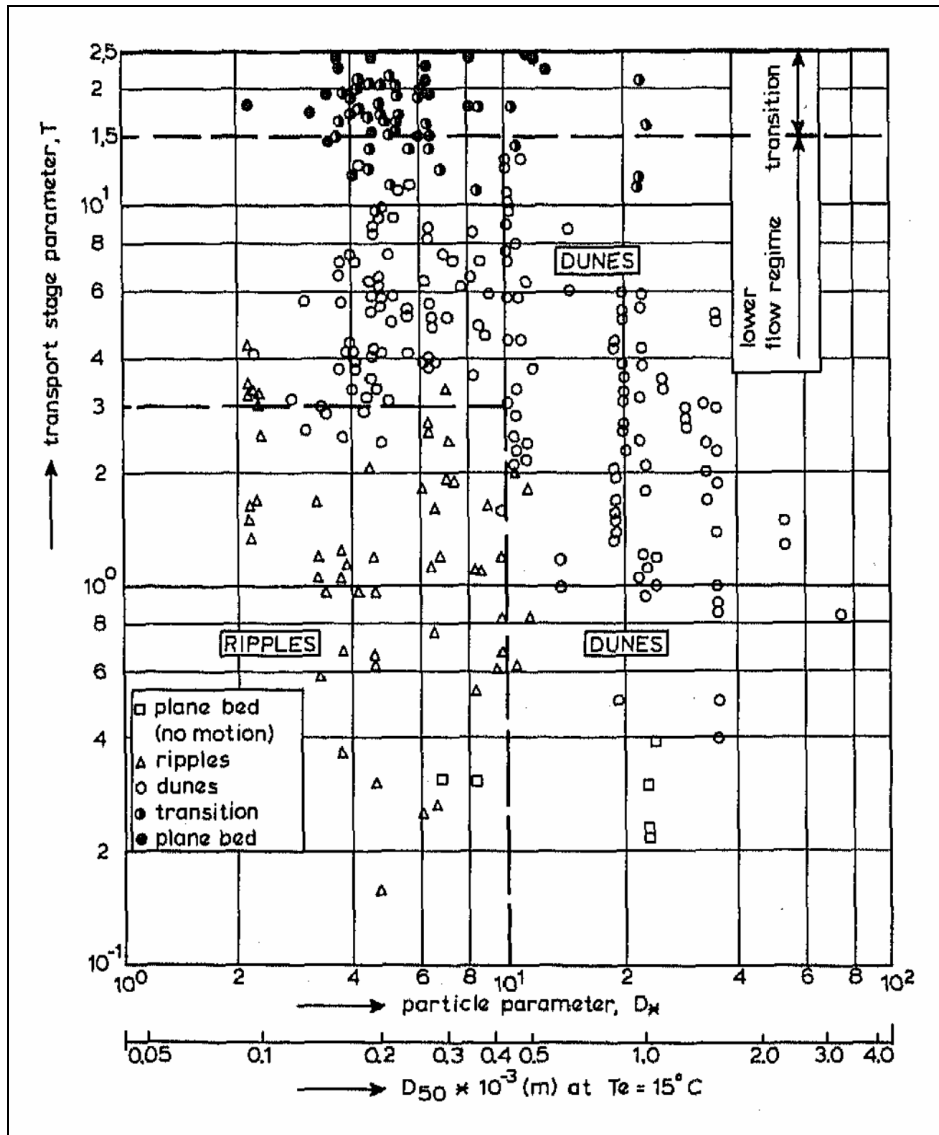
Figure A1.3 Diagram for bed form classification in lower and transitional flow (Van Rijn, 1984)

Figure A1.3 shows a bed form classification diagram for lower and transitional flow based on a large number of reliable flume and field experiments (Van Rijn, 1984).
T gives the grain shear stress (τ') in relation to the critical shear stress (τ_c),

$$T = \frac{\tau' - \tau_c}{\tau_c}$$

(A.1.2)

And d_*, the dimensionless grain size, depends on the densities of water and sand (respectively ρ and ρ_s), and the kinematic viscosity (v) and the gravitational acceleration (g)

$$d_* = d\left(\frac{(\rho_s - \rho)g}{\rho v^2}\right)^{1/3}$$

(A.1.3)

Appendix 2 Equilibrium predictors

Flume experiments and field studies show that equilibrium height of river dunes for steady flow can be described as a function of the median grain size (d_{50}) and water depth (H). The method of Van Rijn (1984) is mainly based on flume data. The influence of the flow strength, quantified by the transport stage parameter T (Van Rijn, 1984) is questioned by Julien & Klaassen (1995), based on analysis of field data of large river.

Van Rijn (1984):	**Julien & Klaasen (1995):**
$$\frac{\Delta}{H} = 0.11\left(\frac{d_{50}}{H}\right)^{0.3}(1 - e^{-0.5T})(25 - T)$$	$$\frac{\Delta}{H} = 2.5\left(\frac{d_{50}}{H}\right)^{0.3}$$
$$\frac{\lambda}{H} = 7.3$$	$$\frac{\lambda}{H} = 2\pi$$
With: Δ = Dune height [m] λ = Dune length [m] H= water depth [m] d_{50} = median grain size [m] $$Transport\ parameter\ T = \frac{\theta - \theta_{cr}}{\theta_{cr}}$$	With: Δ = Dune height [m] λ = Dune length [m] H=water depth [m] d_{50} = median grain size [m]

Table A4.1: Equilibrium dune dimension predictors

The equilibrium length of river dunes is in both methods described as a function of the water depth. Both estimators are applicable for flow and sediment characteristics that match with a river dune regime (Appendix 1) given that the flow strength exceeds the critical shear stress (Appendix 2).

Appendix 3 Critical shear stress

If the flow velocity is zero, the sand remains immobile. Then if velocity increases a velocity is reached at which particles start to move. This is called the initiation of motion or incipient motion.
It is commonly used to measure the threshold of motion in terms of the bed shear stress or bed shear velocity. Shields (1936) stated the dimensionless shear stress or Shields parameter θ as a function of the shear stress (τ_b), fluid density (ρ), gravitational acceleration (g) and relative density of sediment grains (Δ = ((ρ$_s$ − ρ)/ ρ) and the representative sediment size (d$_{50}$)

$$\theta = \frac{\tau_b}{\rho g (\Delta d)} \quad = \quad \frac{u_*^2}{g \Delta d_{50}} \tag{A.3.1}$$

Van Rijn (1993) determined the critical Shields parameter for the initiation of motion as a function of the dimensionless grain diameter D∗:

$$D_* = d_{50} \left(\frac{\Delta g}{v^2} \right)^{1/3} \tag{A.3.2}$$

In which Δ is the relative density of sediment (ρ$_s$ − ρ / ρ) , g the gravitational acceleration, v the kinematic viscosity and d$_{50}$ the representative sediment size.
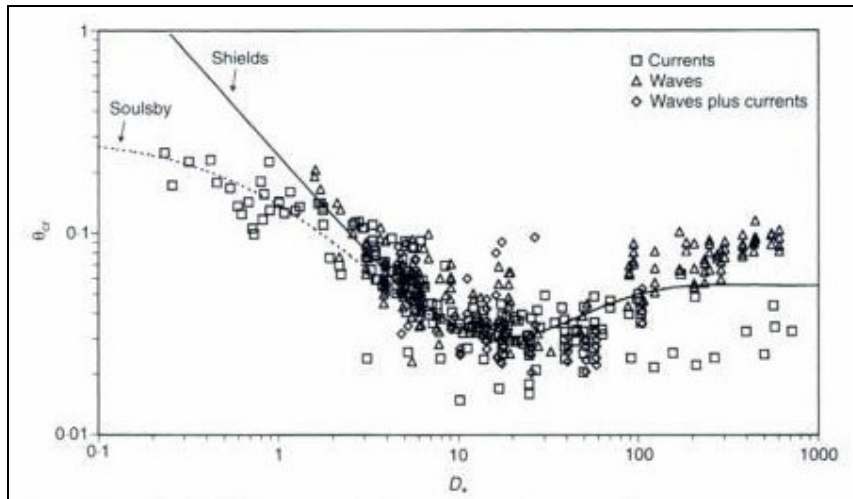
Figure A.3.1 Critical Shields as a function of dimensionless grain size (Soulsby, 1998)

For different dimensionless grain sizes the empirical determined values for the critical Shields parameter are (Van Rijn, 1993):

$$\theta_{cr} = \frac{0.24}{D_*} \qquad if \quad 1 < D_* \leq 4$$

$$\theta_{cr} = \frac{0.14}{D_*^{0.64}} \qquad if \quad 4 < D_* \leq 10$$

$$\theta_{cr} = \frac{0.04}{D_*^{0.1}} \qquad if \quad 10 < D_* \leq 20 \tag{A.3.3}$$

$$\theta_{cr} = 0.013 D_*^{0.29} \quad if \quad 20 < D_* \leq 150$$

$$\theta_{cr} = 0.055 \qquad if \quad D_* > 150$$

When the Shields parameter (formula A.3.1) exceeds the critical shear stress (formula A.3.3) sediment movement will take place.
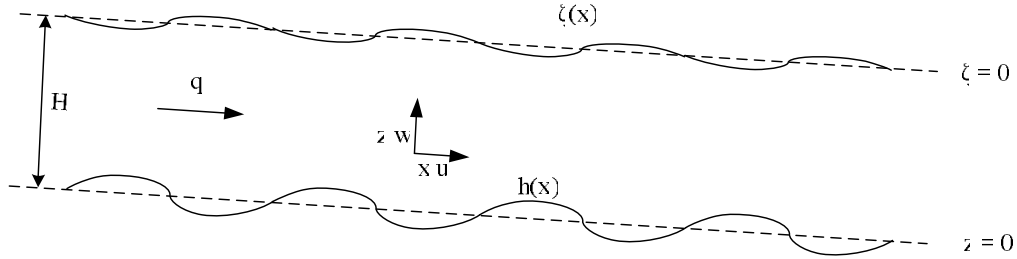
Appendix 4 Extended model description DuDe

Figure A4.1: Definitions of flow parameters

The flow velocities u and w are respectively in the horizontal (x) and vertical (z) direction (see figure A4.1). A_v is the eddy viscosity, which is assumed constant in this model. The water surface elevation is denoted by ζ. Flow over a sloping bed is driven by the force as a result of the gravitational acceleration (g) and depends therefore on the bed slope (i_b).
To describe flow over a given bed configuration, hydrostatic shallow water equations are used.
Assuming no variations perpendicular to the flow direction and considering incompressible flow, the momentum equation in x-direction reads:

$$u\frac{\partial u}{\partial x} + w\frac{\partial u}{\partial z} = A_v\frac{\partial^2 u}{\partial z^2} - g\frac{\partial \zeta}{\partial x} + gi_b \tag{A4.1}$$

The principle of mass conservation is described by the continuity equation (A4.2).
The continuity equation reduces, given the assumptions mentioned earlier to:

$$\frac{\partial u}{\partial x} + \frac{\partial w}{\partial z} = 0 \tag{A4.2}$$

To solve the shallow water equations, boundary conditions are needed. Starting with no flow through the bed:

$$u\frac{\partial h}{\partial x} = w\bigg|_{z=h(x)} \tag{A4.3}$$

Furthermore, at the water surface there is no shear (due to wind, for example):

$$\frac{\partial u}{\partial z} = 0\bigg|_{z=H+\zeta} \tag{A4.4}$$

And no flow through the free surface:

$$u\frac{\partial \zeta}{\partial x} = w\bigg|_{z=H+\zeta} \tag{A4.5}$$

Periodic boundaries are applied on the right and left boundary of the domain. When using periodic boundary conditions an additional equation is needed to guarantee uniqueness of the solution:

$$\frac{1}{L}\int_0^L \zeta dx = 0 \tag{A4.6}$$

In which L is the length of the periodic domain. (Van den Berg & Van Damme, 2005)

To predict the sediment transport, which is assumed to be mainly bedload transport, the bed shear stress needs to be accurately described. Because the bed shear stress can be derived from the velocity distribution near the bed a correct description of the velocity profile is essential. Because u approaches zero (no slip) at the bed, calculating τ_b based on velocity gradients is problematic in de viscous sublayer. Velocity gradients near the bed do not predict the bed shear stress accurately in the viscous sublayer. As described by Paarlberg (2006), Soulsby (1990) has made a comparison for different turbulence models for boundary layer flows. It turns out that a basic turbulence closure (constant eddy viscosity A_v) in combination with a partial slip condition results in a good representation of the vertical flow structure and therefore in good estimation of the volumetric bed shear stress τ_b [m²s⁻²]:

$$\tau_b \equiv A_v \frac{\partial u}{\partial z} = Su \Big|_{z=h(x)} \tag{A4.7}$$

In which S [ms⁻¹] is a slip parameter and A_v [m²s⁻¹] the eddy viscosity which is defined as a constant value.
Both parameters depend on the bed shear velocity u∗:

$$u_* = \sqrt{gHi_b}$$

The slip parameter is found to be directly related to the bed shear velocity:

$$S = \beta_1 u_* \tag{A4.8}$$

The eddy viscosity depends not only on the bed shear velocity, but also on the mean water depth:

$$A_v = \beta_2 \frac{1}{6} \kappa H u_* \tag{A4.9}$$

κ = von Kármán constant, β_1 and β_2 are calibration factors ($\beta_1 = 0.5, \beta_2 = 0.5$).

With the shallow water equations and the given boundary conditions, the flow over a given bed configuration can be solved and the sand water coupling can be made. The local bed shear stress determines the sediment transport and consequently determines the local bed changes. The sediment transport equations are explained in the next section.

Sediment transport and bed evolution

The model does not predict turbulent bursts. Therefore a minimal disturbed signal is used as initially disturbed bed. The model needs bed gradients to generate bed elevation. A sinusoidal bed profile, or a random signal with an amplitude of only $0.1*d_{50}$ is used as input to imitate the small bed defects to start with. The propagation of these initial disturbances is a result of the coupled flow and sediment transport formula.
In most of the existing transport formulas, sediment transport is expressed as a function of the dimensionless shear stress or Shields parameter θ:

$$\theta = \frac{\tau_b}{\rho g \Delta d_{50}} \tag{A4.10}$$

The dimensionless shear stress can be determined as a function of the bed shear stress (τ_b), fluid density (ρ), gravitational acceleration (g), relative density of sediment grains ($\Delta = ((\rho_s - \rho)/\rho)$) and the representative sediment size (d_{50}). The relative density of sediment is determined based on the density of the sediment (ρ_s) and the density of the fluid (ρ).
The basis for the sediment transport equation used in the DuDe model is first described by Meyer-Peter and Müller (1948). They stated a power law relationship between sediment flux and bed shear stress. The formula of Meyer-Peter-Müller is an empirical formula which only concerns bed load transport. The non-dimensional transport rate Φ_b is described by:

$$\phi_b = \left\langle \begin{array}{ll} m(\theta - \theta_c)^n & if \ \theta > \theta_c \\ \\ 0 & if \ \theta \le \theta_c \end{array} \right. \tag{A4.13}$$

In which, m and n are empirical constants and θ and θ_c are respectively the Shields parameter and the critical Shields parameter. The critical Shields parameter depends on the dimensionless grain size (see Appendix 3).

The volumetric bed load transport rate (q_b) can be described by (Fredsoe & Deigaard, 1992):

$$q_b = \phi_b \sqrt{\Delta g d^3} \tag{A4.14}$$

The volumetric bed load transport can now be expressed as:

$$q_b = \left\langle \begin{array}{ll} \sqrt{\Delta g d^3}) \ m(\theta - \theta_c)^n & if \ \theta > \theta_c \\ \\ 0 & if \ \theta \le \theta_c \end{array} \right. \tag{A4.15}$$

This formula has been modified, as proposed by Komarova & Hulscher (2000), to incorporate two bed slope effects. Firstly (i): as described by Whitehouse (1995), a sloping bed can enhance or reduce the sediment transport rate once sediment is in motion depending on the direction of the slope. For example sediment being transported down a slope will experience a component of its immersed weight acting down slope. Secondly (ii): a sloping bed will change the value of the threshold shear stress for initiation of motion (Bagnold, 1956).

Intuitively a positive slope (upwards in the direction of flow) increases the threshold shear stress for particle motion. The second bed slope effect is described mathematically by Fredsoe and Deigaard (1992).

The volumetric sediment transport rate q_b [m^{2}s^{-1}] depends on the local volumetric bed shear stress τ_b [m^{2}s^{-2}] (see formula 2.2.5). The threshold shear stress increases or decreases depending on the local bed slope (ii) mentioned earlier with a factor λ_1. The volumetric transport rate is also directly influenced by the local bed slope as a result of the other slope effect (i) with a factor λ_2. The parameter α is a proportionality constant = 0.5 s^{2}m^{-1} and β = 1.5 is a nonlinearity parameter.

The local bed slope h_x is the first derivative of h to x. ϕ_s is the angle of repose of sediment, which depends on the grain diameter and angularity (roundedness) of the sediment (Simons, 1957 in: Chang 1988) and is about 30º for sand in rivers.

$$q_b = \alpha(\tau_b - \lambda_1 \tau_{cr,0})^\beta \lambda_2 \qquad\qquad \lambda_1 = \frac{1 + h_x / \tan\phi_s}{\sqrt{1 + (h_x)^2}}$$

$$\tag{A4.16}$$

$$\tau_{cr,0} = \theta_{cr} g \Delta d_{50} \qquad\qquad \lambda_2 = \frac{1}{1 + h_x / \tan\phi_s}$$

The critical bed shear stress is initially determined by the critical Shields parameter for the initiation of motion (θ_{cr} = 0.047 [-]), the gravitational acceleration (g = 9.81 [ms^{-2}]) the relative density of sediment (Δ = 1.65 [-]) and the median sediment grain size (d_{50} [m])
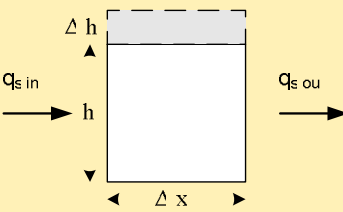
The role of the bed slope can be described by a simple example (see intermezzo).

Intermezzo: The influence of a negative bed slope of 5% on the local sediment transport rate

Input parameters :

$H = 0.153m$

$d_{50} = 0.8*10^{-3}m$

$\phi_s = 30°$

$h_x = -0.05 \ (\approx -3°)$

$u = 0.5ms^{-1}$

$i_b = 1.2*10^{-3}$

$\Delta = 1.65$

$\alpha = 0.5$

$\beta = 1.5$

The initial conditions for the waterdepth, median grain size and other physical input parameters are chosen consistent with the conditions for which the model is calibrated and in the same range as the flume conditions mentioned in chapter 3.

Flux calculation :

$\tau_b \approx ghi_b \approx 1.8*10^{-3}m^2s^{-2}$

$\tau_{cr,0} = \theta_{cr}g\Delta d_{50} = 0.6*10^{-3}m^2s^{-2}$

$\lambda_1 = \dfrac{1 + h_x/\tan\phi_s}{\sqrt{1+\left(h_x\right)^2}} = \dfrac{0.91}{1.00} = 0.91$

$\lambda_2 = \dfrac{1}{\sqrt{1 + h_x/\tan\phi_s}} = 1.05$

$q_{s1} = \alpha(\tau_b - \tau_{cr,0})^{\beta} = 2.08*10^{-5}m^2s^{-1}$

$q_{s2} = \alpha(\tau_b - \lambda_1\tau_{cr,0})^{\beta} = 2.22*10^{-5}m^2s^{-1}$

$q_{s3} = \alpha(\tau_b - \tau_{cr,0})^{\beta}\lambda_2 = 2.18*10^{-5}m^2s^{-1}$

$q_{s4} = \alpha(\tau_b - \lambda_1\tau_{cr,0})^{\beta}\lambda_2 = 2.33*10^{-5}m^2s^{-1}$

Note that the critical shear stress is of the same order as the bed shear stress and is therefore of great importance in the determination of the local sediment flux.

$\lambda_1 < 1$, implying a decrease in threshold shear, which is in compliance with the negative bed slope (h_x)

$\lambda_2 > 1$, implying an increase in local flux, which is in compliance with the negative bed slope (h_x)

The indirect bed slope effect (λ_1) and direct bed slope effect (λ_2) result respectively in a flux increase of 7% and 5%.This shows the importance of both bed slope effects.

When applied together they cause an increase of 12% given a local bed slope of -0.05 (-3º).

Bed level changes occur as a result of gradients in the sediment flux distribution, based on the Exner (1920) equation:

$$\frac{\partial h}{\partial t} = -\frac{1}{(1-\varepsilon_0)}\frac{\partial q_b}{\partial x}$$ (A4.17)

This can be explained physically based on continuity of mass, the difference between mass inflow and outflow will be compensated by the change in bed level. A correction is applied for the porosity of the sediment ($\varepsilon_p = 0.4$), because the sediment flux is calculated as volume solid material, and to determine the change in bed elevation including voids, compensation for this 40% void volume is needed.

Explanation of the bed update formula of Exner (1920)	
	$$\frac{1}{1-\varepsilon_p}(q_{s,in}\Delta t - q_{s,out}\Delta t) + \Delta h\Delta x = 0$$ $$\frac{1}{1-\varepsilon_p}\Delta q\Delta t + \Delta h\Delta x = 0 \qquad divide\,by\,\Delta x\Delta t:$$ $$\frac{1}{1-\varepsilon_p}\frac{\Delta q}{\Delta x} + \frac{\Delta h}{\Delta t} = 0 \qquad \Delta x \to 0\,\Delta t \to 0:$$ $$\frac{\partial h}{\partial t} = -\frac{1}{(1-\varepsilon_p)}\frac{\partial q_s}{\partial x}$$

Parameterization of flow separation

River dunes become asymmetric due to unidirectional flow. The top migrates faster than the trough, resulting in a gentle stoss side and a steep lee side. If the lee side of a dune becomes too steep for the flow to follow the bed, flow separates (figure 2.2). The boundary between the normal flow zone and the flow separation zone is called the separation streamline (SSL). The area underneath the SSL is called the flow separation zone (FSZ). The separation streamline touches the bed again at the flow reattachment point (FRP).
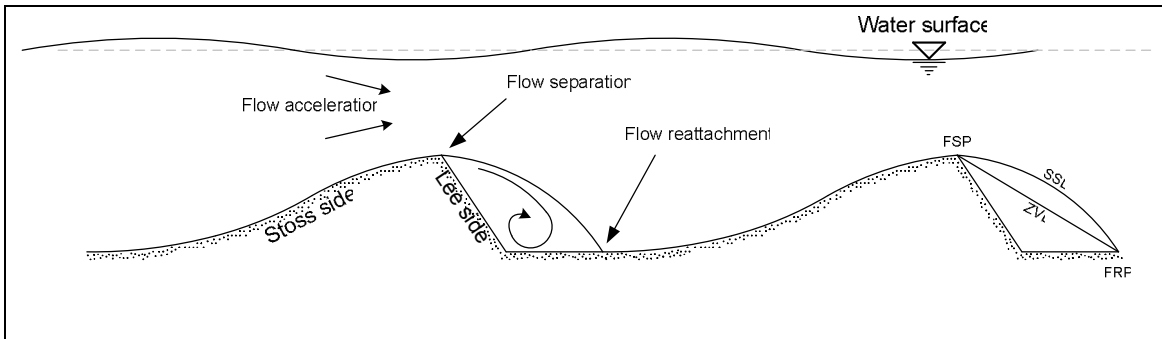
Figure A4.2: Schematisation of river dunes with flow separation characteristics

Some researchers prefer to use the expression flow reattachment zone, because the place of flow reattachment is not fixed (Walker & Nickling, 2002; Raudkivi, 2006). However, in the model a fixed point needs to be determined in order to locate the boundaries of the flow separation zone.
Due to a constant eddy viscosity in the model, the model does not account for flow separation. Therefore a parameterization based on dune height and the local bed angle at the points of separation is used as described by Paarlberg et al. (2007). The shape of the flow separation zone is found to be independent of flow conditions. (Paarlberg et al. 2007)
The parameterization of flow separation is based on a method developed for aeolian dune development by Kroy et al. (2002). In this method the separation streamline is parameterized in a form as simple as possible. Subsequently, this separation streamline is used as imaginary bed level for the flow calculation, neglecting all flow inside the flow separation zone. The shear stresses inside the flow separation zone are set to zero, because they typically do not exceed threshold shear stress and are therefore of no interest for morphological purposes. The difficulty in this approach lies in the determination of the separation streamline.
The first step to derive this separation streamline is to determine the length of the flow separation zone. Paarlberg et al. (2007) have derived a relation between dune length and the local bed slope at the flow separation point.

The separation streamline can be described by a third order polynomial:

$$\tilde{s}(\xi) = \frac{s(\xi)}{H_b} = s_3(\xi)^3 + s_2(\xi)^2 + s_1(\xi) + s_0 \qquad \text{(A4.18)}$$

$$\xi = x - x_s$$

In which s(ξ) is the z-coordinate of the separation streamline, ξ is a relative coordinate, described as the distance from the location of the flow separation point in stream wise direction along the dune. x is the absolute location of a point, x_s is the location of the first upstream flow separation point from that point.

The coefficients s_0 and s_1 are determined using characteristics at the point of flow separation, assuming smooth connection at the flow separation point (ξ=0). The starting angle of the separating streamline is equal to the local bed slope at the flow separation point (α_s)

$$s_0 = \tilde{s}(0) = 1$$
$$s_1 = \tilde{s}'(0) = \tan\alpha_s \qquad \text{(A4.19)}$$

s_2 and s_3 are determined based on regression analysis of flume data (Paarlberg et al., 2007). Based on numerous flume data they found a function of the local bed slope at the flow separation point (α_s), that predicts the length of the separation zone (L_{st}) compared with the dune height at the brinkpoint H_b as:

$$L_s' = L_{st} / H_b = 7.24\tan\alpha_s + 5.26 \qquad \text{(A4.20)}$$

The coefficients s2 and s3 can determined if the location of the reattachment point is known and and the slope of the separation streamline at the flow reattachment point are known. In case of a horizontal bed at the flow separation point, the average angle of the separation streamline at the reattachment point (ξ = L's) is (tan α_r')av = -0.51 (σ = 0.12), yielding:

$$s_3 = \frac{2}{(L's)_{av}} + \frac{(\tan\alpha_r')_{av}}{(L_s')_{av}^2} \qquad \text{(A4.21)}$$

$$s_2 = -s_3(L_s')_{av} - \frac{1}{(L_s')_{av}^2} \qquad \text{(A4.22)}$$

In the case of a negative bed slope at the flow separation point, the angle of the separation streamline at the flow reattachment point is not known, because only limited data with such cases are used. To be able to use one boundary condition less at te flow reattachment point, the parameterization of the separation streamline is restricted to a second order polynomial (i.e. $s_3 = 0$), if tan $\alpha_s < 0$, yielding:

$$s_2 = \frac{\tan\alpha_s}{L_s'} - \frac{1}{L_s'^2} \qquad \text{(A4.23)}$$

When the separation streamline is calculated it is used as a imaginary bed. The flow over this parameterized bed can be calculated and bed shear stresses can be derived. When taken into account that the flow inside the flow separation zone is recirculating and the shear stress does not exceed the critical shear stress, the bed shear stress over the flow separation zone needs a correction. The average bed shear stress and thus the flux inside the flow separation zone is set to zero. The bed shear stress distribution over the stoss side of the downstream dune is based on experimental data, as described by Paarlberg et al. (2006).

The shear stress is approximated with a third order polynomial as a function of the dimensionless position along the dune (χ), see figure and formula A4.18.
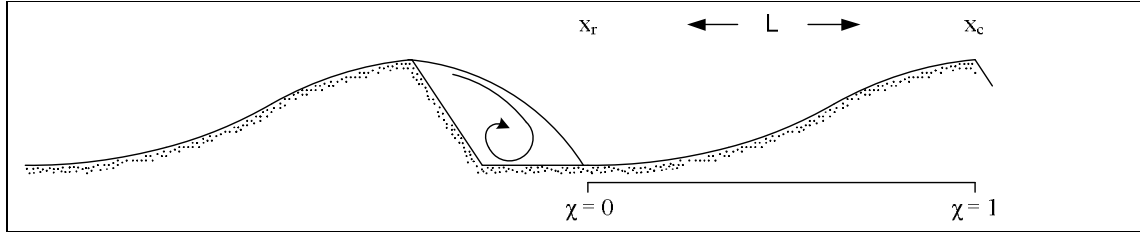
Figure A4.3: Dimensionless position along the dune

The length of the stoss side (L) is given by $L = x_c - x_r$
χ ranges from $\chi = 0$ at the flow reattachment point to $\chi = 1$ at the crest of the dune.
The dimensionless coordinate is given by $\chi = (x-x_r)/L$

$$\tau'(\chi) == \begin{cases} 0 & if \ \chi < 0 \\ a_3(\chi)^3 + a_2(\chi)^2 + a_1(\chi) + a_0 & if \ \chi_r \leq \chi \leq \chi_c \end{cases} \qquad (A4.24)$$

The derivation of these coefficients can be found in Paarlberg et al. (2006) and is partly based on calibration with experimental data sources.
The parameterization of flow separation has one more important implication for the dune evolution. Namely, by setting the bed shear stress and thus the flux inside the flow separation zone to zero, no migration of the lee side is modelled.
The solution lies in the assumption that all sediment that passes over the dune crest avalanches down the lee side, with a lee side angle at the angle of repose. The angle of the lee side of a dune when flow is separated is determined by the angle of repose of the sediment.
Bed level changes outside the flow separation zone are described by equations A4.16 and A4.17, but inside the flow separation zone this is impossible as a result of the zero bed shear stress inside the flow separation zone. Therefore the migration of the lee side is parameterized. Since the bed is parameterized with the determination of the separation streamline, bed shear stresses at the crest of a dune are known. The assumption needed to determine the migration of the lee side is that all sediment that passes the crest of a separating dune will avalanche down the lee-side, which is in general agreement with observations in flume experiments.
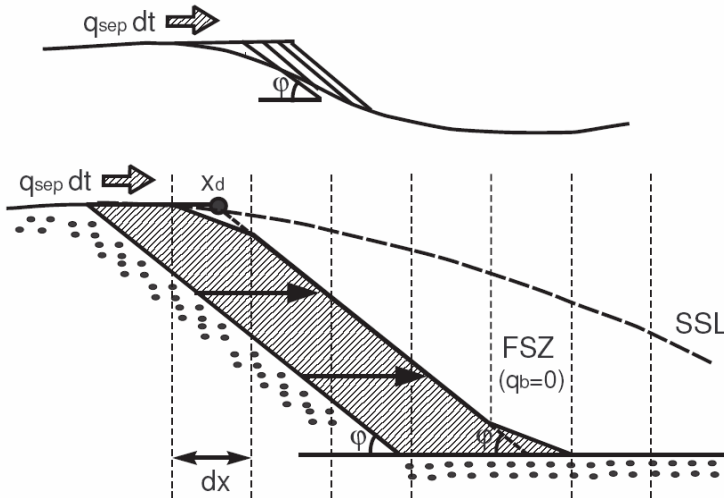

Figure 2.4: Parameterization of the migrating lee-side; the flux over the crest avalanches down resulting in a displacement per time step depending on the flux over the crest and the height of the dune. [Paarlberg et al., 2006]

Therefore the migration of the lee side is determined by the quotient of the flux and the dune height. For a detailed description of this parameterization of flow separation, see Paarlberg et al. (2006)

Appendix 5 Flood wave experiments

Field studies (e.g. Wilbers & TenBrinke, 2003) show a phase lag between the moment of maximum river discharge and the appearance of the highest dunes. A flood wave is simulated by stepwise increase and decrease of the discharge (table A5.1).
Unsteady (flood wave) experiments are performed using the three flow conditions for which steady flow experiments are conducted. The flood wave experiments started with equilibrium dunes for the smallest discharge.

Flow stage	Discharge [Ltr/s]	Duration [min]
A (T24)	27.2	25
B (T23)	36.0	40
C (T22)	43.7	40
D (T23)	36.0	100
E (T24)	27.2	180

Table A5.1: Flood wave design

Table 3.2 shows that the Froude number for the three stages of the flood wave experiment is almost equal, but the water depth (H) and bed shear velocity (u_*) increase with increasing discharge. The dune height increases in the second and third stage of a flood wave as a result of increasing flow depth and discharge. Figure A5.1 also shows a hysteresis effect for the dune height as observed in a field study by Ten Brinke et al. (1999).
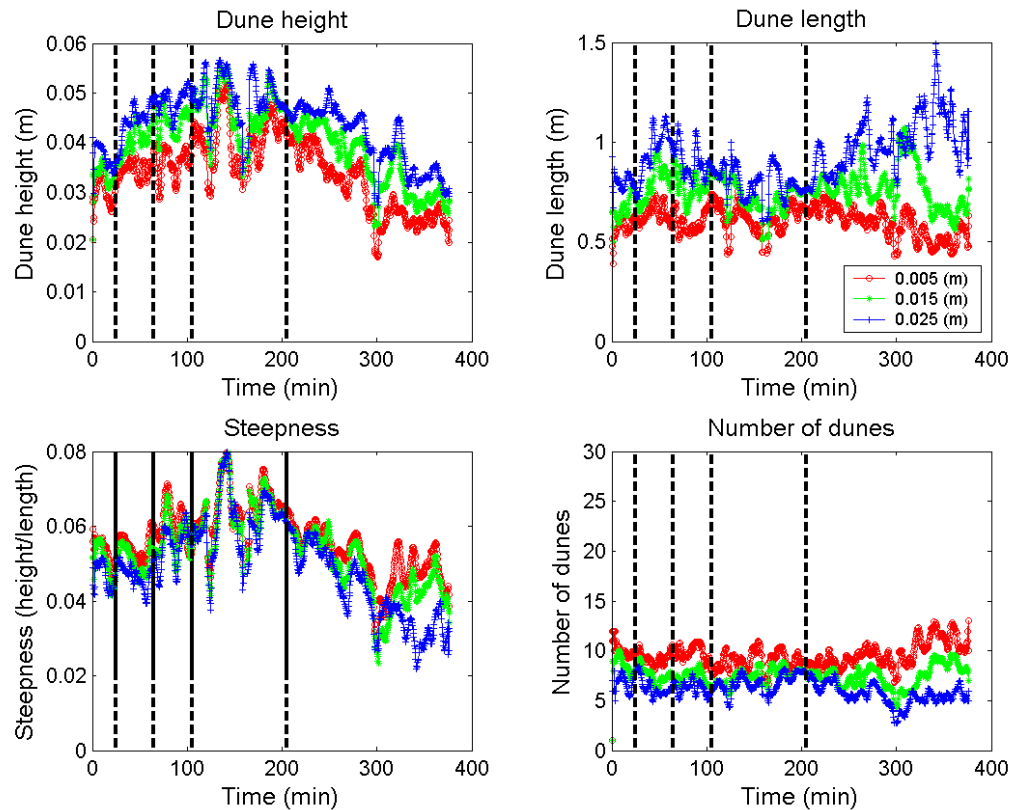
Figure A5.1: Experiment T21, dune dimensions (height, length, steepness and number of dunes) during flood wave for different minimum dune heights (red = 0.005, green = 0.015 and blue = 0.025); vertical lines indicate moments where discharge is changed.

Water levels in the falling stage are higher than in the rising stage (figure A5.2). This is also an effect of hysteresis. Dunes need time to develop and are increasingly disturbing the water column above. In the first falling stage (stage D), where the discharge and water level drop already, the dune height still increases. The decrease of dune height during the flood wave sets in, in the last stage. The decrease of dune height takes more time than the increase in height. The mean dune length remains constant during all stages.
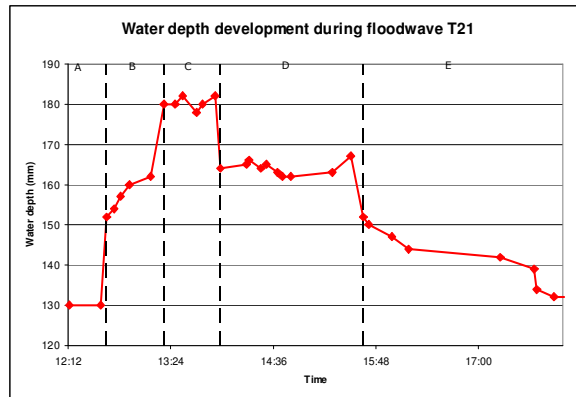
Figure A5.2: Water depth during flood wave

Appendix 6 Results experiments

Bed profiles over time for experiment T22

T22

Dune height

Dune length

Steepness

Number of dunes

Flow	Test	Flow parameters									
Cond	Numbers	PUMP setting	b [m]	Q [l/s]	q [m2/s]	H_0 [m]	b/H_0 0	i_0 0	U [m/s]	$u*_1$ [m/s]	$u*_2$ [m/s]
VII	22	20	0.44	43.74	0.0994	0.1500	2.93	0.0015	0.65	0.047	0.037

b = flume width, Q = discharge, q = specific discharge, H0 = initial water depth, i0 = initial water surface and bed slope
U = average flow velocity, u* = shear velocity, with u*1=sqrt(g*H0*i0), and u*2=based on ADV measurements (see exp. set up)
Note, for experiment T22,23,24, water depth is changed during experiment, such that w/s slope is equal to bed surface slope

Non-dimensional parameters

Flow	Test	Non-dimensional parameters					
Cond	Numbers	Fr	Re_gr	Y	Y/Ycr	Us/Usc	Us/Usc from theta
VII	22	0.536	39.93	0.1604	4.64	1.709	2.153

Fr = Froude number = U/sqrt(g*H0), Re_gr = grain Reynolds number = u*1*D50/visc, with D50 = average grain size and visc = 1*10^{-6}
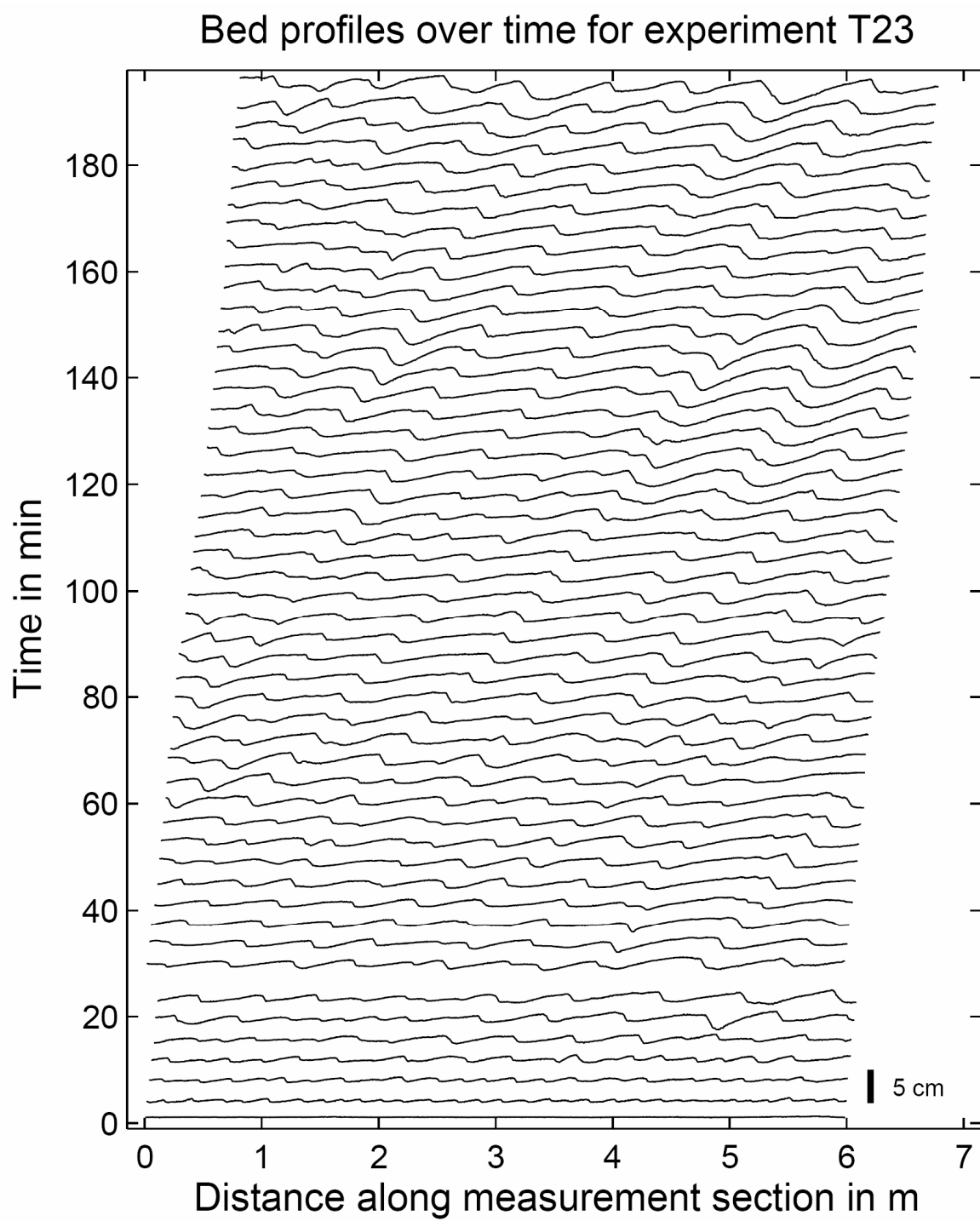Y = theta = Shields number, Us = u*, Usc = u*c = critical shear velocity (based on Shields number)

Expected equilibrium dune dimensions

Flow	Test	Coleman	Van Rijn (1993)		Julien&Klaassen (1995)		1/3H	6H
Cond	Numbers	time to eq. [s]	Δeq [m]	Leq [m]	Δeq [m]	Leq [m]	Δeq [m]	Leq [m]
VII	22	4859	0.063	1.095	0.079	0.942	0.050	0.900

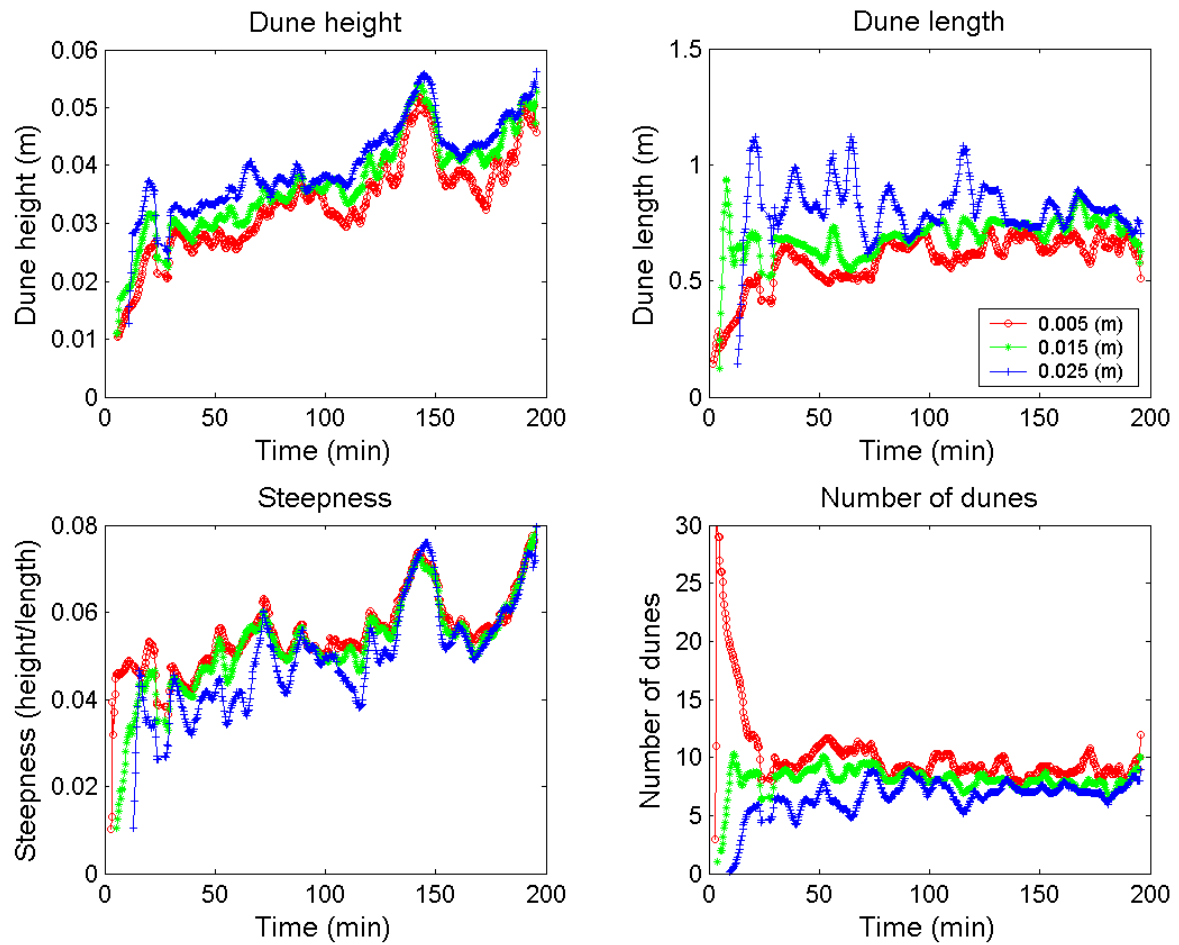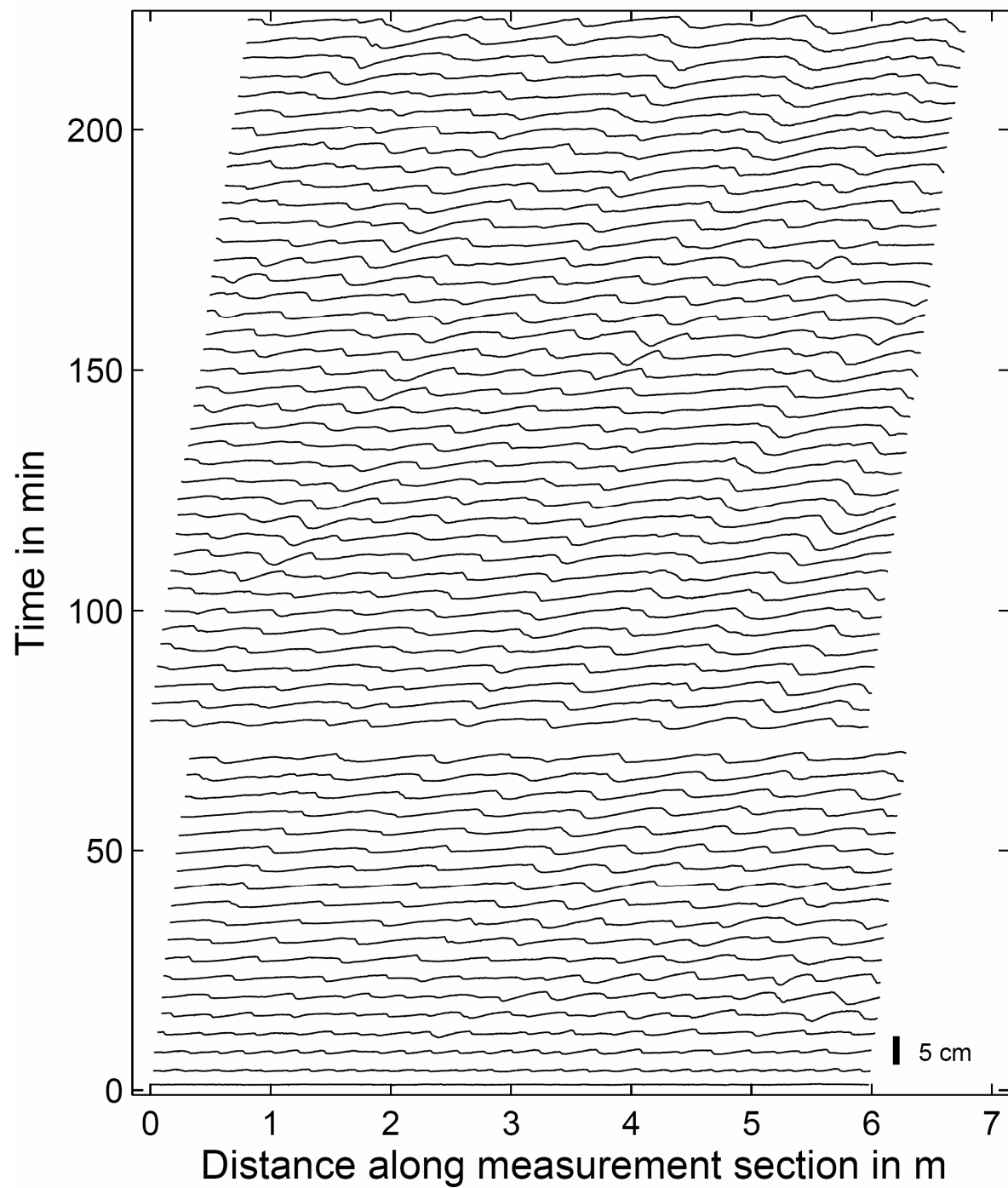Coleman = Coleman et al. (2005), Δ= dune height, L = dune length

Observed equilibrium dune dimensions

Flow	Test	Measured equilibrium characteristics				
Cond	Numbers	time to eq. [s]	Heq [m]	Δeq [m]	Leq [m]	Δ/L eq [-]
VII	22	3300	0.190	0.050	0.075	0.066

Bed profiles over time for experiment T23

T23

Dune height

Dune length

Legend:
- 0.005 (m)
- 0.015 (m)
- 0.025 (m)

Steepness

Number of dunes

Flow	Test	Flow parameters									
Cond	Numbers	PUMP setting	b [m]	Q [l/s]	q [m2/s]	H_0 [m]	b/H_0 0	i_0 0	U [m/s]	$u*_1$ [m/s]	$u*_2$ [m/s]
II	23	17	0.44	35.94	0.0817	0.1250	3.52	0.0015	0.62	0.043	0.036

b = flume width, Q = discharge, q = specific discharge, H0 = initial water depth, i0 = initial water surface and bed slope
U = average flow velocity, u = shear velocity, with u*1=sqrt(g*H0*i0), and u*2=based on ADV measurements (see exp. set up)*
Note, for experiment T22,23,24, water depth is changed during experiment, such that w/s slope is equal to bed surface slope

Non-dimensional parameters

Flow	Test	Non-dimensional parameters					
Cond	Numbers	Fr	Re_gr	Y	Y/Ycr	Us/Usc	Us/Usc from theta
II	23	0.561	36.45	0.1337	3.86	1.671	1.965

*Fr = Froude number = U/sqrt(g*H0), Re_gr = grain Reynolds number = u*1*D50/visc, with D50 = average grain size and visc = 1*10^{-6}*
Y = theta = Shields number, Us = u, Usc = u*c = critical shear velocity (based on Shields number)*

Expected equilibrium dune dimensions

Flow	Test	Coleman	Van Rijn (1993)		Julien&Klaassen (1995)		1/3H	6H
Cond	Numbers	time to eq. [s]	Δeq [m]	Leq [m]	Δeq [m]	Leq [m]	Δeq [m]	Leq [m]
II	23	3449	0.052	0.913	0.070	0.785	0.042	0.750

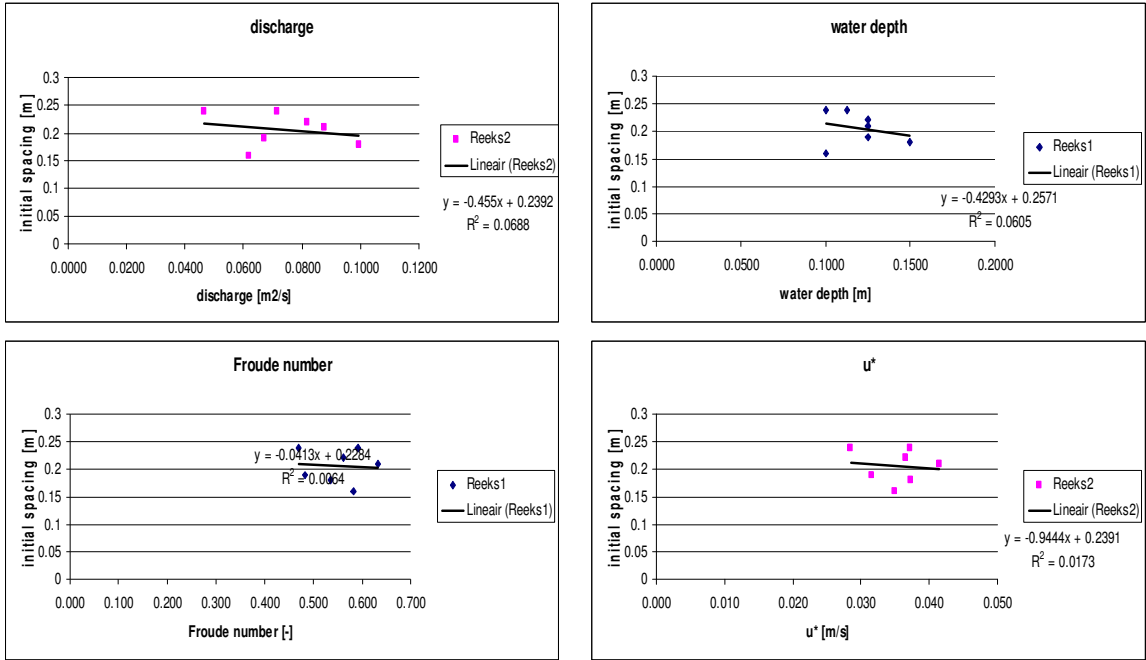*Coleman = Coleman et al. (2005), Δ= dune height, L = dune length*

Observed equilibrium dune dimensions

Flow	Test	Measured equilibrium characteristics				
Cond	Numbers	time to eq. [s]	Heq [m]	Δeq [m]	Leq [m]	Δ/L eq [-]
II	23	6800	0.160	0.044	0.070	0.066

Bed profiles over time for experiment T24

T24

Dune height

Dune length

Steepness

Number of dunes

Flow	Test	Flow parameters									
Cond	Numbers	PUMP setting	b [m]	Q [l/s]	q [m2/s]	H0 [m]	b/H0 0	i0 0	U [m/s]	u⋅1 [m/s]	u⋅2 [m/s]
IV	24	14	0.44	27.19	0.0618	0.1000	4.40	0.0015	0.58	0.038	0.035

b = flume width, Q = discharge, q = specific discharge, H0 = initial water depth, i0 = initial water surface and bed slope
U = average flow velocity, u* = shear velocity, with u⋅1=sqrt(g*H0*i0), and u⋅2=based on ADV measurements (see exp. set up)
Note, for experiment T22,23,24, water depth is changed during experiment, such that w/s slope is equal to bed surface slope

Non-dimensional parameters

Flow	Test	Non-dimensional parameters					
Cond	Numbers	Fr	Re_gr	Y	Y/Ycr	Us/Usc	Us/Usc from theta
IV	24	0.583	32.61	0.1070	3.09	1.600	1.758

Fr = Froude number = U/sqrt(g*H0), Re gr = grain Reynolds number = u⋅1*D50/visc, with D50 = average grain size and visc = 1*10^{-6}
Y = theta = Shields number, Us = u*, Usc = u*c = critical shear velocity (based on Shields number)

Expected equilibrium dune dimensions

Flow	Test	Coleman	Van Rijn (1993)		Julien&Klaassen (1995)		1/3H	6H
Cond	Numbers	time to eq. [s]	Δeq [m]	Leq [m]	Δeq [m]	Leq [m]	Δeq [m]	Leq [m]
IV	24	2267	0.039	0.730	0.060	0.628	0.033	0.600

Coleman = Coleman et al. (2005), Δ= dune height, L = dune length
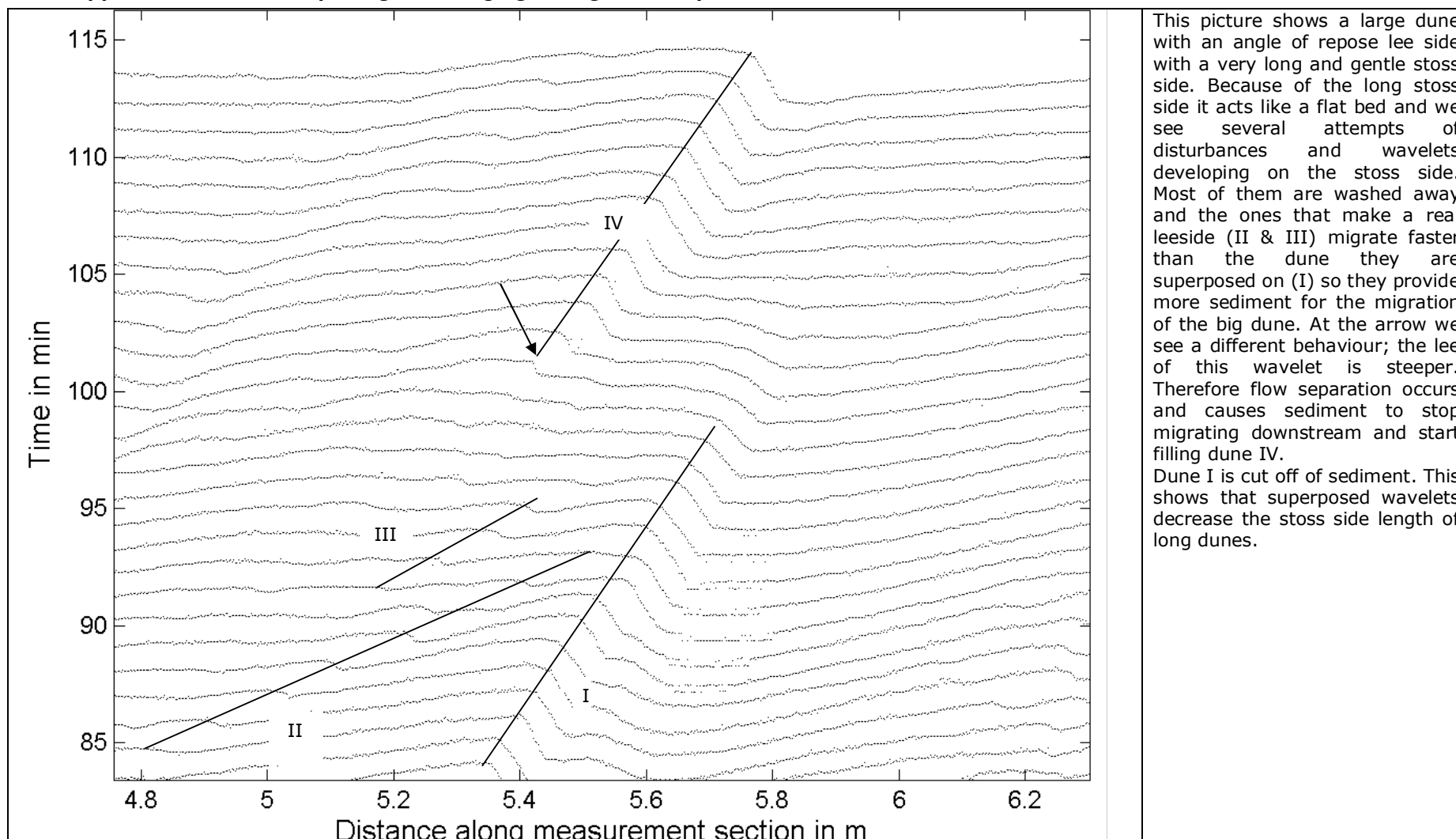
Observed equilibrium dune dimensions

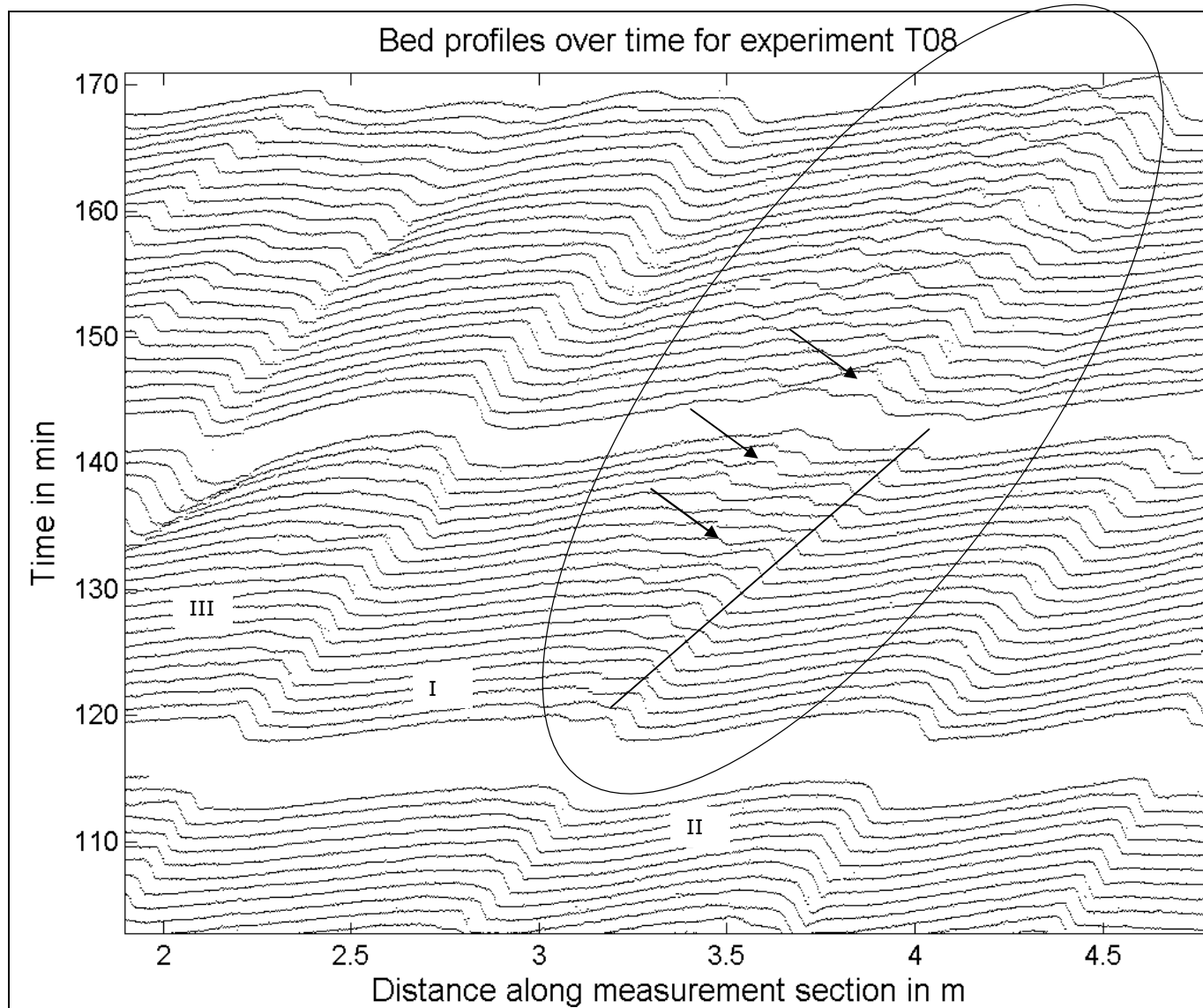| Flow	Test	Measured equilibrium characteristics				
Cond	Numbers	time to eq. [s]	Heq [m]	Δeq [m]	Leq [m]	Δ/L eq [-]
IV	24	6000	0.130	0.036	0.070	0.051

Appendix 7 Influence of flow parameters on the initial spacing of river dunes

Coleman et al. (2005) conclude based on their experiments that the initial spacing of small dunes can be estimated based on median grain size and is independent of flow parameters.
Based on the measured initial spacing of river dunes during the experiments in New Zealand, this theory is confirmed. discharge (q), waterdepth (Δ) , bed shear velocity (u_*) and Froude number, do not correlate with the measured initial spacing.
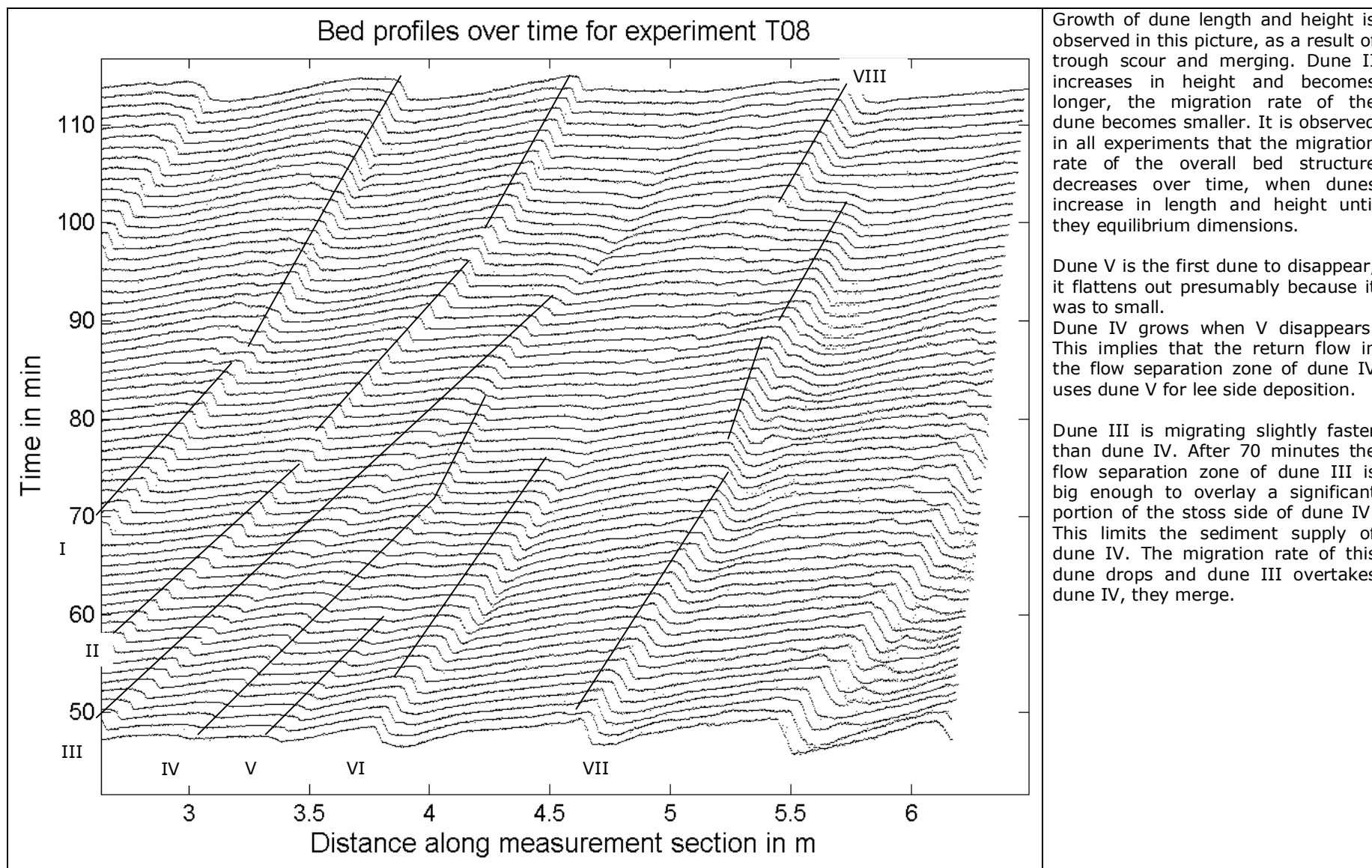
Appendix 8 Details on splitting and merging during flume experiments

This picture shows a large dune with an angle of repose lee side with a very long and gentle stoss side. Because of the long stoss side it acts like a flat bed and we see several attempts of disturbances and wavelets developing on the stoss side. Most of them are washed away and the ones that make a real leeside (II & III) migrate faster than the dune they are superposed on (I) so they provide more sediment for the migration of the big dune. At the arrow we see a different behaviour; the lee of this wavelet is steeper. Therefore flow separation occurs and causes sediment to stop migrating downstream and start filling dune IV.

Dune I is cut off of sediment. This shows that superposed wavelets decrease the stoss side length of long dunes.

Bed profiles over time for experiment T08

In this pictures we see well-developed dunes migrating at almost the same pace. The same effect occurs as we saw in the last picture. Dune I is less steep than the dunes (II & III) next to it. Therefore my suggestion is that again chances for initiation of superposed wavelets are growing.

When a leeside of one of these wavelets grows big enough (see arrow) it starts cutting off the sediment supply to the next big crest so this one starts lowering, but if the climbing dune reaches the front of the dune its on, they will continue together to migrate downstream. So a continuous process is seen (inside the circle) of small fast migrating superposed bed features that keep breaking down and filling up the front of dune (I) until it reaches a certain threshold steepness, and the dune gets stable again.

Bed profiles over time for experiment T08

Growth of dune length and height is observed in this picture, as a result of trough scour and merging. Dune II increases in height and becomes longer, the migration rate of the dune becomes smaller. It is observed in all experiments that the migration rate of the overall bed structure decreases over time, when dunes increase in length and height until they equilibrium dimensions.

Dune V is the first dune to disappear, it flattens out presumably because it was to small.
Dune IV grows when V disappears. This implies that the return flow in the flow separation zone of dune IV uses dune V for lee side deposition.

Dune III is migrating slightly faster than dune IV. After 70 minutes the flow separation zone of dune III is big enough to overlay a significant portion of the stoss side of dune IV. This limits the sediment supply of dune IV. The migration rate of this dune drops and dune III overtakes dune IV, they merge.

Bed profiles over time for experiment T08

This picture shows an even stronger magnified picture of the merging of dune III and IV shown on the previous picture.

The merging of two dunes is marked with an arrow. The dunes tend to grow in height and length over time.
It looks that dune I migrates faster because of a longer stoss side and a higher absolute crest height which results in a higher shear stress and therefore higher sediment transport at the crest.

Dune III is close to dune IV, so there is already influence of the flow separation zone of dune I. The flow separation zone of dune III occupies a large portion of the stoss side of dune IV. This limits the sediment transport to the crest of dune IV. The migration of this dune decreases even more, until the return flow inside the flow separation zone scours the last remains of the dune crest of dune IV at minute 83 (see arrow).

Appendix 9 Numerical stability analysis

A stability analysis is conducted to investigate whether superimposed fearures can grow on top of existing dunes.
A situation in which several asymmetrical dunes have developed is chosen as initial situation (b_0).
On top of this bed profile, a sine is applied with a given wavelength resulting in b'_0. Both situations are run with the model for one time step (b_1 and b'_1)
(see figure A9.1)
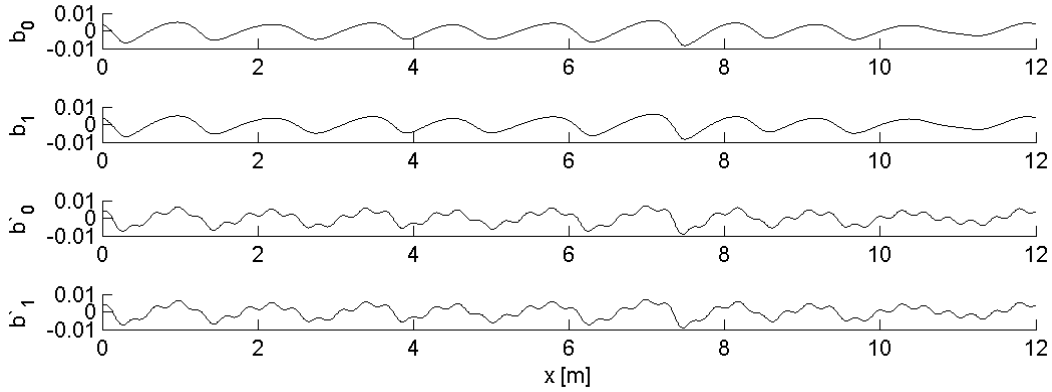
Figure A9.1: Input for the stability analysis

The initially applied superposed sine at t_0 (b'_0 - b_0) grows and migrates over time and changes into the signal at t_1 (b'_1 - b_1) To investigate whether this signal grows locally, plots are made of every superposed signal at t_0 and t_1 and are compared. One of these plots is shown in figure A8.2, The amplitude of the superposed signal after one time step shows no growth regardless of the location. This is important information, because the superposed signal is applied over the complete domain and it would be realistic to assume that there is variation in growth regarding the location of the superposed feature (e.g. on the stoss or lee side) Therefore, this check is performed for every wavelength.
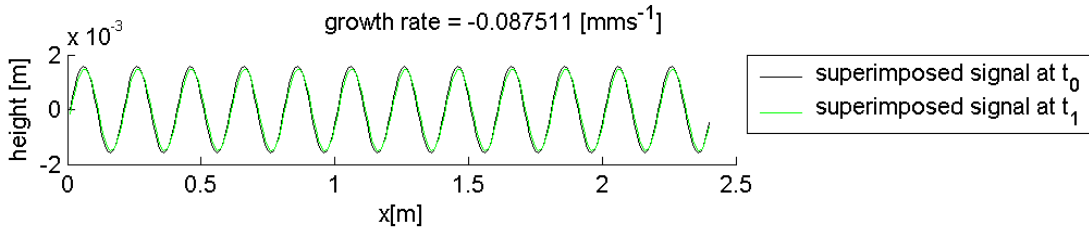
Figure A9.2: Negative growth of a superposed sine (wavelength = 0.2 m; comparison of (b'_0 - b_0) and (b'_1 - b_1))
The mean absolute value of the applied sine after one time step divided by the mean absolute value of the original applied sine gives a ratio for overall growth of the superposed feature.
The growth ratio of the applied sine is given by a numerical scheme:

$$\text{Amplitude growth [m]} = \frac{\pi}{2Npx}\left[\sum_{i=1}^{Npx}\left|b'_1(i)-b_1(i)\right|-\sum_{i=1}^{Npx}\left|b'_0(i)-b_0(i)\right|\right] \qquad (A.9.1)$$

Npx = gridpoints in the x-direction [-]

With a numerical time step (Δt = 1s) this absolute amplitude growth is equal to the amplitude growth rate [ms^{-1}]
This growth rate is plotted for several wavelengths to investigate which wavelengths grow and which will disappear, when applied on a developed bed profile (see figure A8.3).
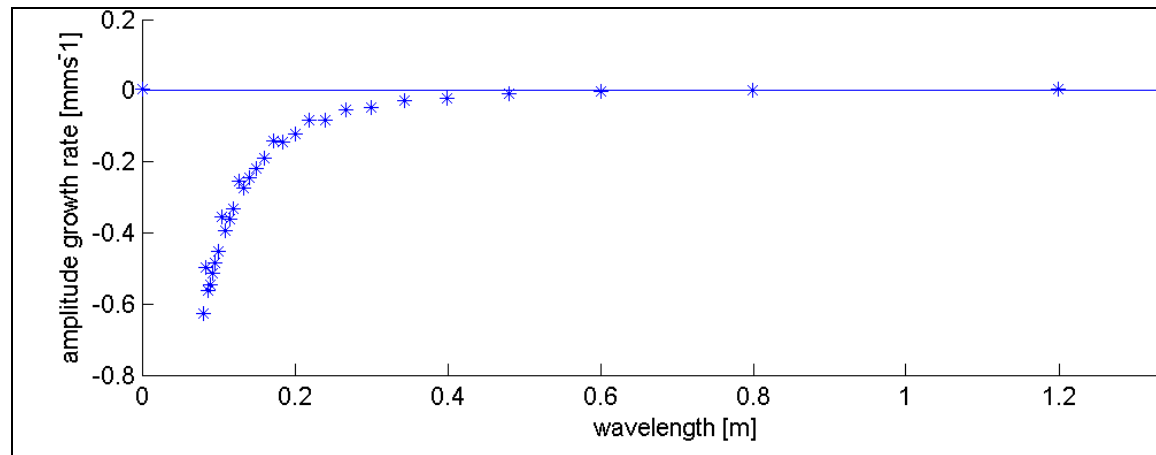
Figure A9.3: Numerical stability analysis for sinusoidal bed disturbances with differing wavelengths

This stability plot shows negative growth for superposed bed features with wavelengths smaller than 80 cm. This implies that the method of initiation of dune splitting by disturbing the bed under the given model settings is not promising. The fastest growing mode is found at a wavelength of 1.2 m, which is slightly higher than the expected equilibrium wavelength based on the flume observations and equilibrium predictors (see table 2.5).

Appendix 10 Model simulations with an angle of repose ϕ_s =63º

Model simulations with the sediment transport formula using ϕ_s =63º shows that, despite the smaller fastest growing mode, dunes merge. Initially they grow faster and steeper (figure A10.1)
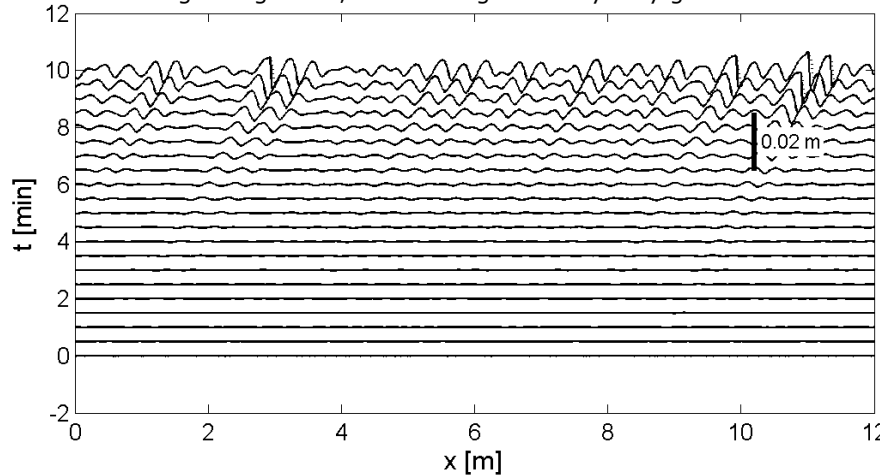
Figure A10.1: Bed form initiation with a Φs of 63 degrees

After 15 minutes, dunes start to merge and the wavelength and wave height increase. The steepness or aspect ratio (H/L) is much bigger (1/10) compared to the situation with an angle of repose of 30º (approx. 1/40). The main conclusion of this section is that the slope terms have influence on both the initial behavior of bed evolution and influence the aspect ratio of bed forms, but do not influence the overall pattern of merging dunes.

These plots show that even with a shorter fastest growing wavelength, big long dunes tend to overtake smaller ones. The most important observation of this rather unusual and unrealistic exploration based on a changed angle of repose is therefore the fact that regardless of the fastest growing wavelength, dunes merge when flow separation is parameterized. Without the inhibition of the migration rate of high and long dunes, it is not possible to simulate dune development obtaining an equilibrium dune length.
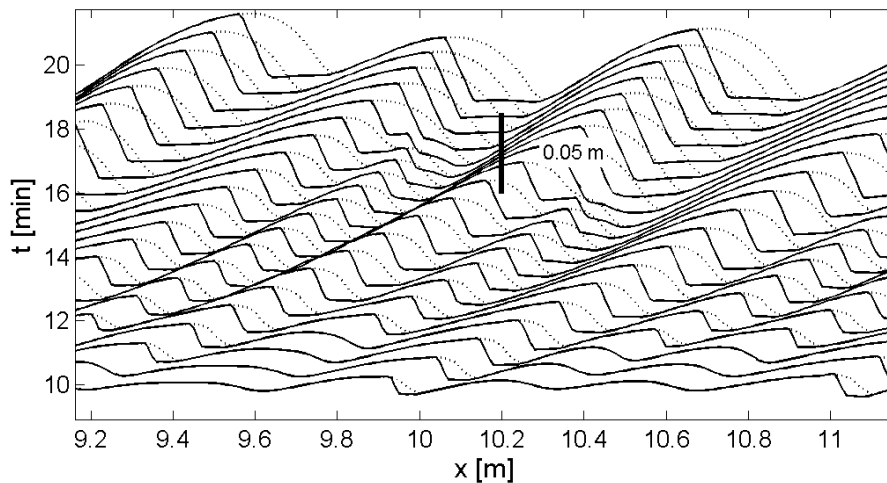
Figure A10.2: Dune merging, exceeding the fastest growing mode for an angle of repose of 63º

88

Appendix 11 Numerical implementation of the superposed wavelet
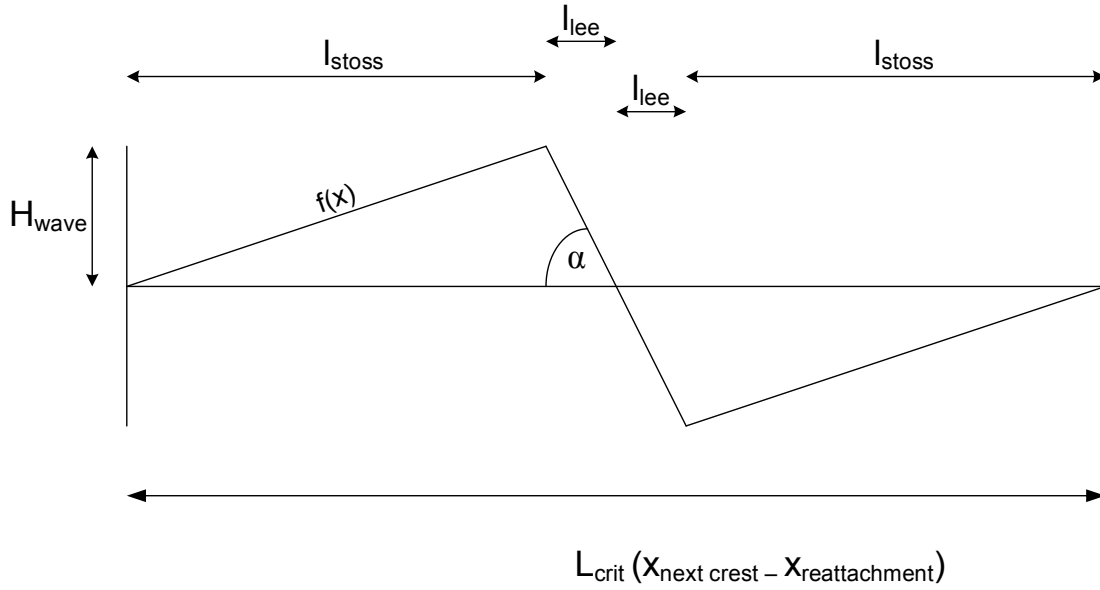
$$l_{lee} = \frac{H}{\tan \alpha}$$

$$l_{stoss} = 1/2L - l_{lee}$$

Analytical :

$$f(x) = \frac{Hx}{l_{stoss}} \qquad\qquad x \le l_{stoss}$$

$$f(x) = H - \tan \alpha(x - l_{stoss}) \qquad l_{stoss} < x < (l_{stoss} + 2l_{lee})$$

$$f(x) = -H + \frac{H(x - l_{stoss} + 2l_{lee})}{l_{stoss}} \qquad x \ge (l_{stoss} + 2l_{lee})$$

Numerical implementation :

$$f(x) = 0$$

$$f(x + \Delta x) = \frac{H\Delta x}{l_{stoss}} \qquad\qquad i \le \frac{l_{stoss}}{\Delta x}$$

$$f(x + \Delta x) = H - \tan \alpha(x - l_{stoss}) \qquad \frac{l_{stoss}}{\Delta x} < i < \frac{(l_{stoss} + 2l_{lee})}{\Delta x}$$

$$f(x) = -H + \frac{H(x - l_{stoss} + 2l_{lee})}{l_{stoss}} \qquad i \ge \frac{(l_{stoss} + 2l_{lee})}{\Delta x}$$

Appendix 12 Sensitivity analysis for β in the sediment transport formula

β =
1.25

β = 1.50

β =
1.75

Dune height

Transport characteristics
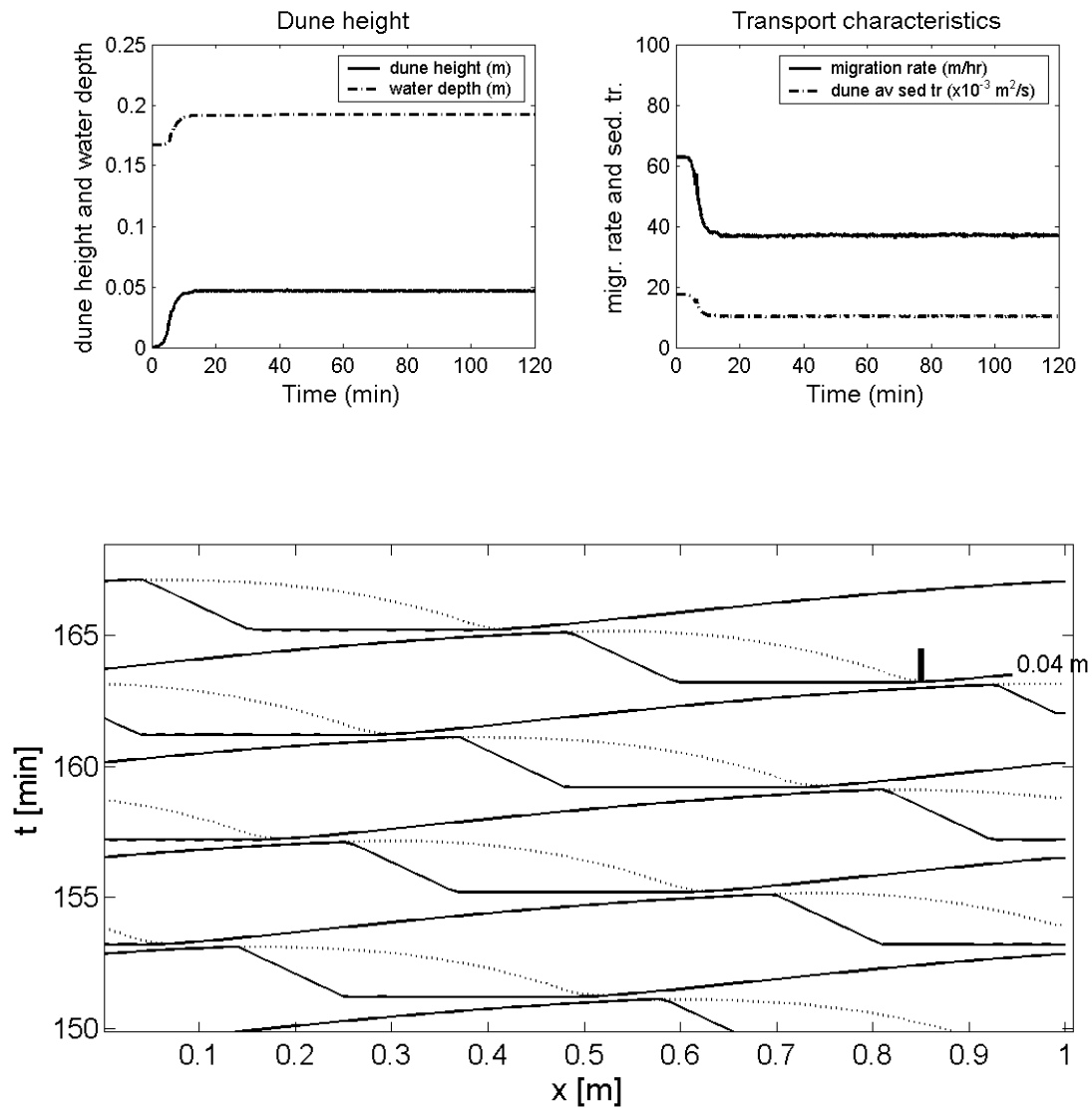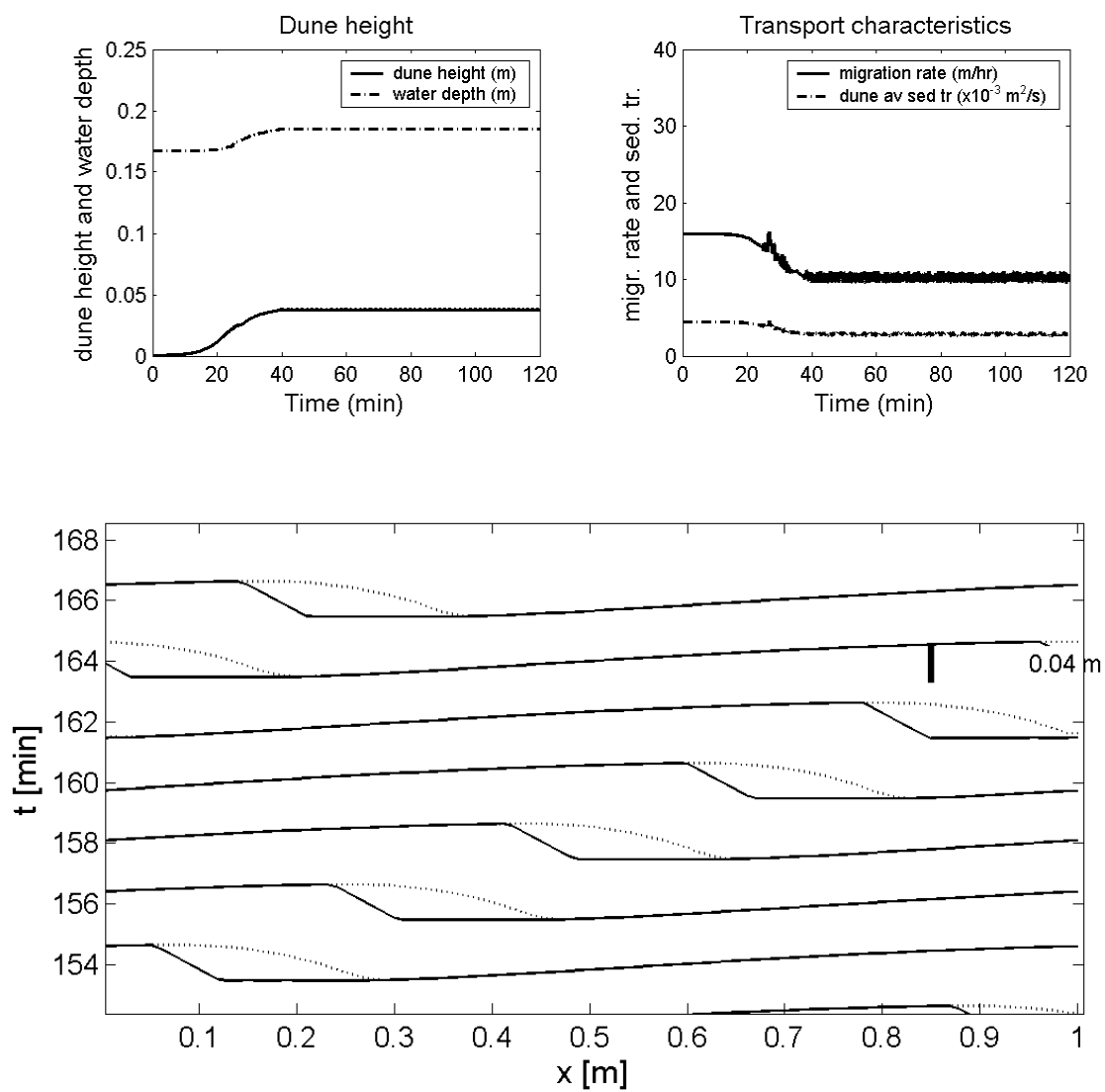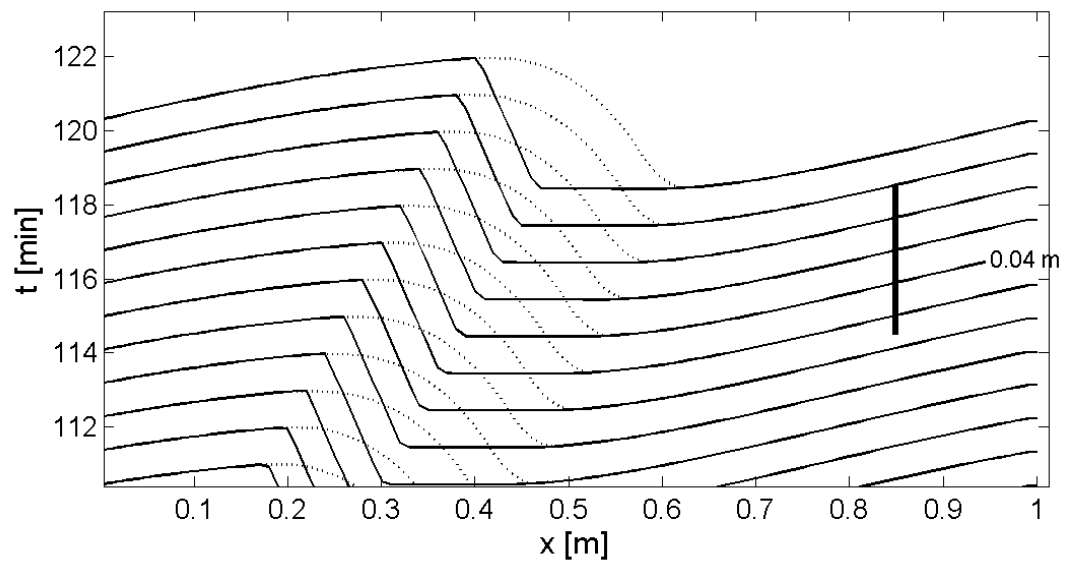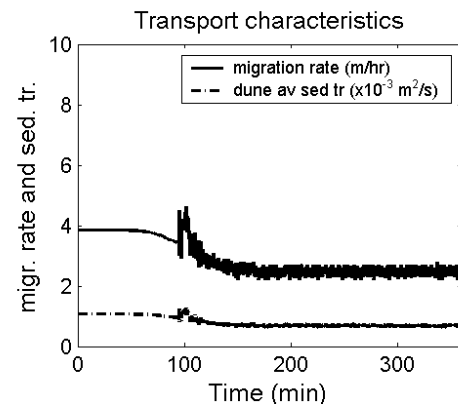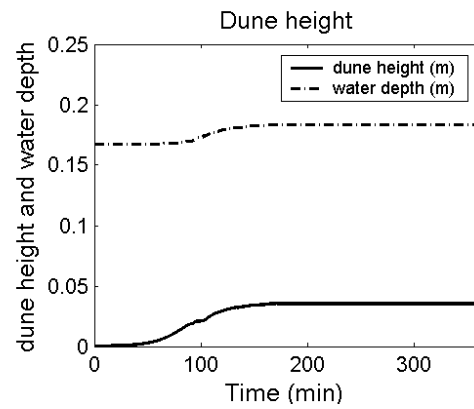
β   =
2.00
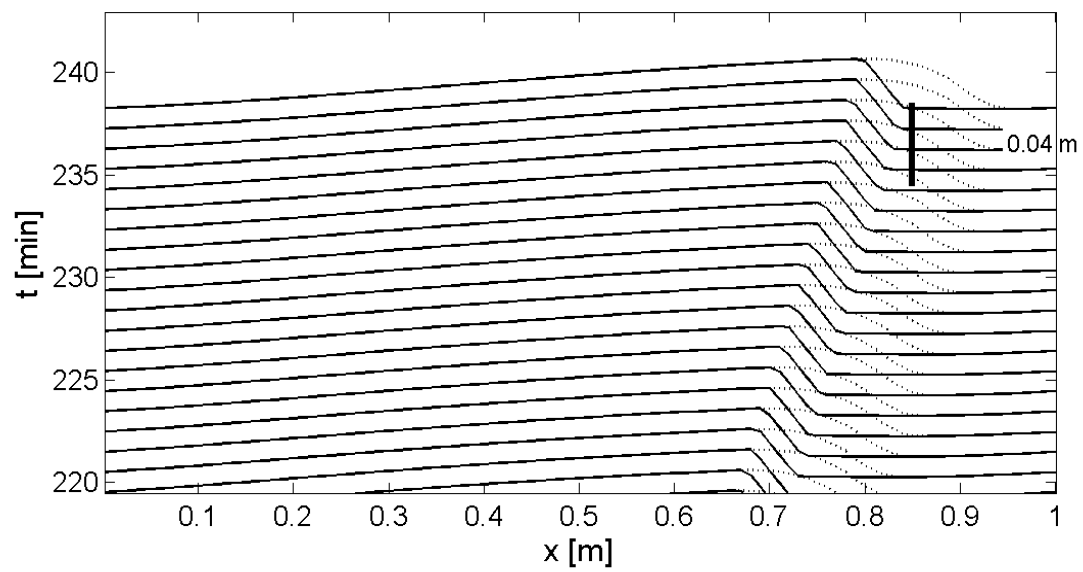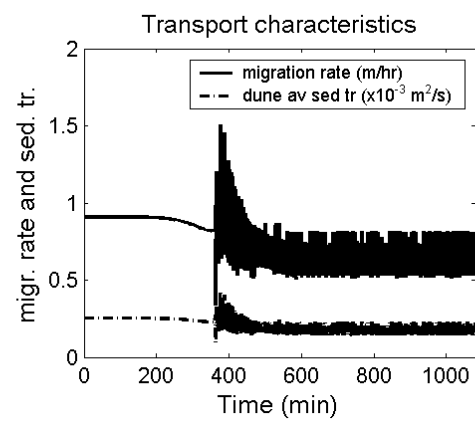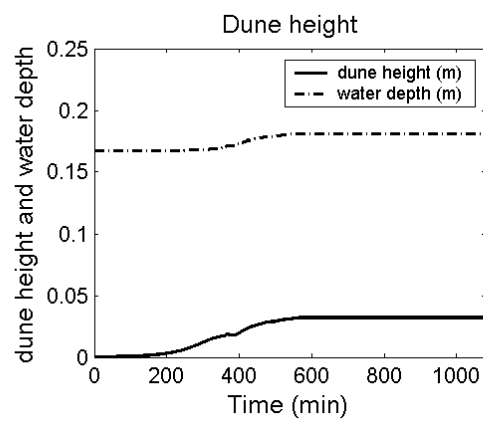
Appendix 13 Sensitivity analysis for H_{wave} and L_{crit}

To investigate the effect of the wavelet parameters H_{wave} and L_{crit} on the equilibrium dimensions and the modelled dune evolution, a sensitivity analysis has been performed for the settings in table A13.1
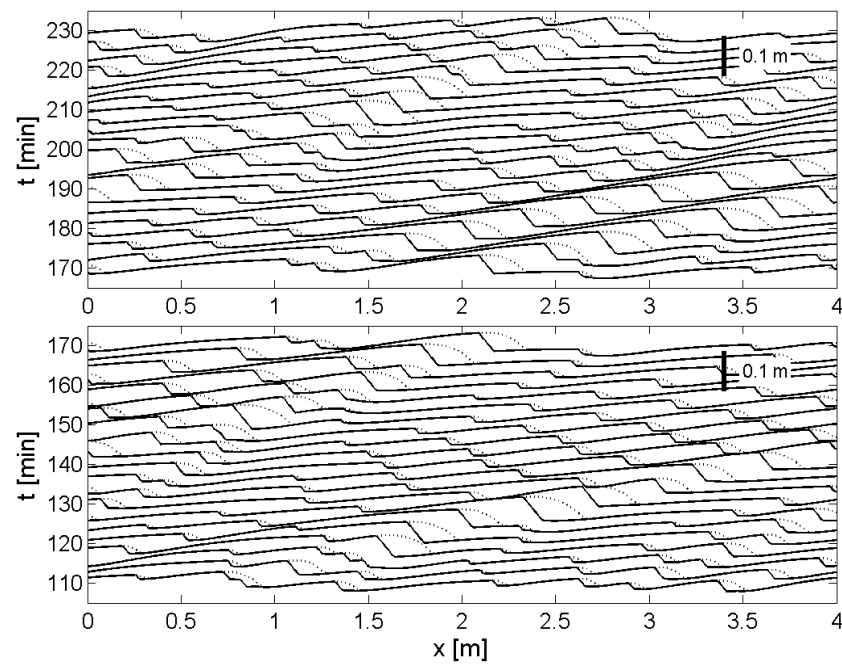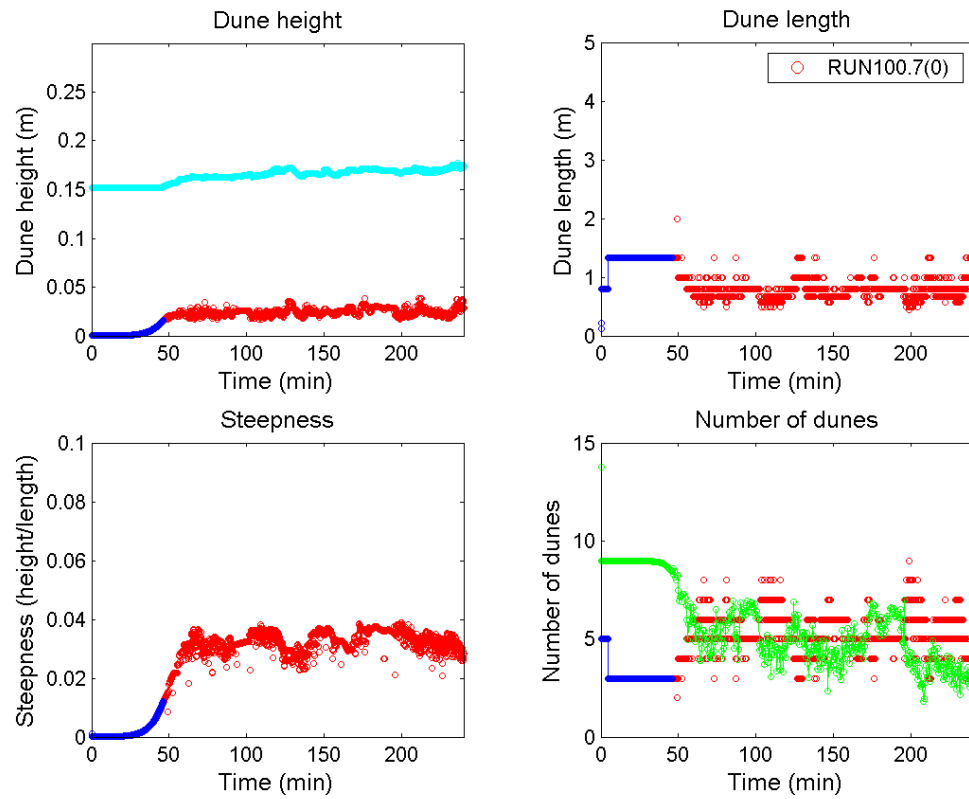
Npz	Npx	L [m]	H_wave [m]	Lcrit [m]
15	800	4	0.003	1
15	400	4	0.006	1
15	400	4	0.012	1
15	400	4	0.006	1.25
15	400	4	0.006	1.5
15	400	4	0.006	1.75
15	400	4	0.006	2

Table A13.1: Model settings for sensitivity analysis (the changed values are marked red)

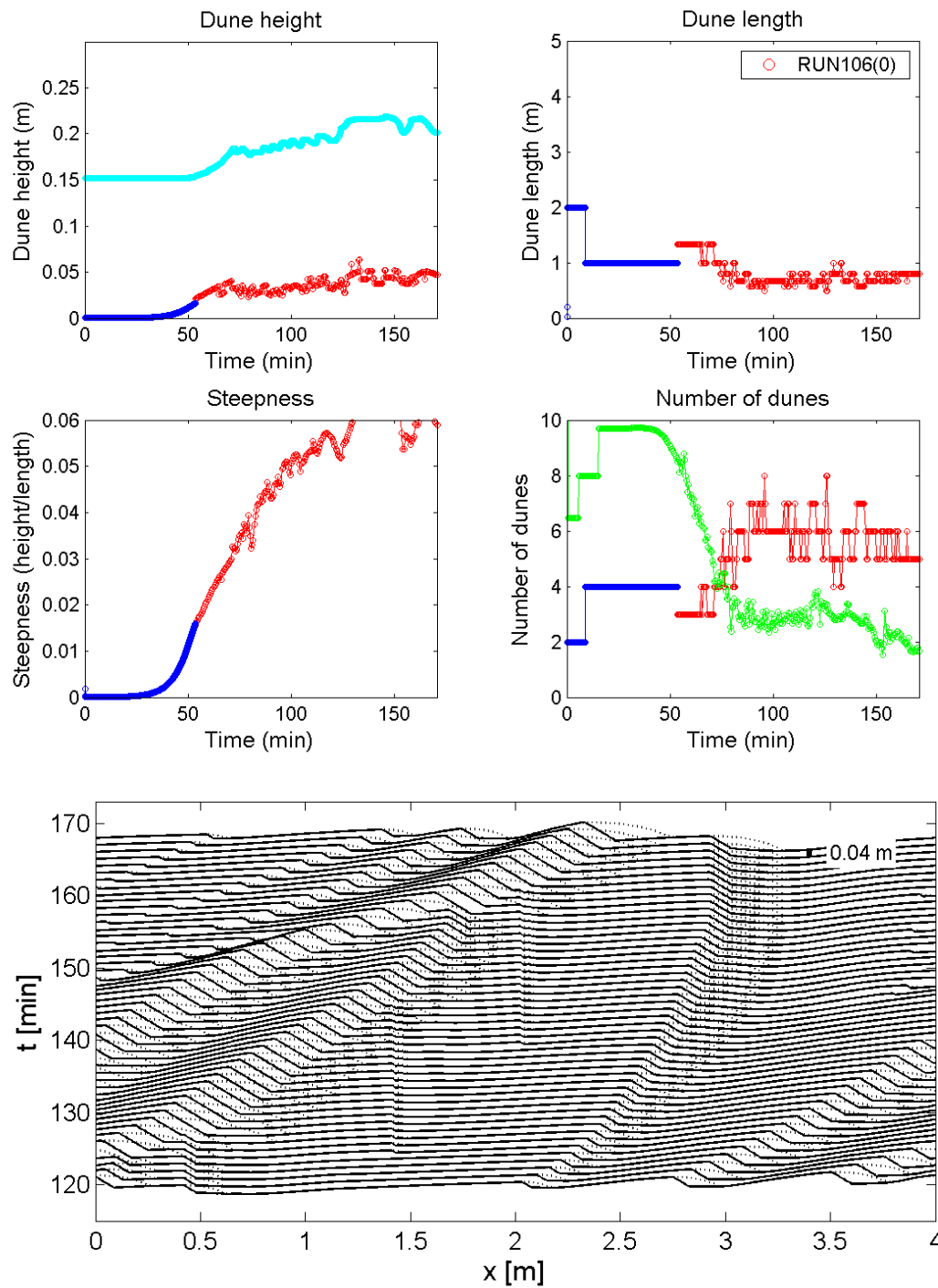| Npz	Npx	L [m]	H_wave [m]	Lcrit [m]
15	800	4	**0.003**	1
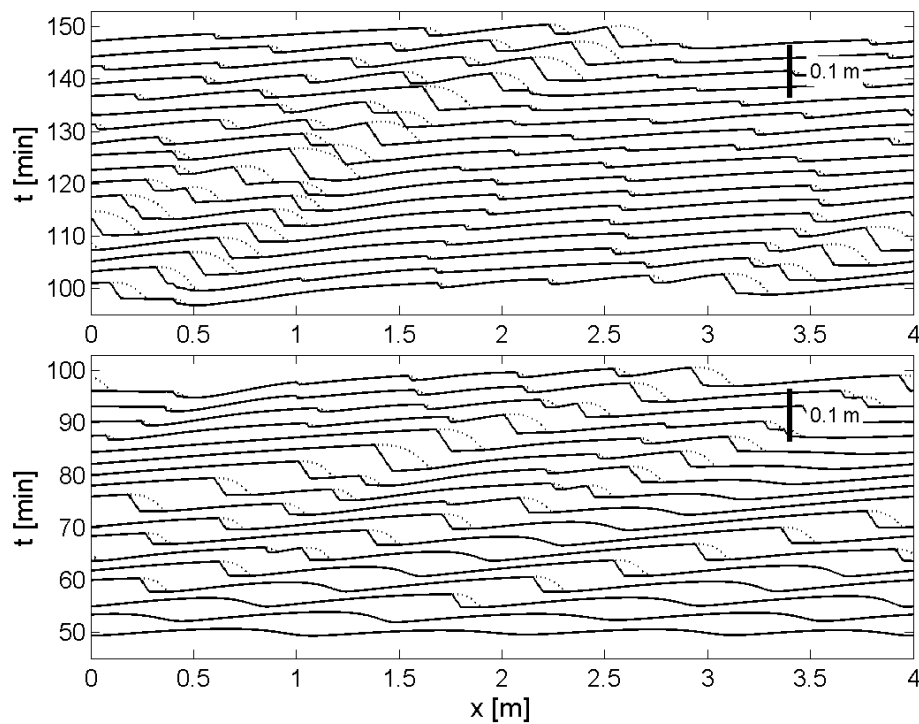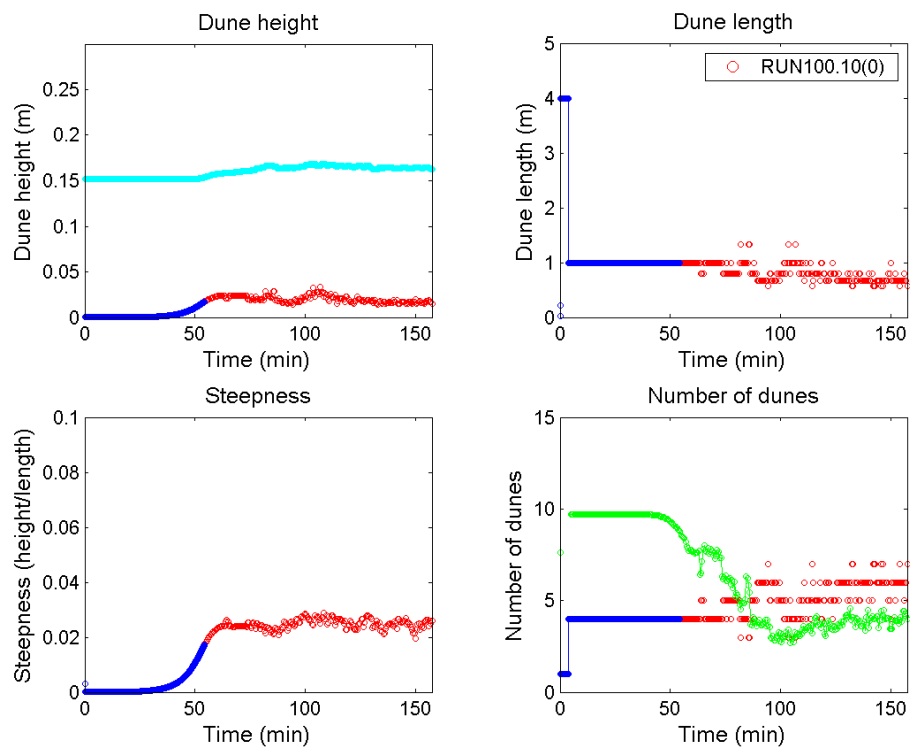
Npz	Npx	L [m]	H_wave [m]	Lcrit [m]
15	400	4	0.006	1

Npz	Npx	L [m]	H_wave [m]	Lcrit [m]
15	400	4	**0.012**	1
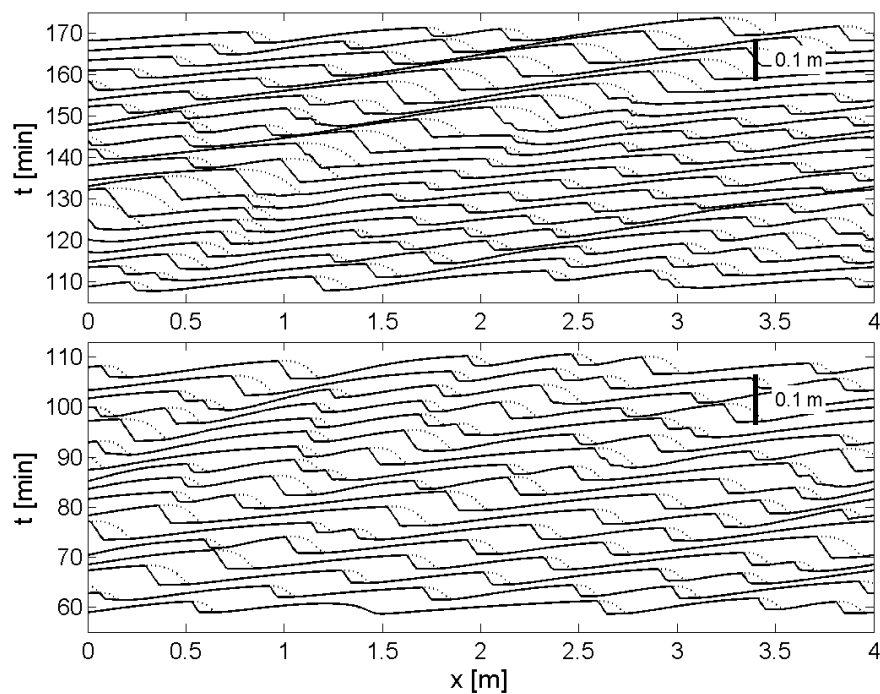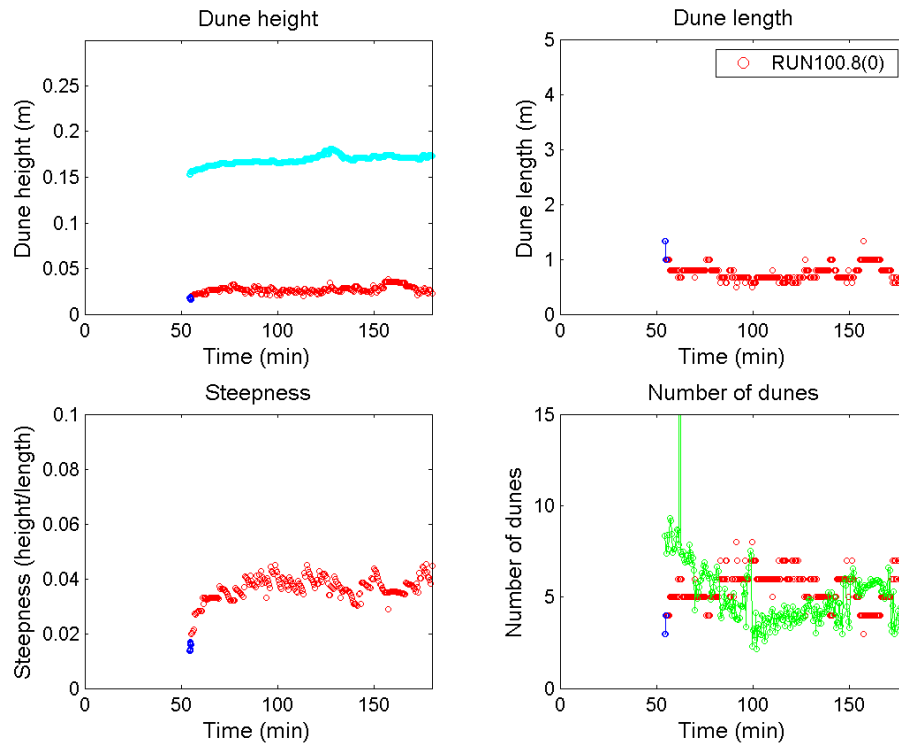
Npz	Npx	L [m]	H_wave [m]	Lcrit [m]
15	400	4	0.006	**1.25**
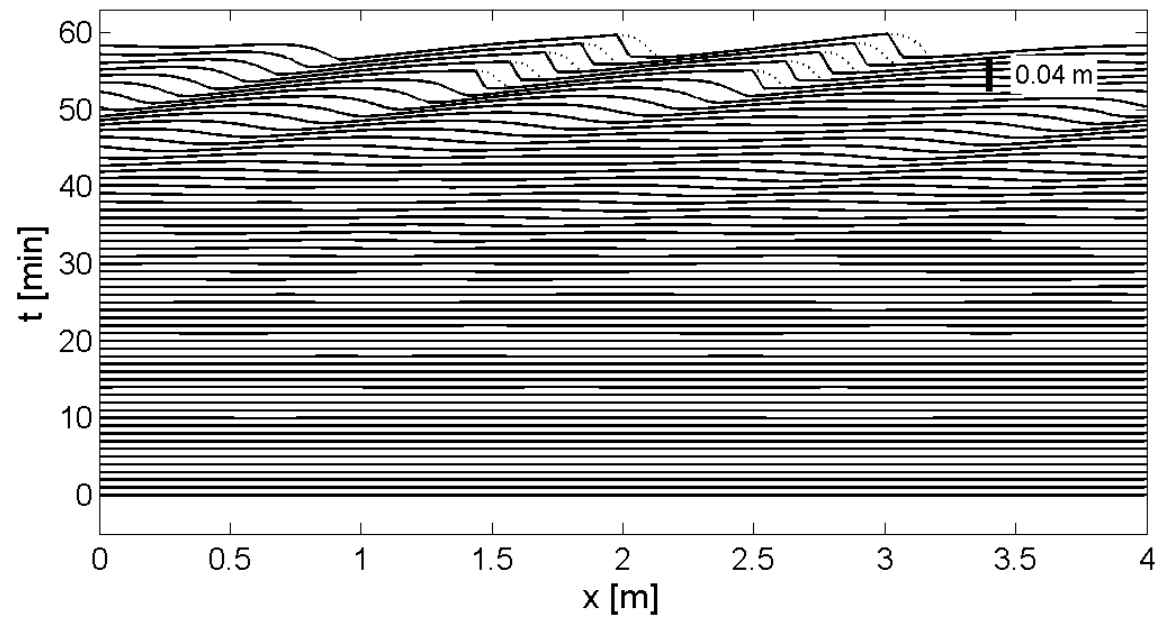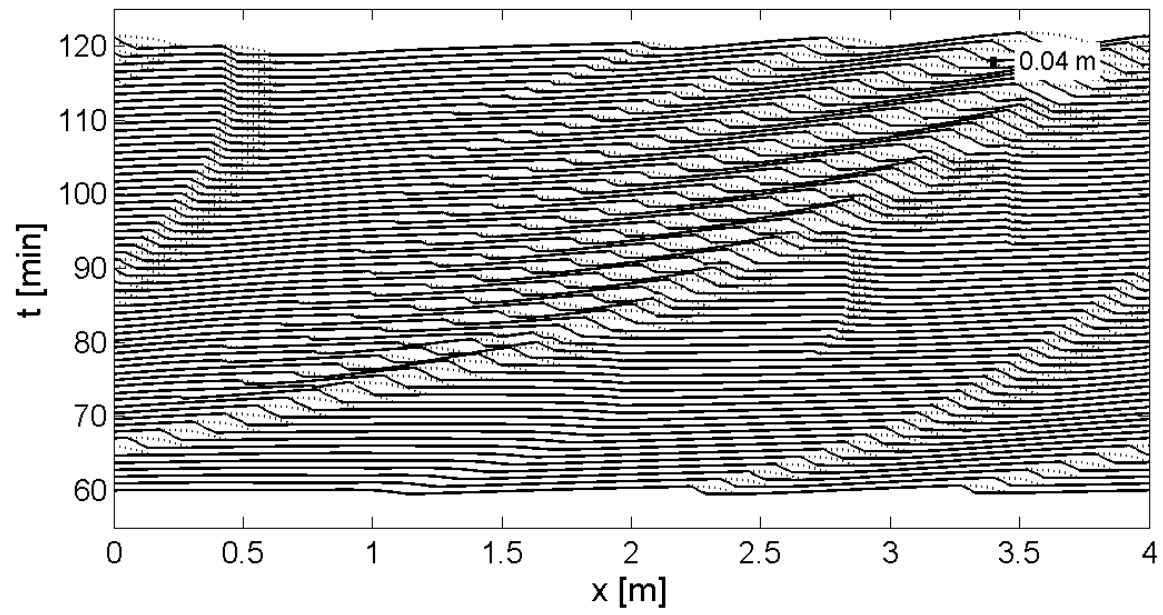
Npz	Npx	L [m]	H_wave [m]	Lcrit [m]
15	400	4	0.006	**1.50**
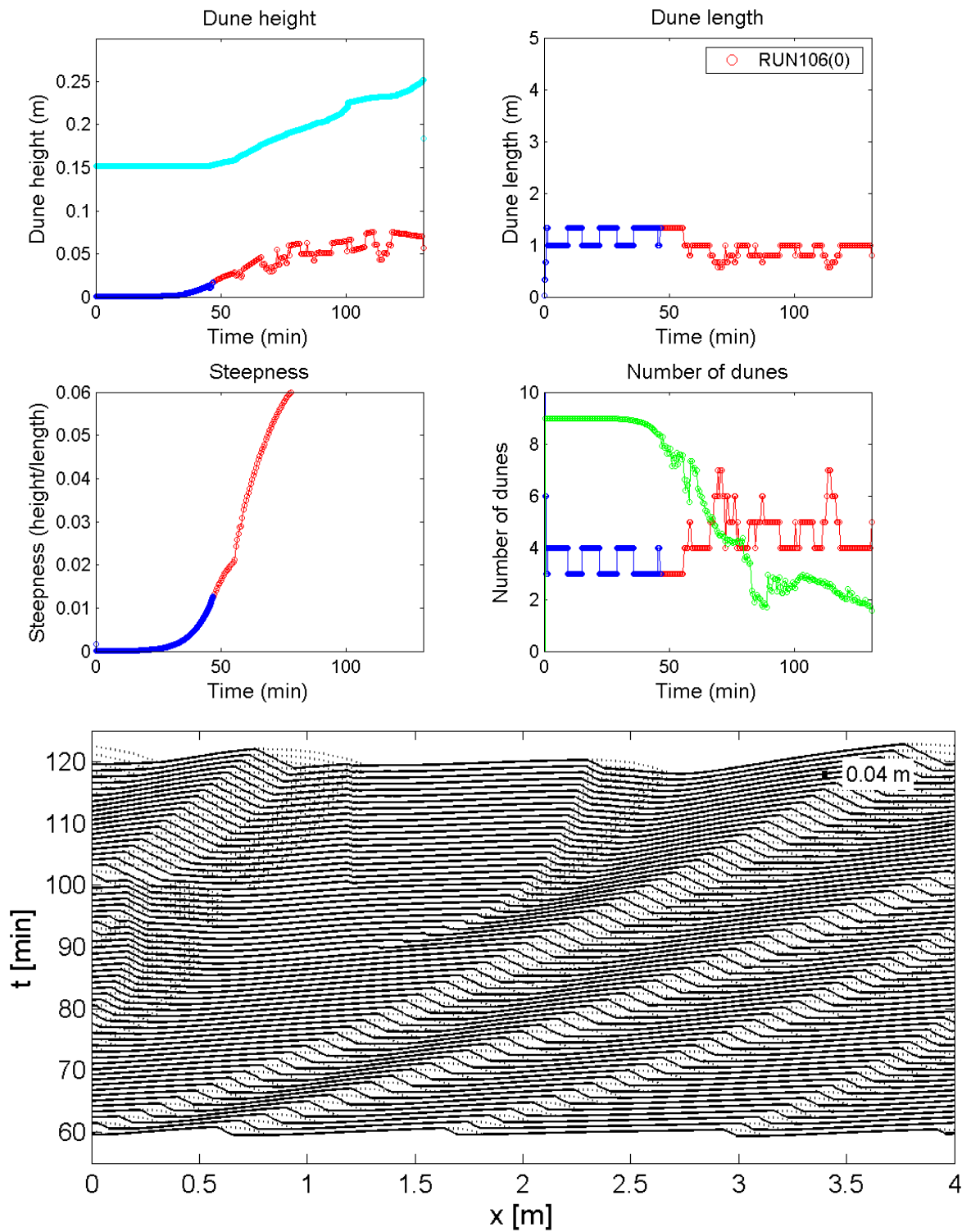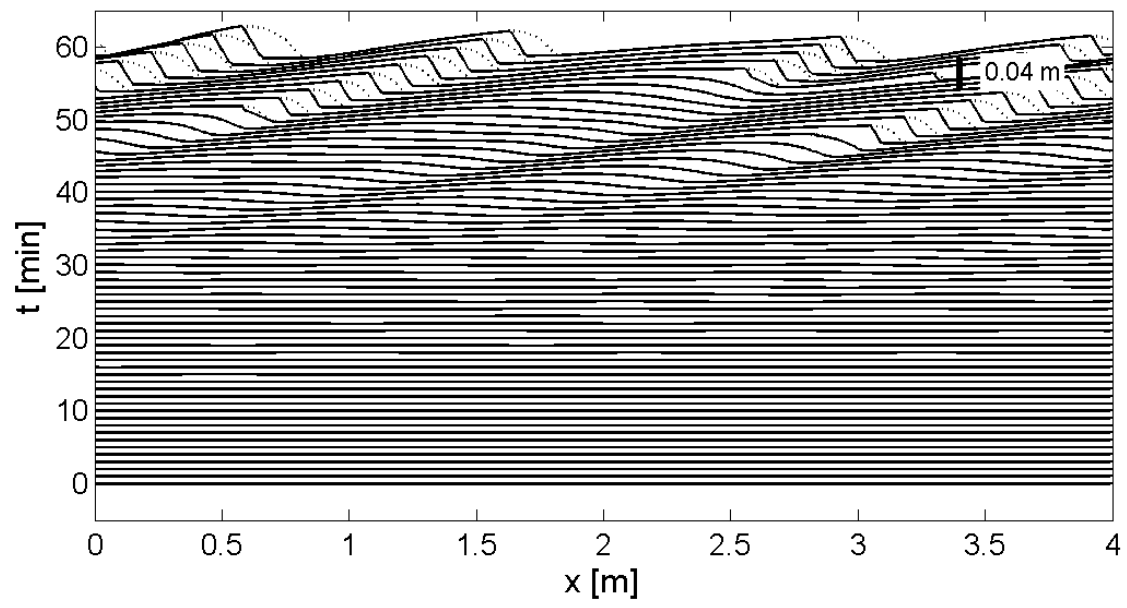
Npz	Npx	L [m]	H_wave [m]	Lcrit [m]
15	400	4	0.006	**1.75**

Npz	Npx	L [m]	H_wave [m]	Lcrit [m]
15	400	4	0.006	**2.00**